

*Alma Mater Studiorum – Università di Bologna*

DOTTORATO DI RICERCA IN  
SCIENZE FARMACEUTICHE

Ciclo XXIV

**Settore Concorsuale di afferenza:** 03/D2

**Settore Scientifico disciplinare:** CHIM/09

**MULTIFUNCTIONAL NANOCARRIERS ENCAPSULATING  
ANTI-ALZHEIMER DRUG FOR NASAL DELIVERY TO  
CENTRAL NERVOUS SYSTEM**

**Presentata da: Giuseppe Corace**

Coordinatore Dottorato

Chiar.mo Prof. Maurizio Recanatini

Relatore

Chiar.mo Prof. Vittorio Zecchi

**Esame finale anno 2012**



*“Imagination is more important than knowledge.  
For knowledge is limited to all we now know and understand,  
while imagination embraces the entire world,  
and all there ever will be to know and understand”*

*Albert Einstein*

*To my Family*

## ACKNOWLEDGMENTS

---

*I would like to express my gratitude to my supervisor, Prof. Vittorio Zecchi for his guidance and knowledge, and all the Drug Delivery Group, to Dr. Federica Bigucci, Dr. Teresa Cerchiara and especially to my unofficial supervisor, Dr. Barbara Luppi who supported me with an invaluable assistance, support and guidance during the research work and thesis revision.*

*I express my sincerest gratitude to Dr. Cristina Cavallari, Prof. Lorenzo Rodriguez and Prof. Adamo Fini for their scientific and friendly support, which never came less, always accompanying me since I was a master student.*

*I am deeply thankful to Prof. Silvana Arelia, Dr. Cristina Angeloni and Dr. Elisa Motori (Dep. Biochemistry "G.*

*Moruzzi") for their studies on neuronal cultures and especially for their willingness and kindness.*

*I would like to express a special thanks to Prof. Martin Brandt and his entire Research Group (Drug Delivery, Institut for Fysik, Kemi og Farmaci, Odense, Denmark), to Prof. Annette Bauer-Brandt, Prof. Judith Kuntsche, Prof. Paul Stain, Max di Cagno, Sarah Fischer, Ulla M. Brinkmann Trettenes, Kerstin Frank and technical support staff (Tina Christiansen and Karen Elmquist) for their hospitality, when I spent my period of research abroad.*

*Thanks also goes out to my master students (Stefano Palmieri, Francesca Cordeschi, Elena Monti, Anna Paola Nunzella, Valentina Iaia, Mariangela Conserva, Mirko Montagnoli, Alice Delucca, Luca Mancini, Yari Delvecchio, Silvia Lelli), teach them has humanly enriched me*

*Finally, the biggest thanks goes to my Family for giving me the strength to follow my dreams.*

*Giuseppe Corace*



## LIST OF PAPERS DISCUSSED

---

This thesis includes the papers listed below:

1. Barbara Luppi; Federica Bigucci; **Giuseppe Corace**; Alice Delucca; Teresa Cerchiara; Milena Sorrenti; Laura Catenacci; Anna Maria Di Pietra; Vittorio Zecchi. *Albumin nanoparticles carrying permeation enhancers for nasal delivery of tacrine hydrochloride.*  
Eur. J. Pharm. Biopharm. 44(4):559-65; 2011  
Reproduced with permission. License Number: 2861131055273. © 2011 Elsevier
2. **Giuseppe Corace**, Barbara Luppi, Cristina Angeloni, Elisa Motori, Silvana Hrelia, Paul C. Stein, Martin Brandl, Roberto Gotti and Vittorio Zecchi  
*Multifunctional Liposomes For Nasal Delivery Of The Anti-Alzheimer Drug Tacrine Hydrochloride. Part 1: Formulation, Characterization, In-Vitro/Ex-Vivo Permeability And Neuronal Uptake Evaluation*  
In preparation for the Journal of Controlled Release
3. **Giuseppe Corace**, Barbara Luppi, Cristina Angeloni, Elisa Motori, Silvana Hrelia, Paul C. Stein, Martin Brandl, Roberto Gotti and Vittorio Zecchi  
*Multifunctional Liposomes For Nasal Delivery Of The Anti-Alzheimer Drug Tacrine Hydrochloride. Part 2: Tocopherol Lateral Diffusion And Neuroprotective Effect Evaluation.*  
In preparation for the Journal of Controlled Release

**My contribution:**

I contributed to all part of above papers except for the thermal analyses (TGA and DSC) reported in the paper 1, that were performed by Dr. Milena Sorrenti and Dr. Laura Catenacci (Department of Pharmaceutical Science, University of Pavia, Pavia, Italy), the evaluation of Tacrine Log D by NMR reported in paper 2, that was performed in collaboration with Prof. Paul C. Stein (Department of Physics, Chemistry and Pharmacy, University of Southern Denmark, Odense, Denmark), the quantification of the Tacrine in the neuronal extract by HPLC reported in the paper 2, that was performed by and in collaboration with Prof. Roberto Gotti (Department of Pharmaceutical Sciences, University of Bologna, Bologna, Italy) the neurotoxicity and neuroprotection reported in paper 3, that were performed by and in collaboration with Dr. Elisa Motori, Dr. Cristina Angeloni and Prof. Silvana Hrelia (Department of Biochemistry “G. Moruzzi”, University of Bologna, Bologna, Italy).



## **INDEX**

---

<b>ABBREVIATION</b>	<b>16</b>
<b>ABSTRACT</b>	<b>17</b>
<b>THEORETICAL SECTION</b>	<b>20</b>
<b>1. AN OVERVIEW ON ALZHEIMER'S DISEASE</b>	<b>21</b>
<b>2. INTRANASAL DRUG DELIVERY</b>	<b>27</b>
2.1. Nasal anatomy and physiology	31
2.1.1. <i>Respiratory region</i>	32
2.1.2. <i>Olfactory region</i>	34
2.1.3. <i>Nasal secretion</i>	35
2.2. Factors influencing the absorption of drugs across the nasal epithelium	36
2.2.1. <i>Physiological barrier</i>	37
2.2.2. <i>Physicochemical characteristics of the drug</i>	40
2.3. Strategy to improve intranasal drug absorption	42
2.4. Micro/nanocarriers for nasal drug delivery	45
2.4.1. <i>Microspheres</i>	45
2.4.2. <i>Nanoparticles</i>	47
2.4.3. <i>Liposomes</i>	48
2.4.4. <i>Nasal inserts</i>	52

---

<b>EXPERIMENTAL SECTION</b>	<b>54</b>
<b>3. ALBUMIN NANOPARTICLES CARRYING CYCLODEXTRINS FOR NASAL DELIVERY OF THE ANTI-ALZHEIMER DRUG TACRINE</b>	<b>55</b>
3.1. Introduction	56
3.2. Materials and Methods	57
3.2.1. <i>Materials</i>	57
3.2.2. <i>Preparation of bovine serum albumin nanoparticles</i>	58
3.2.3. <i>Nanoparticle loading and determination of loading efficiency</i>	59
3.2.4. <i>Particle size, zeta-potential measurements and morphology</i>	60
3.2.5. <i>Thermogravimetric analysis (TG), Differential scanning calorimetry (DSC) and Fourier Transform Infrared Spectroscopy (FT-IR)</i>	60
3.2.6. <i>Mucoadhesion properties</i>	61
3.2.7. <i>In-vitro release studies</i>	62
3.2.8. <i>Ex-vivo permeation studies across sheep nasal mucosa</i>	62
3.2.9. <i>Statistical analysis</i>	62
3.3. Results	63
3.3.1. <i>Particle characteristics</i>	63
3.3.2. <i>Nanosphere loading and determination of loading efficiency</i>	64
3.3.3. <i>Thermogravimetric analysis (TG), Differential scanning calorimetry (DSC) and Fourier transform infrared (FT-IR) spectroscopy</i>	64
3.3.4. <i>Mucoadhesion properties</i>	67
3.3.5. <i>In-vitro release studies</i>	67
3.3.6. <i>Ex-vivo permeation studies across sheep nasal mucosa</i>	69
3.4. Discussion	69
3.5. Conclusions	72

<b>4. MULTIFUNCTIONAL LIPOSOMES FOR DELIVERY OF THE ANTI-ALZHEIMER DRUG TACRINE HYDROCHLORIDE BY THE NASAL ROUTE. PART 1: FORMULATION, CHARACTERIZATION, IN-VITRO/EX-VIVO PERMEABILITY AND NEURONAL UPTAKE EVALUATION</b>	<b>73</b>
<b>4.1. Introduction</b>	<b>74</b>
<b>4.2. Materials and Methods</b>	<b>76</b>
4.2.1. <i>Materials</i>	76
4.2.2. <i>Determination of THA octanol/phosphate buffer solution PBS (pH 7.4 and 6.0) distribution coefficient (LogD)</i>	76
4.2.3. <i>Preparation of liposomes</i>	77
4.2.4. <i>Liposome size distribution and zeta-potential measurements</i>	78
4.2.5. <i>Determination of encapsulation efficiency</i>	79
4.2.6. <i>Ex-vivo Mucoadhesion Studies</i>	81
4.2.7. <i>Evaluation of THA apparent permeability (<math>P_{APP}</math>) using the Phospholipid Vesicle-based Permeation Assay (PVPA)</i>	82
4.2.8. <i>Evaluation of THA permeability (P) using Ex-vivo Sheep Nasal mucosa Permeation Assay (ENSPA)</i>	83
4.2.9. <i>Assessment of tacrine uptake/association in SH-SY5Y cell line</i>	84
4.2.10. <i>Statistical analysis</i>	84
<b>4.3. Results and discussion</b>	<b>85</b>
4.3.1. <i>Evaluation of THA LogD</i>	85
4.3.2. <i>Physical properties of liposomes</i>	86
4.3.3. <i>Ex-Vivo mucoadhesion study</i>	87
4.3.4. <i>THA permeability</i>	88
4.3.5. <i>THA neuronal uptake/association</i>	90
<b>4.4. Conclusions</b>	<b>91</b>

<b>5. MULTIFUNCTIONAL LIPOSOMES FOR DELIVERY OF THE ANTI-ALZHEIMER DRUG TACRINE HYDROCHLORIDE BY THE NASAL ROUTE. PART 2: TOCOPHEROL LATERAL DIFFUSION AND NEUROPROTECTIVE EFFECT EVALUATION</b>	<b>92</b>
5.1. Introduction	93
5.2. Materials and Methods	96
5.2.1. <i>Materials</i>	96
5.2.2. <i>Liposome Formulations and characterization</i>	96
5.2.3. <i>Cell culture and treatments</i>	97
5.2.4. <i>Determination of neuronal viability</i>	98
5.2.5. <i>Intracellular ROS formation</i>	99
5.2.6. <i>Assessment of Neuroprotection</i>	99
5.2.7. <i>Evaluation of <math>\alpha</math>-Tocopherol intermembrane transfer</i>	100
5.3. Results and discussion	101
5.3.1. <i>Effect of THA and loaded liposomes on neuronal viability</i>	101
5.3.2. <i>Effect of THA solution and loaded liposomes on intracellular ROS production</i>	104
5.3.3. <i>Assessment of Neuroprotection</i>	108
5.3.4. <i>Evaluation of Toc intermembrane transfer</i>	110
5.4. Conclusion	111
<b>6. CONCLUDING REMARKS</b>	<b>112</b>
<b>7. REFERENCES</b>	<b>114</b>

**ABBREVIATION**

---

A $\beta$	Amyloid- $\beta$ peptides;
AchEIs	Acetylcholinesterase inhibitors;
AD	Alzheimer's disease;
ANOVA	Analysis of Variance;
BACE1	$\beta$ -secretases;
BBB	Blood-Brain Barrier;
$\beta$ CD	$\beta$ -cyclodextrin;
BuChEIs	Butyrylcholinesterase inhibitors;
BSA	Bovine Serum Albumin;
Cho	Cholesterol;
CNS	Central Nervous System;
DLS	Dynamic Light Scattering;
DMEM	Dulbecco's modified Eagle's medium;
DSC	Differential Scanning Calorimetry;
DCFH-DA	2',7'-dichlorofluorescein-diacetate;
ENSPA	Ex-vivo Nasal Sheep Permeation Assay;
EPC	L- $\alpha$ -phosphatidylcholine from egg yolk;
ER	Electrical resistance;
FCS	Fetal calf serum;
FDA	United States Food and Drug Administration;
FT-IR	Fourier Transform Infrared spectroscopy;
HP $\beta$ CD	Hydroxypropyl $\beta$ -cyclodextrin;
MW	Molecular Weight;
NFTs	Intraneuronal Neurofibrillary Tangles;
nP	Albumin nanoparticles;
NMR	Nuclear Magnetic Resonance;
NRM	Nicotinic Receptor Modulator;
$\Omega$ 3	Eicosapentaenoic acid and Docosahexaenoic acid;
P	Permeability Coefficient;
P <sub>APP</sub>	Apparent Permeability Coefficient;
PBS	Phosphate Buffer Solution;
PCS	Photon-Correlation Spectroscopy;
PVPA	Phospholipid Vesicle based barrier Permeation Assay;
ROS	Reactive Oxygen Species;
SBE $\beta$ CD	Sulphobutylether $\beta$ -cyclodextrin;
TGA	Thermogravimetric analysis;
THA	Tacrine hydrochloride;
Toc	$\alpha$ -tocopherol;
USHNC	Uptake Studies in Human Neuronal Cell;

## ABSTRACT

---

Alzheimer's disease (AD) is a fatal neurodegenerative condition characterized clinically by progressive memory loss and irreversible cognitive deterioration. It has been shown that there is a progressive degeneration of the brain cholinergic neurons which leads to the appearance of cognitive symptoms of the disease. At present, there are no therapeutic interventions able to stop the progression nor to treat brain degeneration. Treatments are therefore aimed at slowing down the worsening course, maintaining, at least temporarily, the cognitive and behavioural symptoms, thus ensuring patients to have good or decent quality of life. One strategy to combat this disease is to increase cholinergic transmission; therefore acetylcholinesterase inhibitors have been developed including tacrine, rivastigmine and donepezil.

Tacrine hydrochloride (1,2,3,4-tetrahydro-9-aminoacridine mono hydrochloride) (THA), a potent, centrally active, reversible cholinesterase inhibitor, was the first drug approved by the United States Food and Drug Administration (FDA) in 1993 for treating the symptoms of mild to moderate Alzheimer disease. THA is available in the market as oral capsule dosage forms. Despite the favourable aqueous solubility, peroral administration of THA is associated with low bioavailability due to hepatic first-pass effect, short elimination half-life, gastrointestinal side effect and reversible dose-dependent hepatotoxicity, the major reasons for its withdrawal. Hence, alternative routes of administration for the centrally active acetylcholinesterase inhibitor tacrine may offer distinct advantages.

Drug delivery from the nose to the Central Nervous System (CNS) can be achieved via olfactory neuroepithelium and can involve paracellular (inter cellular spaces and tight junction), transcellular (passive diffusion, active transport and transcytosis) and/or neuronal transport. Moreover, the transport via trigeminal nerve system from the nasal cavity to CNS has also been described. THA delivery into CNS through intranasal route has been reported either in humans or animal models of Alzheimer's disease and its administration by intranasal route not only has been found useful for

circumventing the blood-brain barrier, but also for avoiding the hepatic first-pass effect, thus allowing lower dosage and side effects.

In this thesis THA delivery from the nose to the CNS was investigated using two multifunctional nanocarriers:

- ***Albumin nanoparticles*** carrying beta cyclodextrin and two different beta cyclodextrin derivatives (hydroxypropyl beta cyclodextrin and sulphobutylether beta cyclodextrin). Bovine serum albumin nanoparticles were obtained using a coacervation method, followed by thermal cross-linking, starting from protein solution at alkaline pH. After preparation, nanoparticles were loaded by soaking from solutions of tacrine hydrochloride and lyophilized. Thermal analysis (Differential Scanning Calorimetry and Thermogravimetric analysis) supported by Fourier Transform Infrared Spectroscopy were performed in order to confirm protein cross-linking in nanosphere structure and possible drug/carrier interaction occurred after the loading process. Moreover, size, polydispersity, zeta potential and morphology of the nanoparticles were investigated as well as drug loading, mucoadhesion properties and *ex-vivo* drug permeation ability. Results indicate that all the nanoparticles presented a mean size and a polydispersity lower than 300 nm and 0.33 respectively, were spherical shaped and negatively charged even after drug loading. Moreover, the presence of the different beta cyclodextrins in the polymeric network affected drug loading and could differently modulate nanoparticle mucoadhesiveness and drug permeation behaviour.
- ***Multifunctional liposomes***, prepared using traditional excipients (cholesterol and phosphatidylcholine), partly enriched with  $\alpha$ -tocopherol (Toc) and/or polyunsaturated fatty acids (eicosapentaenoic acid and docosahexaenoic acid) ( $\Omega$ 3). The aim with these special ingredients was to increase drug bioavailability, possibly due to enhanced liposome fusion with mucosal epithelial cells and, at the same time, to improve the therapeutic effect due to their antioxidant and anti-inflammatory properties. Here, several liposome formulations were prepared using the reverse phase evaporation technique followed by membrane filter extrusion. In particular, liposome capacity to enhance drug permeation was evaluated by means of different assays: Ex-vivo Nasal Sheep Permeation Assay

(ENSPA), Phospholipid Vesicle based barrier Permeation Assay (PVPA) and Uptake Studies in Human Neuronal Cell (USHNC). All liposome formulations showed a mean diameter in the range of 175 nm to 219 nm with polydispersity index lower than 0.22, a lightly negative zeta potential and excellent encapsulation efficiency. Moreover, along with good mucoadhesive properties, liposomes containing Toc and  $\Omega 3$  showed markedly increased tacrine permeability which may be due to fusion of liposomes with cellular membrane, a hypothesis, which is also supported by cellular uptake studies. Multifunctional liposomes have high potential as new systems for CNS-delivery of anti-Alzheimer drugs via the nasal route. In the last part of the thesis are reported the antioxidant and neuroprotective properties of our multifunctional liposomes. Particularly, liposome formulations and THA solution at different concentrations were tested to evaluate possible neurotoxicity, neuroprotection, antioxidant effect and reduction of ROS production in the neurons, using human neuronal cell line SH-SY5Y. The MTT assay confirmed the non-toxicity of all liposome formulation. Caspase-3 test showed that the formulations containing Toc and especially those containing both Toc and  $\Omega 3$  presented markedly neuroprotective effect, reducing the activation of apoptosis initiator enzyme (caspase 3), after treatment with hydrogen peroxide. The intracellular ROS generation (in neurons) was investigated using the 2',7'-dichlorofluorescein-diacetate (DCFH-DA) as a well-established compound to detect and quantify intracellular produced  $H_2O_2$ . Also in this case, liposomes containing Toc and  $\Omega 3$  showed a better activity than other formulations. In conclusion, liposomes enriched with Toc and  $\Omega 3$  presented the best permeation profile and antioxidant activity, even when compared to liposomes containing Toc alone. To explain this behaviour, Tocopherol intermembrane transfer was evaluated confirming that  $\Omega 3$  can enhance the intermembrane Toc diffusion.

## THEORETICAL SECTION



*The Thinker (A. Rodin 1902, Musée Rodin, Paris)*

## 1. AN OVERVIEW ON ALZHEIMER'S DISEASE

---

Alzheimer's disease (AD) the most common form of dementia among older people, it is characterized by the breakdown of connections between neurons and their eventual death [1]. AD is taking on the contours of a global epidemic, latest estimates tell us that more than 35 million people worldwide are living with dementia. Unless we can change the course of this disease, this number is expected to double by 2030 and more than triple by 2050. Has been reported in the Journal of Alzheimer's association that in the United States [2], AD is the sixth leading cause of all deaths and is the fifth leading cause of death in Americans aged 65 years. An estimated 5.4 million Americans have AD; every 69 seconds, someone in America develops AD; by 2050, the time is expected to accelerate to every 33 seconds. Over the coming decades, the baby boom population is projected to add 10 million people to these numbers. In 2050, the incidence of AD is expected to approach nearly a million people per year, with a total estimated prevalence of 11 to 16 million people. Dramatic increases in the numbers of "oldest-old" (those aged 85 years) across all racial and ethnic groups will also significantly affect the numbers of people living with AD. In 2010, nearly 15 million family and other unpaid caregivers provided an estimated 17 billion hours of care to people with AD and other dementias, a contribution valued at more than \$202 billion. Medicare payments for services to beneficiaries aged 65 years with AD and other dementias are almost 3 times higher than for beneficiaries without these conditions. Total payments in 2011 for health care, long-term care, and hospice services for people aged 65 years with AD and other dementias are expected to be \$183 billion (not including the contributions of unpaid caregivers) [3].

This heterogeneous, progressive disease of the central nervous system still is of unknown etiology with the exception of the rare familial cases of autosomal-dominant inheritance of gene defects. The two main types of AD currently

recognized are a generally later-onset sporadic form, representing about 95% of all cases, and autosomal-dominant familial forms involving specific mutations in one of three genetic loci (APP, presenilin 1, and presenilin 2) and typically associated with the early-onset of AD symptoms. Neuropathological examination of the AD brain shows the presence of characteristic markers such as intraneuronal neurofibrillary tangles (NFTs) composed of hyperphosphorylated tau protein and senile plaques, which are due to the deposition of amyloid- $\beta$  peptides ( $A\beta$ ), derived from the altered cleavage, operated by  $\beta$ - and  $\gamma$ -secretases, on the  $A\beta$  precursor protein (APP), resulting in over production and aggregation of neurotoxic forms of  $A\beta$ . The relationships between  $A\beta$  and the pathogenesis of the disease seems well established. In fact,  $A\beta$  aggregates are neurotoxic and also promote the hyperphosphorylation of tau protein, thus causing before neuronal dysfunction and subsequently neuron death [4-6].

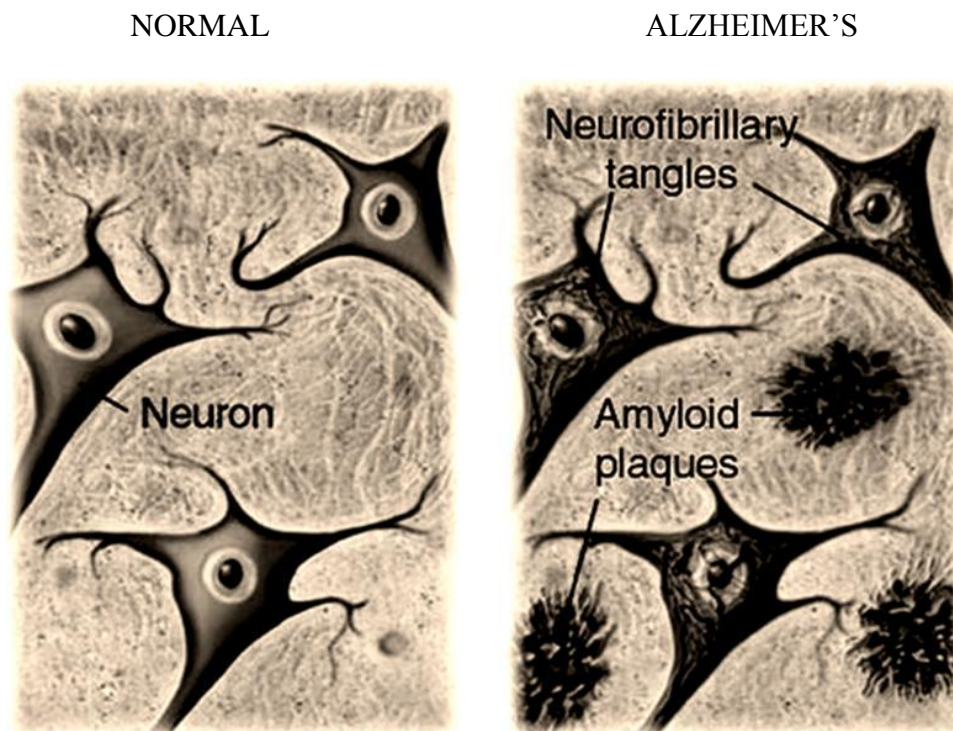


**Fig. 1.1** Alzheimer's hallmarks © 2000 - 2012 American Health Assistance Foundation

Moreover, the possibility that soluble forms of  $A\beta$ , including protofibrils and oligomers, may also be more toxic than  $A\beta$ , has recently been taken into account. In

fact, the presence of soluble A $\beta$  increases the caspases activation [7]. Caspases are a family of serine-aspartyl proteases whose activation normally leads to cell apoptosis. Caspases are involved in the cleavage of numerous proteins, including APP, presenilin (PS1, PS2) and tau [8,9], which, as mentioned above, are involved in AD. Recently, has been shown that their activation does not necessarily conduct neurons to the apoptosis process; in fact, caspases can be activated for long time without neuronal death [10] carrying out their deleterious actions on neurons and promoting the AD progression [5]. Based on these notions, oxidative stress (OS) is increasingly taking a key role in the pathogenesis and progression of several neurodegenerative disorders including AD. OS and A $\beta$  are closely intertwined; particularly, OS increases the production of A $\beta$  [11], due to the increase of  $\beta$ -secretase,  $\gamma$ -secretase

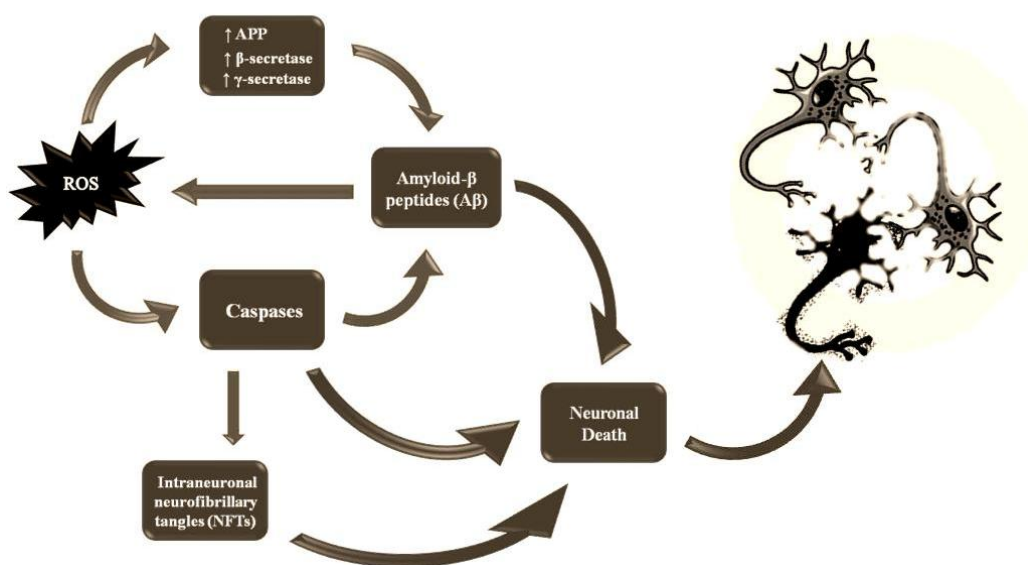


**Fig. 1.2 Implication of the ROS in the pathogenesis of AD**

and APP protein expression and activity [12], and A $\beta$  promotes OS in-vivo and in-vitro [13], creating a vicious cycle that forwards the disease (Fig. 1.2). In addition, is

well known that reactive oxygen species (ROS) activate the caspases with everything that goes with it.

One of the first clinical manifestations of AD include the gradual progression of cognitive impairment affecting multiple domains. The clinical hallmark of AD includes the impaired recent memory like difficulty learning new information; moreover, it can also occur disturbances in language, apraxia, mental confusion, behavioural changes and loss of executive control functions such as insight and judgment[14]. Despite the causes of this disease are still obscure, it is seen that the cognitive impairment is closely related to a destruction of cholinergic neurons and a deficiency of acetylcholine (ACh) at the level of the hippocampus a structure of the brain essential for memory and learning “cholinergic hypothesis”. Regarding the decrease in central cholinergic activity has been given the most attention for the treatment of disease; in fact, the initial pharmacologic strategy for AD is focused on increasing cholinergic transmission in the brain[15]. Among different strategies employed to increase synaptic levels of ACh, there is the inhibition of the neurotransmitter degradation, using acetylcholinesterase inhibitors (AChEIs) or butyrylcholinesterase inhibitors (BuChEIs), this last enzyme is a minor constituent in normal brains but in the brains of AD patients is increased in association with plaques and tangles, so its inhibition is very important to improve cholinergic transmission. Among the cholinesterase inhibitors approved, there are tacrine hydrochloride (tacrine) and rivastigmine tartrate (rivastigmine) that act on both AChE and BuChE, donepezil hydrochloride (donepezil ) which instead inhibits only AChE and galantamine hydrochloride (galantamine) that besides the acetylcholinesterase inhibitor activity has also an allosteric nicotinic receptor modulator (NRM) activity, which has been shown to stimulate the presynaptic release of acetylcholine and other neurotransmitters in laboratory preparations. In addition to cholinergic hypothesis has been recently highlighted the implication of excitatory neurotransmitter glutamate in the pathogenesis of AD; on the basis of this, has been inserted in the pharmaceutical treatment of the disease also the class of NMDA antagonist, of which the only commercially available drug is the memantine hydrochloride (memantine). Neuropharmacologic and pharmacokinetic properties of the currently available anti-Alzheimer drug are summarized in Table 1.1.

**Table 1.1 Anti-Alzheimer drug available on the market [15]**

	<b>Tacrine (Cognex®)</b>	<b>Donepezil (Aricept®)</b>	<b>Rivastigmine (Exelon®)</b>	<b>Galantamine (Razadyne®) (RazadyneER®)</b>	<b>Memantine (Namenda™)</b>
<b>Manufacturer/ Distributor</b>	West-Ward Horizon	Eisai Pfizer	Novartis	Janssen Shire	Merz Forest
<b>Mechanism(s)</b>	AChEI, BuChEI	AChEI	AChEI, BuChEI	AChEI, NRM	NMDA antagonist
<b>Dose Forms (mg)</b>	10, 20, 30, 40	5, 10	1.5, 3, 4.5, 6	4, 8, 12 4mg/ml 8, 16, 24	5, 10
<b>Dose Frequency</b>	4x /day	1x /day	2x /day	2x /day 1x /day	2x /day
<b>Serum T<sub>1/2</sub> (hrs)</b>	1.3 – 2	70	2 – 8	6 – 8	60 – 80
<b>Dose Range</b>	40 – 160 mg/d	5 – 10 mg/d	3 – 12 mg/d	8 – 24 mg/d	5 – 20 mg/d
<b>Target Dose</b>	80 – 160 mg/d	5 – 10 mg/d	6 – 12 mg/d	16 – 24 mg/d	10 – 20 mg/d
<b>Dose Titration</b>	6 wks.	4 – 6 wks.	4 – 6 wks.	4 wks.	1 wk.
<b>Metabolism</b>	CYP1A2	CYP2D6, 3A4	Non-hepatic	CYP2D6,3A4	Non-hepatic
<b>Protein-binding</b>	75%	96%	40%	18-19%	45%

	<b>Tacrine (Cognex®)</b>	<b>Donepezil (Aricept®)</b>	<b>Rivastigmine (Exelon®)</b>	<b>Galantamine (Razadyne®) (RazadyneER®)</b>	<b>Memantine (Namenda™)</b>
<b>Taken with food</b>	Yes	Not necessary	Yes	Yes	Not necessary
<b>Hepatotoxicity</b>	Yes	No	No	No	No

**Table 1.1 Continued**

These drugs do not stop the evolutionary process of the disease but are only able to determine the significant improvement of cognitive performance and a gradual slowing of the functional deficit, but their side effects often require discontinuation of treatment. For this reason, today, many studies are directed to the search for new pharmacological approaches to allow, either alone or in combination with the cholinesterase inhibitors, to obtain a better clinical response. Moreover, in recent years, increasing attention has been reserved to the formulation of innovative pharmaceutical systems, and to the investigation of administration routes, alternatives to the oral route, which serves to improve the performance of drugs already in use. Moreover, considering the key role of oxidative stress in the pathogenesis and progression of the disease, it would be deliverable to combine the approved AD therapy with the treatment of the OS.

Finally, during the past several years, we have witnessed enormous growth in scientific information regarding AD. To this point, however, little of this information has been translated into effective treatments. The future goal of the scientific research is to join together all the knowledges acquired. In fact, AD is a multifactorial disease and then must be addressed with a multidisciplinary strategy, uniting to drug discovery the development of new pharmaceutical systems capable to delivery the active molecules directly into Central Nervous System (CNS), increasing the therapeutic efficacy and at the same time reducing side effects.

## 2. INTRANASAL DRUG DELIVERY

Though great progress have been achieved regarding our understanding of the pathogenic basis of neurological disease, there are only a small number of effective drugs for treating these diseases. Every day new potentially active molecules are synthesized but they are discarded for their toxicity or low bioavailability. In fact, the main limitation for a drug active on the central nervous system (CNS) is precisely to carry it in the CNS, that as well known is overprotected by the blood-brain barrier (BBB) (Fig. 2.1) that segregates the brain interstitial fluid from the circulating blood. In particular, BBB histological morphology comprises two plasma membranes in series, separated by about 0.3  $\mu\text{m}$  of endothelia cytosol [16]. This barrier ensures the interface between the cerebral capillaries and the brain tissue over a surface of

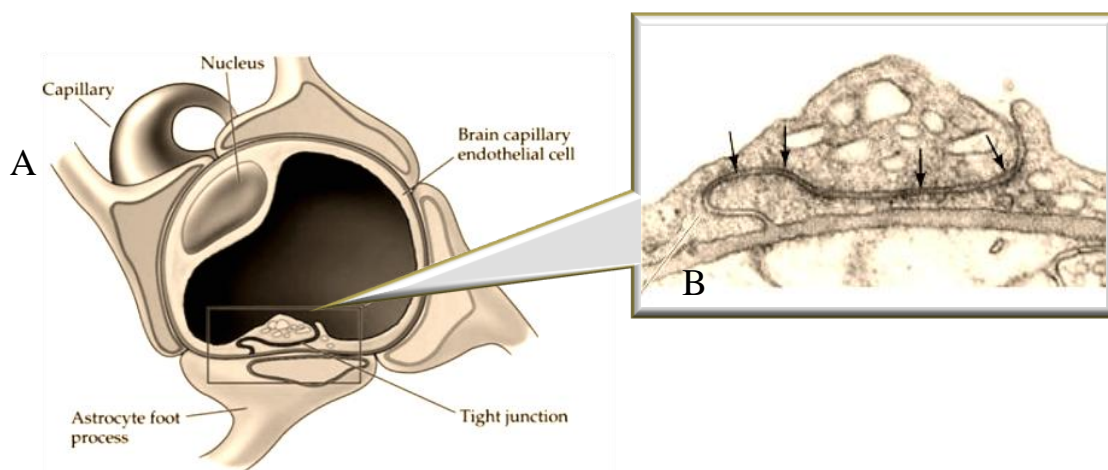


**Fig. 2.1 Blood-Brain Barrier (BBB).** (A) Diagram of a brain capillary in cross section and reconstructed views, showing endothelial tight junctions and the investment of the capillary by astrocytic end feet. (B) Electron micrograph of boxed area in (A), showing the appearance of tight junctions between neighboring endothelial cells (arrows). A from Goldstein and Betz, 1986; B from Peters et al., 1991.

interface of about 12  $\text{m}^2$  [17]. The cells of the capillary endothelium are closely connected via intercellular connections; the tight junctions that act as zips closing the

inter-endothelial pores that normally exist in endothelial membranes, resulting in a greater transendothelial electric resistance (1500-2000  $\Omega\cdot\text{cm}^2$ ) compared to that of other tissues like skin, bladder, colon, lungs (3-33  $\Omega\cdot\text{cm}^2$ ) [18]. This makes the blood–brain barrier resistant to the free diffusion of molecules across the membrane and prevents most molecules from reaching the CSN from the blood stream. Less than 2% of all small-molecule drugs, and virtually no large-molecule drugs can cross the BBB. The obstacle imposed by those brain protective mechanisms has increased the interest in developing strategies to overcome them when brain drug exposure is required[19].

Recently, much interest has been given to the exploitation of the nasal route for delivery of drugs, a lot of excellent reviews have been published examining in detail some particular aspects concerning to potential therapeutic applications of intranasal route of drug delivery [20-23]. Indeed, intranasal administration offers a variety of attractive options for local and systemic delivery of several drugs (Table 2.1). The nasal mucosa is richly vascularized and provides a series of unique attributes, all of which may help to maximize the patient’s safety, convenience and compliance. The nasal mucosa is, compared to other mucous membranes, easily accessible and provides a practical entrance portal for small and large molecules.

**Table 2.1 Advantages and limitations of intranasal administration [24]**

Nasal administration	
ADVANTAGES	LIMITATIONS
Drug degradation that is observed in the gastrointestinal tract is absent.	The histological toxicity of absorption enhancers used in nasal drug delivery system is not yet clearly established.
Hepatic first pass metabolism is avoided. Rapid drug absorption and quick onset achieved.	Relatively inconvenient to patients when compared to oral delivery systems since there is a possibility of nasal irritation.
The bioavailability of larger drug molecules can be improved by means of absorption enhancer or other approach.	Nasal cavity provides smaller absorption surface area when compared to GIT.

The nasal bioavailability for smaller drug molecules is good. Drugs that are orally not absorbed can be delivered to the systemic circulation by nasal drug delivery.	There is a risk of local side effects and irreversible damage of the cilia on the nasal mucosa, both from the substance and from constituents added to the dosage form.
Studies so far carried out indicate that the nasal route is an alternate to parenteral route, especially, for protein and peptide drugs.	Certain surfactants used as chemical enhancers may disrupt and even dissolve membrane in high concentration.
Convenient for the patients, especially for those on long term therapy, when compared with parenteral medication.	There could be a mechanical loss of the dosage form into the other parts of the respiratory tract like lungs because of the improper technique of administration.
Drugs possessing poor stability in g.i.t. fluids are given by nasal route.	
Polar compounds exhibiting poor oral absorption may be particularly suited for this route of delivery.	

---

Intranasal administration offers a rapid onset of therapeutic effects, no first-pass effect, no gastrointestinal degradation or lung toxicity, non invasiveness, essentially painless application, and easy and ready use by patients. In addition, due to the olfactory region of nasal mucosa, drugs can be directly transported to the brain. It was realised that the olfactory region is mayor site for entry viruses into the brain, to confirm this Shoshkes Reiss C. et al [25] inoculated on mice nasal epithelium, vesicular stomatitis virus; they reported as virus was transmitted along the olfactory nerve to the CNS within 12 h. Drug delivery into CNS through intranasal route has been reported [26-29] either in humans or animal models of Alzheimer's disease [30-31], brain tumours [32-33], epilepsy [34], pain [35] and sleep disorders [36]. Has been reported in literature that the drug uptake into the brain from the nasal mucosa mainly occurs via three different pathways (Fig. 2.2):

- Systemic pathway by which part of the drug is absorbed into the systemic circulation subsequently reaches the brain by crossing the BBB;

- Olfactory pathway
- Trigeminal neural pathway

Drugs through olfactory and trigeminal pathways travels from the nasal cavity to cerebrospinal fluid (CSF) [37].

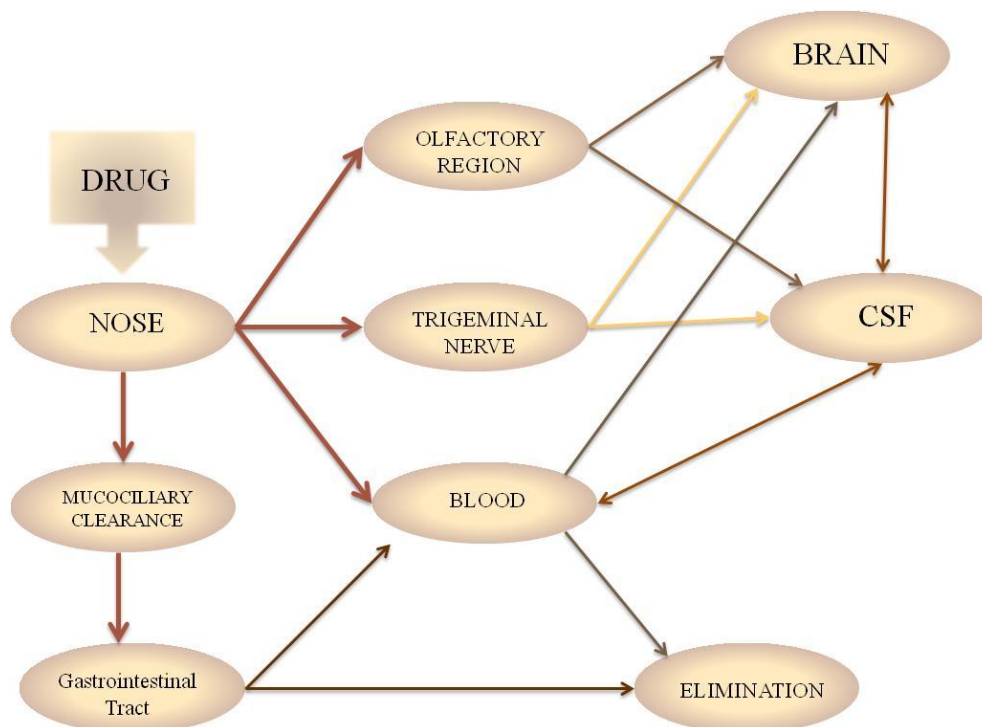


**Fig. 2.2 Brain drug uptake through different pathways after intranasal administration**

The drug can cross the olfactory path by one or a combination of mechanisms. These include transcellular or simple diffusion across the membrane, paracellular transport via movement between cells and transcytosis by vesicle carriers.

## 2.1. Nasal anatomy and physiology

The primary functions of the nasal cavity in humans and animals are breathing and olfaction. The structure and function of this cavity are related to the resonance of produced sounds, filtration of particles, mucociliary clearance, immunological activities and heating humidification of the inspired air before it reaches the lung [38]. In order to accomplish drug delivery to CNS, the drugs have to efficiently permeate across the nasal mucosa. For effective administration of drugs through the nasal route, its anatomical and physiological features must be concomitantly taken into consideration in designing delivery system for the CNS. Therefore, an understanding of the anatomy and physiology of nasal mucosa is imperative [39]. The nasal cavity is subdivided along the centre into two halves by the nasal septum.

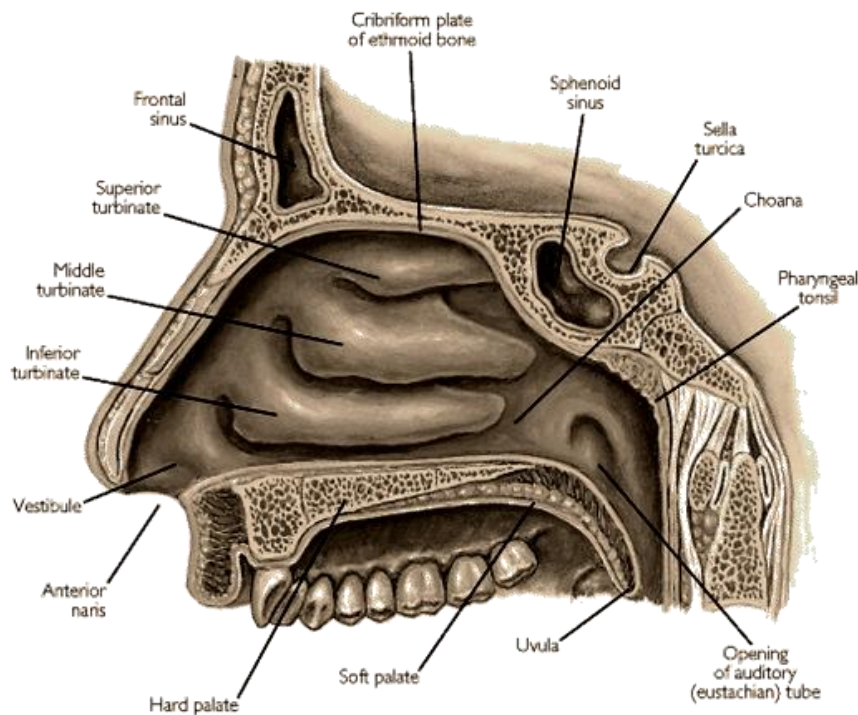


**Fig. 2.3** Section of the human nasal cavity, from SEER's web based Training Module [SEER, 2007, [http://training.seer.cancer.gov/module\\_anatomy/images/illu\\_nose\\_nasal\\_cavities.jpg](http://training.seer.cancer.gov/module_anatomy/images/illu_nose_nasal_cavities.jpg)]

The two cavities open to the facial side through the anterior nasal apertures and to the rhinopharynx via the posterior nasal apertures and each of two nasal cavities can be subdivided into different regions: nasal vestibule, inferior turbinate, middle turbinate,

superior turbinate, olfactory region, frontal sinus, sphenoidal sinus, and cribriform plate of ethmoid bone (Fig. 2.3). The total surface area of the nasal cavity in human adult is about 150 cm<sup>2</sup> and total volume is about 15 ml. The olfactory region in men covers an area of about 10 cm<sup>2</sup> and is positioned on superior turbinate on opposite septum. The respiratory region contains three nasal turbinates: superior, middle, and inferior which project from the lateral wall of each half of the nasal cavity. The presence of these turbinates creates a turbulent airflow through the nasal passages ensuring a better contact between the inhaled air and the mucosal surface. The nasal epithelial membrane provides a significant barrier to the free diffusion of substance across them [40-42]. The presence of tight junction between neighboring epithelial cells cancels the free diffusion of hydrophilic molecules through the epithelium via paracellular route. Tight junctions are located at the boundary between apical and basolateral domains in epithelial cell periphery. The structure and function of this cavity are related to the resonance of produced sounds, filtration of particles, mucociliary clearance, immunological activities and heating humidification of the inspired air before it reaches the lung [38].

### ***2.1.1. Respiratory region***

The respiratory region is the largest, it is considered as the major site for drug absorption into systemic circulation having the highest degree of vascularity, it consists of an epithelium resting on a basement membrane and a lamina propria [43]. The anterior part of respiratory region covered with squamous epithelium, which changes to transitional epithelium and converts in the posterior part of the cavity to a pseudostratified columnar epithelium. The pseudostratified epithelium, also named the respiratory epithelium, consists of four dominated cell types; ciliated columnar cells, non-ciliated columnar cells, goblet cells and basal cells (Fig. 2.4). The basal cells are situated on the basal membrane and don't extend to the apical epithelial surface, as do the other three cell types. It is also rich in dendritic cells important for local immune response (IgA). A total of 15-20 % of the respiratory cells covered by

layer of long cilia of size 2-4  $\mu\text{m}$ . The cilia move in coordinated way to propel mucus across the epithelial surface towards the pharynx [41]. The respiratory cells are also covered by about 300 microvilli per cells. Mucus layer consists of low viscosity sol layer that surrounds the cilia and a more viscous gel layer forming a layer on the top of the sol layer and covering the tips of the cilia. The epithelial cells are closely

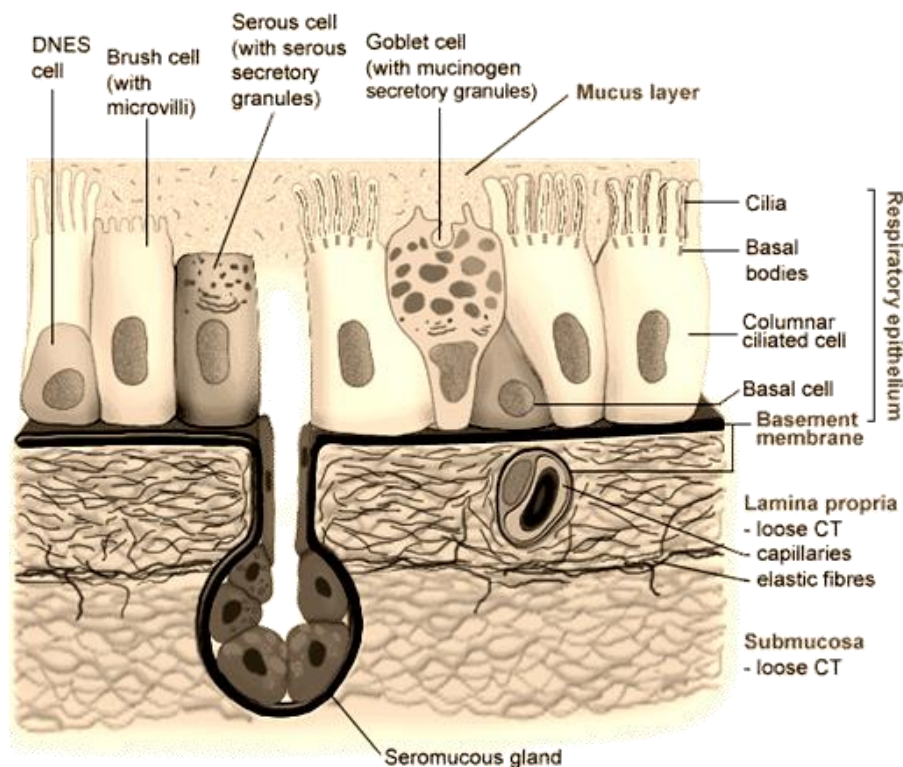


**Fig. 2.4** The respiratory epithelium is covered by a mucus layer (gel and sol layer) and the cell types arising from the basement membrane are: ciliated and non-ciliated cells (with microvilli), goblet cell, and basal cell. Modified from *Histology of the Respiratory System* McGill Molson Medical Informatics Project (Dr Morales) <http://alexandria.healthlibrary.ca>

connected on apical surface, surrounded by intercellular junction whose specialized sit and structural components are commonly known as junction complex [22, 40]. Its is innerved by trigeminal nerves, which enter the brain both through the pons and separately through the cribioform plate under the olfactory bulbs [44].

### 2.1.2. Olfactory region

The olfactory region is situated between the nasal septum and the lateral walls of each of the two nasal cavities and just below the cribriform plate of the ethmoid bone separating the cranial cavity from nasal cavity. In men, the epithelium is restricted to a small area in the roof of the nasal cavity of about 10 cm<sup>2</sup> as compared to an area of about 150 cm<sup>2</sup> in dogs, which reflects the major importance of the sense of smell to the dog [40]. The olfactory epithelium is innervated by olfactory nerves (Fig. 2.5) which is responsible for the transport of drugs from nasal cavity to the CNS along the intraneuronal/extraneuronal olfactory pathway region provides a potential advantage

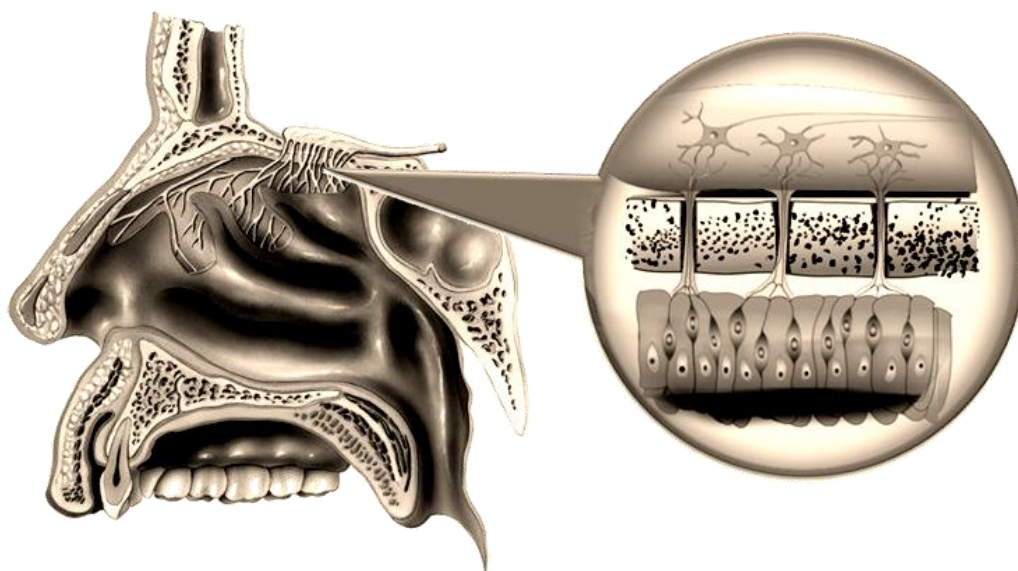


**Fig. 2.5 Diagram of the olfactory area showing the olfactory epithelium, bulb and tract. Modified from Adams et al. (1989).**

where a drug may be exposed to neurons that may be facilitated it across into cerebro-spinal fluid when administered intranasally [38, 41]. Various studies in animal models have conformed that, at early time points after nasal administration, the concentration of cocaine in the brain was higher after nasal administration than after intravenous injection, thereby showing the existence pathway from nose to brain [45]. Fehm et al. reported a significant accumulation of insulin In cerebrospinal fluid after a single administration of 40 IU insulin, whereas no increase was seen in insulin plasma levels [46]. It should be stressed that the blood supply to the nasal

mucosa is pertinent with regards to systemic drug delivery. The arterial blood supply to the nasal cavity is derived from both the external and internal carotid arteries. The terminal branch to the maxillary artery supplies the sphenopalatine artery, which in turn supplies the sphenopalatine artery, which in turn supplies the lateral and medial wall of the nasal chamber. The anterior and posterior ethmoid branches come from the ophthalmic artery, which is a branch of carotid artery. These vessels supply the anterior portion of the nose. The veins of the nasal cavity drain into the sphenopalatine foramen and then into sphenopalatine foramen pterygoid plexus [47].

### ***2.1.3. Nasal secretion***

The epithelium in a clean, non-infected, non-allergic and non-irritated nose is covered by a mucus layer, which is secreted by goblet cells and serous glands in the nasal mucosa and sub-mucosa [38]. About 90-95% of mucus layer consists of water with electrolyte, serum protein, immunoglobulins and lipids; while 3% consists of mucin [48]. The mucus moved through the nose at an approximate rate of 5 to 6 mm/min, so is renewed every 10 to 15 minutes. The nasal mucus performs a number of physiological functions; is including physically and enzymatically protection, water-holding capacity; permits efficient heat transfer and acts as adhesive and transports particulate matter towards the nasopharynx [49]. The average pH in the anterior of the nose is 6.40; while, the pH in the posterior of the nasal cavity is 6.27 [50]. Generally, the normal pH of the nasal secretions in adult ranges from 5.5-6.5, whereas in infants and young children it ranges from 5.0- 6.7 [38]. A change in the pH of mucus can affect the ionization and thus increases or decreases the permeation of drug, depending on the nature of the drug. The effect of altering nasal pH on the absorption of certain drugs has been studied in animals and animal models. Morimoto et al. demonstrated in rat an enhanced absorption of vasopressin by a reduction in pH; it should be noted however that, this pH reduction caused an adverse effect on ciliary beat [51].

## 2.2. Factors influencing the absorption of drugs across the nasal epithelium

Drug delivery from the nose to the CNS can be achieved via olfactory neuroepithelium and can involve paracellular (inter cellular spaces and tight junction), transcellular (passive diffusion, active transport and transcytosis) and/or neuronal transport. The factors influencing nasal absorption are related to nasal physiology, the physico-chemical characteristics of the compound and the properties of specific drug formulation [52] (Fig. 2.6).

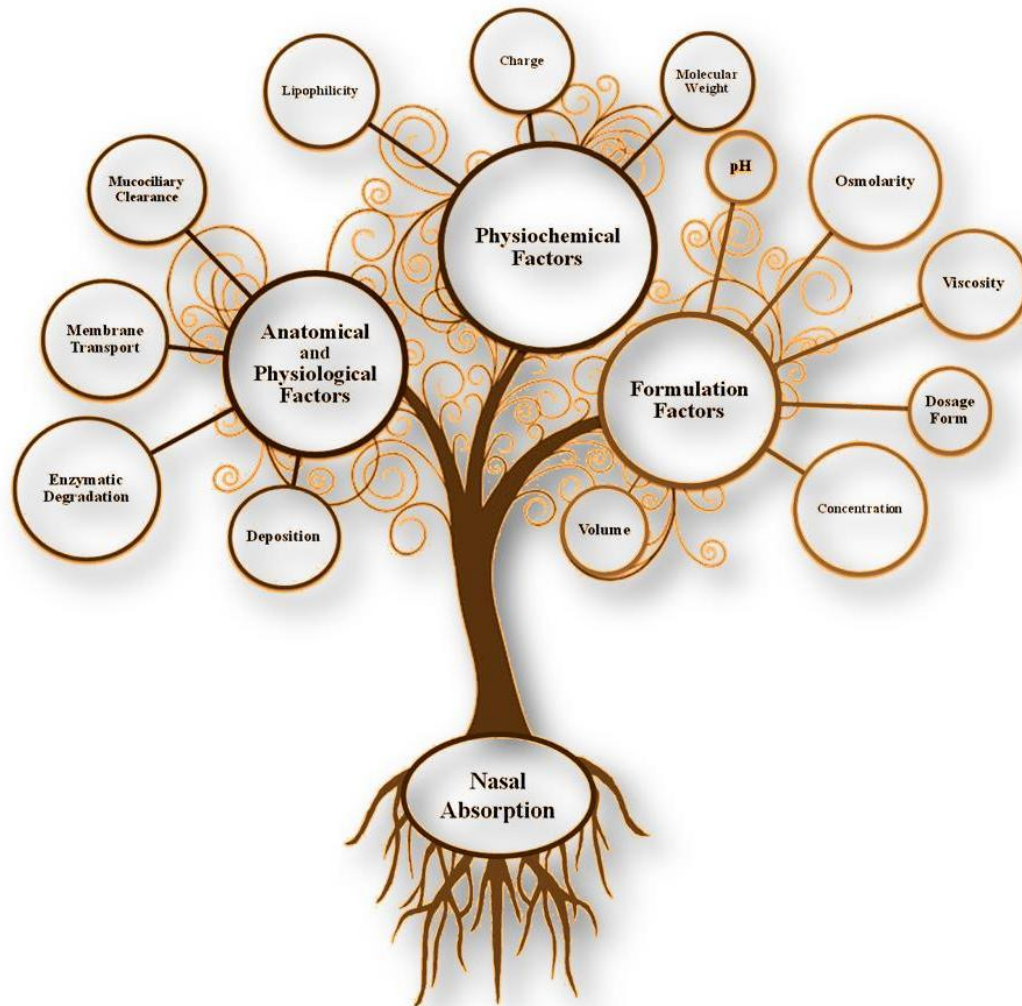


**Fig. 2.6 Factor influencing nasal absorption. The three main factors are: Anatomical and Physiological nasal characteristics, drug Physicochemical properties and the characteristics of the Formulations.**

### **2.2.1. Physiological barrier**

The nasal mucociliary clearance system transports the mucus layer that covers the nasal epithelium towards the nasopharynx by ciliary beating. Its function is to protect the respiratory system from damage by inhaled particulate and substances. Impairment of nasal mucociliary clearance can result in diseases of the upper airways. One of the functions of the upper respiratory tract is to prevent noxious substances (allergens, bacteria, viruses & toxin) from reaching the lungs. Generally, when such materials adhere to, or dissolve in the mucus lining of the nasal cavity, they were transported towards the nasopharynx for eventual discharge into the gastrointestinal tract. Clearance of this mucus and the adsorbed/dissolved substances into the gastrointestinal tract is called the mucociliary clearance (MCC) [49]. Nasal clearance proceeds at average rate of about 5-6 mm/min [38]. With a beat of ~ 100 stokes per min, the cilia transport the mucus with speed of 5 mm/min and formulations administered on the human respiratory epithelium has been found to be cleared from the nasal cavity with half-life of clearance of about 20 min. Nasal mucociliary clearance also has implications for nasal drug absorption. Drugs are cleared rapidly from the nasal cavity after intranasal administration, so it is important a fast systemic drug absorption. Several strategies are discussed to increase the residence time of drug formulations in the nasal cavity, resulting in improved nasal drug absorption [53]. Indeed, reducing the mucociliary clearances increases the time of contact between a drug and the mucus membrane and subsequently enhances drug permeation; vice versa increasing mucociliary clearances decreases drug permeation. Therefore, strategies to increase the nasal bioavailability of drugs that are poorly absorbed from the nasal mucosal can be aimed either at increasing the nasal membrane permeability or by decreasing the mucociliary clearance rate [54]. Zaki N.M. et al. developed a mucoadhesive in situ gel reducing nasal mucociliary clearance and improving the bioavailability of the antiemetic drug, metoclopramide hydrochloride. Definitely, the prolong contact time has been attributed to the rheological properties of the formulation, which reduce or delay its clearance from the mucosa and may result in specific interactions of the polymer in the gel with mucus components [55]. A large number of methods have been used to assess

mucociliary function, these methods study the mucociliary system whole (in-vivo) or as its separate components (in-vitro or ex-vivo) i.e., the ciliary activity and mucus layer [54].

Another important barrier to the drug nasal absorption is its enzymatic metabolism; in fact, though drugs administered nasally avoid first pass hepatic metabolism, there is a wide range of metabolic enzymes located in the nasal mucosa that may limit the bioavailability of some drugs, especially those containing peptides or proteins [56]. Nasal mucosa acts as an enzymatic barrier to the delivery of drug; indeed, has been reported the presence in substantial amounts in the nasal cavity of a large number of enzymes [57], which include:

- ❖ *Cytochrome P-450*: it was apparent that nasal tissue contained high levels of P-450 isozymes (10 forms) that very actively catalyzed the oxidation of certain substrates. Thus, the turnover rate (nanomoles of substrate per picomoles of P-450 per minute) for nasal microsomal, P-450-dependent aniline hydroxylation was six time higher than for liver Cytochrome P-450.
- ❖ *Aldehyde Dehydrogenases*: is a polymorphic enzyme responsible for the oxidation of aldehydes to carboxylic acids. The formaldehyde dehydrogenases are most abundant in olfactory mucosa, while acetaldehyde dehydrogenase activity is most abundant in the nasal respiratory tissue. Another interesting difference in the location of these enzymes is the presence of formaldehyde dehydrogenase in olfactory sensory cells, while aldehyde dehydrogenase is absent from those cells.
- ❖ *15-lipoxygenase*: is an enzyme that catalyzes the oxidation of arachidonic acid to yield 15-hydroperoxyarachidonate (15-HPETE) which is rapidly converted to 15-hydroxy-5,8,11,13-eicosatetraenoate (15-HETE). The 15-hydroperoxides are preferentially formed in neutrophils and lymphocytes. It was seen that this enzyme is more active in nasal epithelial cells than bronchial cells.
- ❖ *Alcohol Dehydrogenases*: are a group of dehydrogenase enzymes that facilitate the interconversion between alcohols and aldehydes or ketones with

the reduction of nicotinamide adenine dinucleotide (NAD<sup>+</sup> to NADH).  
 $\text{CH}_3\text{CH}_2\text{OH} + \text{NAD}^+ \rightarrow \text{CH}_3\text{CHO} + \text{NADH} + \text{H}^+$ .

- ❖ *Carboxylesterases*: is an enzyme that catalyzes the chemical reaction a carboxylic ester + H<sub>2</sub>O  $\rightleftharpoons$  an alcohol + a carboxylate. Carboxylesterase activities in the nasal cavity are among the highest of any activities found there, but little is known about the biochemistry of the nasal forms.
- ❖ *Epoxide Hydrolases*: also known as epoxide hydratase) functions in detoxication during drug metabolism. It converts epoxides to trans-dihydrodiols, which can be conjugated and excreted from the body. Metabolizes especially styrene oxide and benzo(a)pyrene-4,5-oxide. High levels of hydrolase activity with these substrates have been reported in rat nasal tissue. Safrole oxide hydrolase activity was reported to be higher in human nasal tissue than in rat nasal tissue.
- ❖ *UDP-Glucuronyl Trasferase*: is a glycosyltransferase that catalyzes addition of the glycosyl group from a UTP-sugar to a small hydrophobic molecule. This reaction is known as glucuronidation reaction. Activities of this UDP-glucuronyl transferase have been observed in the nasal tissues of the rat and of the dog. With 1-naphthol as the substrate, Gervasi and co-workers could not detect glucuronidation in human nasal respiratory tissue homogenates.
- ❖ *Glutathione S-Transferase(GTS)*: Are an enzyme family that catalyse the conjugation of reduced glutathione — via a sulfhydryl group — to electrophilic centers on a wide variety of substrates. This activity detoxifies endogenous compounds such as peroxidised lipids, as well as breakdown of xenobiotics. GSTs may also bind toxins and function as transport proteins, and, therefore, an early term for GSTs was “ligandin”. The mammalian GST super-family consists of cytosolic dimeric isoenzymes of 45–55 kDa size that have been assigned to at least six classes: Alpha, Mu, Pi, Theta, Zeta and Omega. Are present in high concentrations in both respiratory and olfactory epithelia. Glutathione S-transferase activity has been demonstrated in human nasal respiratory tissue by using 1-chloro-2,4-dinitrobenzene as the substrate. The activity in human nasal tissue was greater than that in rat nasal tissue.

- ❖ *Rhodanese*: is a mitochondrial enzyme that detoxifies cyanide (CN<sup>-</sup>) by converting it to thiocyanate (SCN<sup>-</sup>). This reaction is important for the decontamination of cyanide, since the thiocyanate formed is relatively harmless. The use of thiosulfate solution as an antidote for cyanide poisoning is based on the activation of this enzymatic cycle. The activity of this enzyme in the rat, cow and human nasal tissues is quite high, and its kinetics in both the rat and human suggests that an isozyme different from that in the liver may be present in the nasal cavity of both species.

Particularly, the nasal cytochrom P450-dependent monooxygenase system has been implicated in nasal metabolism of nasal decongestants, alcohol, nicotine and cocaine [58]. Histochemical, immunohistochemical, and biochemical localization of many nasal xenobiotic metabolizing enzymes indicate that these enzymes are often highly localized in specific tissues, cells, and portions of cells. Finally, the nasal cytochromes P-450, in contrast to those of the liver, are relatively resistant to induction but are easily inhibited. On the basis of this, the nasal route is still considered to be superior to the oral route. Various approaches have been used to overcome these degradations. These include the use of protease and peptidase inhibitors such as bacitracin, amastatin, boroleucin and puromycin, which have been reported to improve the absorption of many drugs [59].

### **2.2.2. *Physicochemical characteristics of the drug***

The physicochemical characteristics of the administered drug, which can influence nasal absorption, include molecular weight, solubility, dissolution rate, charge, partition coefficient, pKa, particle size and the presence of polymorphism [47]. Molecular weight (MW), size and lipophilicity or hydrophilicity play a key role in nasal drug permeation. Generally, the permeation of drugs less than 300 Da is not significantly influenced by the physicochemical properties of the drug, they can permeate through aqueous channels of the membrane (paracellular mechanism). On the contrary, for a large number of therapeutic agents including peptides and

proteins, which have MW larger than 1 kDa, bioavailability is low and can be directly predicted from knowledge of MW. In general, the bioavailability of these large molecules ranges from 0.5% to 5% [60], but can be increased formulating these molecule in combination with enhancer substances, which open the tight junctions. Other factors also can affect transport pathways are the pH and the osmolarity of the formulation; in fact, several authors have reported how modifying these two parameters in the formulation can increase the drug bioavailability [61]. Drug lipophilicity is one of the most important physicochemical characteristic that a drug has to possess to improve nasal permeability; in fact, though the nasal mucosa was found to have some hydrophilic characteristics, it appears that this mucosa are primarily lipophilic in nature and the lipid domain plays an important role in the barrier function of these membranes [62]. Generally, the permeation of the compound through nasal mucosa increases on increasing the lipophilicity. It should be noted however, that the lipophilicity is in contrast with the drug solubility in the aqueous medium. Whereas water represents the 95% of the nasal secretions, drug solubility is probably the most crucial factor in determining absorption through nasal mucosa. Poorly aqueous soluble drugs may require high doses, making this administration route impractical. The problem can be overcome by enhancing drug solubility using various techniques. Finally, tied to solubility there is the dissolution rate that is equally important; especially for particulate nasal products, administered as either powder inhalation or in the form of suspensions, where the dissolution rate becomes extremely important; in fact, particles deposited in the nostrils need to be dissolved prior to absorption, otherwise drug is moved away by mucociliary clearance without being absorbed.

### 2.3. Strategy to improve intranasal drug absorption

The poor nasal bioavailability of many substances (in particular, peptide and protein drugs) can be substantially improved by the use of absorption enhancer. The acceptability of these enhancer is not only dependent on their promoting effect but also on their safety profile for systemic and local adverse effects. Nasal drug formulations must not alter the histology and physiology of the nose in the sense that the mucosa must retain its functionality as a barrier toward external substances and microorganism. The histological toxicity refers to the alteration of mucosa, including membrane protein removal, cell loss, excessive mucus discharged, cytotoxicity, and disturbing of the normal enzymatic balance. In literature there is a lot of studies that reported the enhancing absorption effect of several substances [63-67]. Generally these substances act as enzyme inhibitors to overcome the enzymatic barrier and permeation enhancer to overcome the physical barrier opening the tight junctions, altering the properties of mucus layer, chelating  $Ca^{++}$  ions in the cell membranes, increasing membrane fluidity. It is possible also a combination of effects, Sayani and Chien listed several enzyme inhibitors the stabilized peptides and at same time enhanced permeation [68]. A classification of the major enhancer molecule used was reported by Ramesh [69]:

- ❖ **Surfactants (*Polyoxyethylene-9-lauryl ether (Laureth-9), Saponin*)**: Sajadi Tabassi SA reported a high reduction of the blood glucose levels following the nasal instillation of solutions containing insulin and *Acanthophyllum* total saponin [70]. The enhancing effect seems to be tied to a reduction in water surface tension; it should be noted however that this effect is also toxic; in fact, caused complete haemolysis of human red blood cells at a concentration of 250  $\mu\text{g/ml}$ .
- ❖ **Bile salts (*Trihydroxy salts (glycol- and taurocholate), Fusidic acid derivatives (STDHF)*)**: Sodium deoxycholate a typical bile salt was used in concentration of 1% to improve the bioavailability of dopamine in beagle dogs via nasal route, a 20% increase in bioavailability of dopamine has been obtained [71]. Several other studies indicate that bile salts can prove to be good optimizers in nasal drug

products. Fusidate derivatives show similar physical and chemical properties to the bile salts, and so have been suggested to enhance absorption in a similar manner. Deurloo MJ described an excellent nasal absorption of insulin due to the enhancing effect of Sodium taurodihydrofusidate (STDHF); particularly, the fusidate derivative at 1% (w/v) enhanced nasal insulin bioavailability from 0.9 to 5.2% and from 0.3 to 18.0% in rabbits and rats, respectively. Emerged so that STDHF is a potent enhancer of nasal insulin absorption, probably both by facilitating insulin transport through the nasal mucosa and possibly also by inhibiting enzymatic degradation [72]. To quantify the toxicity of these substances, Zezhi Shao et al. investigated in nasal rat the protein and enzyme release following the administration of four bile salts, one fusidate derivative [73]. Deoxycholate (NaDC) was found to possess the maximum protein solubilizing activity, followed by taurodihydrofusidate (STDHF), cholate, glycocholate (NaGC), and taurocholate (NaTC) in a descending order.

- ❖ **Chelators (*Salicylates, Ethylenediaminetetraacetic acid (EDTA)*):** It was seen that the mechanism of action of ethylene-diamine-tetraacetic acid (EDTA) includes depletion of  $\text{Ca}^{2+}$  from tight junctional areas, thus allowing the junctions to open. In fact, the integrity of the tight junctions, which may be seen as barriers to the paracellular diffusion of molecules, is dependent on extracellular  $\text{Ca}^{2+}$ . The effect of EDTA on nasal absorption was studied, results showed a promoting effect of EDTA on absorption of fluorescein isothiocyanate-dextran with various molecular weights after nasal administration to [74].
  
- ❖ **Fatty acid salts (*Oleic acid, Caprylate (C8), Caprate (C10), Laurate (C12)*), Phospholipids (*Lysophosphatidylcholine (lyso-PC), Didecanoyl – PC*):** Saturated (for example, lauric, myristic and capric acid) and unsaturated fatty acids (for example, oleic acid, linoleic acid and linolenic acid) have penetration enhancing property of their own and they have been studied since a long time. Fatty acid esters such as ethyl or methyl esters of lauric, myristic and oleic acid have also been employed as the oil phase of emulsion. Tugrul T. Kararli evaluated the enhancing effect of the oleic acid/monolein emulsion on the nasal

absorption of *O*-(*N*-morpholino-carbonyl-3-*L*-phenylaspartyl-*L*-leucinamide of (2*S*,3*R*,4*S*)-2-amino-1-cyclohexyl-3,4-dihydroxy-6-methylheptane, a renin inhibitor; in comparison with a control PEG 400 solution. Results highlighted that the percent absolute bioavailability of the compound was enhanced from 3–6% (PEG 400 solution) to 15–27% when the emulsion formulations were used [75]. The phospholipid didecanoylphosphatidylcholine (DDPC) has shown absorption-enhancing properties in the nasal absorption of insulin and growth hormone. Agerholm *et al.* suggested that the major transport route of human growth hormone after intranasal administration to rabbits *in vivo* formulated with DDPC was transcellular through lethally damaged ciliated cells [76].

- ❖ **Cyclodextrins ( $\alpha$ ,  $\beta$ , and  $\gamma$ -cyclodextrins and their derivatives):** Cyclodextrin (CDs) are cyclic oligosaccharides showing a polar outer surface and an apolar interior cavity able to include lipophilic guest molecules. CDs can enhance lipophilic drug absorption by the solubilisation and protection against physicochemical and enzymatic degradation [77]. Thus CDs are also able to enhance hydrophilic drug absorption by the extraction of specific lipids from biological membranes, leading to an increase in membrane permeability and fluidity [78]. The extent of protection and absorption enhancement seems to depend CDs strongly on the nature of the drug used as well as on the CD used. For example, *in vivo* studies in rats have demonstrated that the addition of 5%  $\alpha$ -CD to nasal preparation of insulin resulted in an absolute bioavailability of approximately 30%; on the contrary,  $\beta$ - and  $\gamma$ -CD did not effect insulin absorption. However, dimethyl-beta-cyclodextrin (DM $\beta$ -CD) gave rise to a large increase in insulin absorption, with a bioavailability of 100% [79]. Based on toxicological studies of the local effects of cyclodextrins on the nasal mucosa DM $\beta$ -CD and randomly methylated beta-cyclodextrin are considered safe nasal absorption enhancers. Their effects were quite similar to controls (physiological saline), but smaller than those of the preservative benzalkonium chloride in histological and ciliary beat frequency studies.

## **2.4. Micro/nanocarriers for nasal drug delivery**

The use of pharmaceutical micro/nanocarriers (micro/nanoparticles, micro/nano emulsion, micelles and liposomes) to enhance the in vivo efficiency of many drugs well established itself over the past decade both in pharmaceutical research and clinical setting. These systems can include, besides the drug, enzymatic inhibitors, nasal absorption enhancers or/and mucoadhesive polymers in order to improve the stability, membrane penetration and retention time in nasal cavity.

### **2.4.1. Microspheres**

Microsphere technology is one of the specialized carriers becoming extremely popular for designing nasal products, as it may provide prolonged and intimate contact with the nasal mucosa and thus increasing absorption and bioavailability [80]. Normally microspheres, due to moisture uptake, dehydrates the nasal mucosa. This result in reversible shrinkage of the cells, providing a temporary physical separation of the tight junctions that increases the absorption of the drugs, also of high molecular weight molecules such as insulin. As mentioned before, one of the most important anatomical region of the nose for the drug absorption is the respiratory region, which is richly vascularised and contains three nasal turbinates, the deposition of the particles in this region depend on the microsystems size. Classically, larger particles including droplets ( $>10\ \mu\text{m}$ ), are deposited in the nasal cavity after inhalation; the larger the particles, the more anterior the deposition. For smaller particles the site of deposition depends on the velocity at which the particles are inhaled and the turbulence in the air flow, however the particles of size smaller than  $1\ \mu\text{m}$  are not normally deposited in the nasal cavity but travel down to the trachea to reach the lung. The ideal microsphere particle size requirement for nasal delivery should range from 10 to  $50\ \mu\text{m}$  as smaller particles than this will enter the lungs. However, studies have reported that a significant portion of small particles are also deposited in the nose [81]. The capacity of removal for the upper respiratory

tract is 100% for the particles with size larger than 10  $\mu\text{m}$ , and approximately 80% for the particles of 5  $\mu\text{m}$ . Clearance capacity drops progressively with further reduction in size and approaches zero for particles at 1-2  $\mu\text{m}$ . Studies have also reported that 4  $\mu\text{m}$  is the sufficient size for the nasal delivery [82].

The rationale behind the use of a microsphere system is the mucoadhesion; in fact, the administration of bioadhesive microsystems (in the powder form) with good mucoadhesive properties would permit such microspheres to swell in contact with the liquid present on nasal mucosa to form a gel and control the rate of clearance from the nasal cavity, thereby allowing poorly absorbed active molecules a longer time on the absorptive surface. It has been shown that microspheres formed by bioadhesive materials are retained in the nasal cavity with half-life clearance of 3h or longer, compared with 15-20 minutes for usual formulations [83]. Numerous examples of microparticulate systems, optimized for nasal administration, produced using different bioadhesive materials have been evaluated in-vivo as nasal drug delivery systems. Intranasal alginate mucoadhesive microspheres of carvedilol, prepared by emulsification cross-linking, showed an availability of 68% compared to intravenous administration of the drug [84]. Another material used by Illum et al, was degradable starch microspheres, was seen that those microparticles increase absorption of human growth hormone and desmopressin [85,86]. Special attention should be reserved to the chitosans, these are biodegradable high weight cationic polysaccharides, that in the last decade have been intensively studied as excipients for drug delivery especially for nasal formulation, due to their mucoadhesive properties and not only. In fact, their mechanism of nasal transport enhancement is a combination of bioadhesion and transient opening of the tight junction in the membranes. The cell-binding activity of chitosans is related to electrostatic interactions between cell surfaces charged negatively and the cationic polyelectrolyte structure. In addition, chitosans have no arresting effect on the mucociliary clearance, and they do not cause significant changes in nasal mucosa histology [87]. Medium molecular weight chitosans are able to enhance the nasal absorption in animals and in human volunteers of polypeptides and other polar drugs, such as insulin, salmon calcitonin, and morphine metabolites (un po di biblio). In relation of these consideration, the combination of a bioadhesive polymers and permeation

relatively nontoxic enhancers can be of promising potential for developing a excellent nasal formulation.

#### **2.4.2. Nanoparticles**

Nanoparticles may offer an improvement to nose-to-brain drug delivery since they are able to protect the encapsulated drug from biological and/or chemical degradation. Nanoparticles are solid colloidal particles ranging in size from 10nm to 1 $\mu$ m. They are made of macromolecular material which can be of synthetic or natural origin. On the basis of the process used for their preparation, two different types of nanoparticles can be obtained (Fig. 2.7), namely nanospheres in which a drug is dispersed in the matrix structure and nanocapsules that present a membrane-wall structure with an oily core containing the drug.

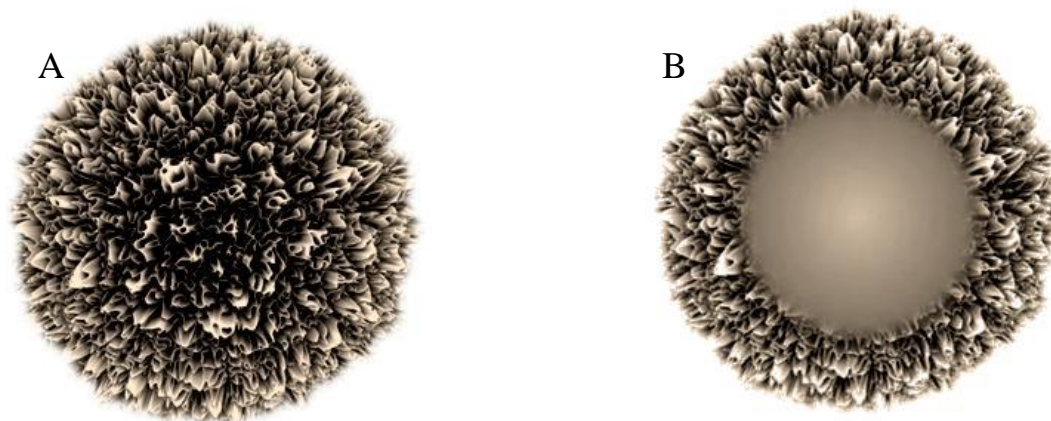


**Fig. 2.7 Difference between (A) nanospheres (matrix structure) and (B) nanocapsules (membrane-wall structure with an oil core)**

Nanoparticulate drug delivery systems can improve significantly the transport of drugs across the nasal mucosa as compared to drugs solutions. The strategy of applying drugs that are encapsulated into nanoparticles to the olfactory epithelium could potentially improve the direct CNS delivery of drugs. If drugs could reach the CNS in sufficient quantity by this route, due to the nanosystem, it could generate

interest in previously abandoned drug compounds (for example Tacrine) and enable an entirely novel approach to CNS drug delivery [88]. Literature on the potential of the nanoparticles as efficient nasal drug delivery system remain still contrasting. In fact, there are examples in the literature where it has been shown that nanoparticles are not as efficient as alternative solution formulations [89]. Although there are other studies that highlighted the enhancing effect of the nanoparticles; for example Seju U et al. evaluated the CNS absorption of olanzapine as a result of intranasal administration of olanzapine-loaded PLGA nanoparticles, they found that in vivo olanzapine was 6.35 and 10.86 times higher uptake of intranasally delivered nanoparticles than olanzapine solution delivered through intravenous and intranasal route, respectively. Highlighted a probable direct transport to the brain after intranasal administration of nanoparticles [90]. Therefore is not yet clear from the published literature whether these nanoparticles are improving delivery by transporting an encapsulated drug across the membrane barrier or merely keeping the system longer in the nasal cavity or protecting the drug from enzymatic degradation. Another explanation could be the uptake of the entire nanoparticles in the neurons, present in the olfactory region or in the trigeminal nerve, due to an endocytosis process. Have been studied various endocytic pathways that are very well provided by Alpesh Mistry et al [88]; generally, nanoparticles may be taken into the neurones and supporting cells by a number of endocytic mechanisms. However, nanoparticles larger than 100 nm are thought to have a restricted access to the brain via the intraaxonal route because their diameter increasingly exceeds that of the axons.

### **2.4.3. Liposomes**

Liposomes consist of one or more concentric lipid bilayers, which enclose one or more internal aqueous volume. The presence of two different environments in the carrier, the aqueous and the phospholipid membrane, makes liposomes a versatile nanocarrier for a broad of hydrophilic, amphipatic and hydrophobic small and macro molecules. Moreover, liposomes present good compatibility, low toxicity, lack of

immune system activation, and targeted delivery of bioactive compounds to the site of actions. Liposomes are classified according their structural parameters [91] (Fig. 2.8) or based on their method of preparation [92]. In the Table 2.2 there is an accurate classification based on structural parameters and on the methods of preparation. Besides being able to prepare liposomes with different methods that allow to obtain very different physical structures, it is also possible to vary the lipid composition and surface properties, thus allowing a large amount of control over the fate of their content. In addition, in liposome bilayer or in the aqueous phase is possible to add substances like tocopherol (see experimental section), which permit to obtain liposomes that in addition to improving drug absorption, they can provide an antioxidant effect, very useful in the treatment of neurodegenerative disease. For these reasons, they have been explored very widely as delivery vehicles.

The basic aspects and the advantages to use liposome like drug delivery system can be summarized in: (1) *protection* - the active materials are protected by virtue of the membrane barrier function and by the possibility to coencapsulate protective agents

**Table 2.2 Liposome classification**

<b>Liposome Classification</b>			
<b>Based on Structural Parameters</b>	<b>Abbreviation</b>	<b>Based on Method of Preparation</b>	<b>Abbreviation</b>
Multilamellar Large Vesicles >0.5 $\mu$ m	<b>MLV</b>	Single or Oligolamellar Vesicles made by Reverse-phase Evaporation	<b>REV</b>
Oligolamellar Vesicles 0.1-1 $\mu$ m	<b>OLV</b>	Multilamellar Vesicles made by Reverse-phase Evaporation	<b>MLV-REV</b>
Unilamellar Vesicles (all size range)	<b>UV</b>	Stable Plurilamellar Vesicles	<b>SPLV</b>
Small Unilamellar Vesicles 20-100nm	<b>SUV</b>	Frozen and Thawed MLV	<b>FAT-MLV</b>
Medium sized Unilammelar Vesicles	<b>MUV</b>	Vesicles prepared by Extrusion methods	<b>VET</b>
Large Unilamellar Vesicles >100nm	<b>LUV</b>	Vesicles prepared by French press	<b>FPV</b>
Giant Unilamellar Vesicles >1 $\mu$ m	<b>GUV</b>	Vesicles prepared by fusion	<b>FUV</b>
Multivesicular Vesicles >1 $\mu$ m	<b>MVV</b>	Dehydration-Rehydration Vesicles	<b>DRV</b>

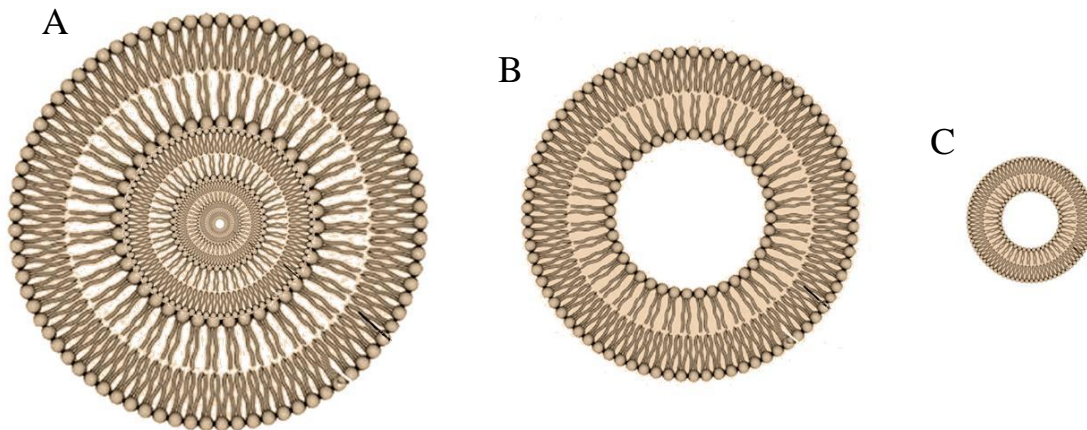


**Fig. 2.8 Liposome classification based on structural parameters. (A) Multilamellar Large Vesicles  $>0.5\mu\text{m}$  (MLV), (B) Large Unilamellar Vesicles  $>100\text{nm}$  (LUV) and (C) Small Unilamellar Vesicles 20-100nm (SUV).**

such as antioxidant molecules; (2) *sustained release* – such release is dependent on the ability to vary the permeability characteristics of the membrane by control of bilayer composition and lamellarity; (3) *controlled release* – drug release is enabled by exploiting lipid phase transitions in response to external triggers such as changes in temperature or pH; (4) *targeted delivery* – such delivery can be achieved by relying on natural attributes such as liposome size and surface charge to effect passive delivery to body organs or by incorporating antibody or other ligands to aid delivery to specific cell types. At the same time drugs can be directed away from vulnerable or unintended targets; (5) *internalization* – this occurs by encouraging cellular uptake via endocytosis or fusion mechanism, for example, to delivery genetic materials into cells. All these features make liposomes excellent candidates for nasal drug delivery; in fact, in addition to these, was also seen that liposomes are able to decrease mucociliary clearance due to their surface viscosity and exchange phospholipids with the membrane and opening “new pores” in the paracellular tight junctions; resulting in an increase in permeability. Moreover, promising results were been shown not only with small molecules but also with large molecules. Numerous examples are reported in the literature, which show the superiority and the convenience of the use of liposomes with respect to the simple solution of the drug; for example Maitani, Y et al [93] reported that insulin presented a better nasal permeability through nasal

mucosa of rabbit, when it was encapsulated in the liposomes compared to insulin solution. Jain, A. K. et al estimated, again using insulin as a model drug, the mucoadhesive properties of liposomes. They reported that liposomes shown to be marginally effective after nasal administration compared to ocular route although better therapeutic profile as the hypoglycaemic effects were prolonged until 72 h [94]. In another study Alsarra, I. A. et al highlighted that acyclovir mucoadhesive liposomes showed good permeability characteristics with enhanced nasal penetration of acyclovir in comparison to free drug suspended in gel. This result could be attributed to both encapsulation in liposomes and incorporation nasal mucoadhesive gel. Nasal bioavailability of acyclovir was 60.72% calculated relative to the serum acyclovir levels over a period of 8h after intravenous injection of acyclovir [95]. Law, S. L. et al studied indeed the effect of liposomes charges on nasal absorption of calcitonin. They reported that positively charged liposomes had a better bioavailability than negative and especially than calcitonin solution. The significant bioavailability enhancement of the positively charged liposomes may be explain with interaction of positively charged liposomes with the negatively charged mucosal surface. This retention allowed an increase in the residence time of calcitonin and thus increased bioavailability [96]. Very important is the opportunity using liposomes, to improve nasal drug delivery to CNS, various studied were done and all confirmed this ability. Arumugam, K. and his collaborators evaluated this ability, encapsulating rivastigmine in liposomes, an acetylcholinesterase inhibitor used in Alzheimer's disease; this drug can be rapidly and completely absorbed after oral administration but is extensively metabolized by hepatic metabolism and by cholinesterase-mediated hydrolysis. They compared intranasal liposome with the oral free drug and found that liposomal formulation can provide ten times higher  $C_{max}$ , higher systemic AUC, and higher concentration in the brain compared to oral administration. The higher rivastigmine brain concentration, following the intranasal liposome administration might also be due to direct transfer of the drug or vesicles system from nasal mucosa to the brain via the olfactory route [97]. Non only small molecule but also protein can be encapsulated in liposomes and delivered to the brain, in an in vivo study Migliore, M. et al. evaluated the effectiveness of cationic liposomes for intranasal administration of proteins to the brain. Was encapsulated in

liposomes as protein model, ovalbumin (OVAL) marked with Alexa 488, and delivery was assessed by fluorescence microscopy. By 6 and 24h after administration, Alexa 488-OVAL deposits were widely distributed throughout brain, with apparent cellular uptake in midbrain by 6h after administration[98].

#### **2.4.4. Nasal inserts**

Nasal inserts are solid formulations that can be administered in the posterior of the nasal cavity [99,100] where they can be transformed rapidly into gels, thus avoiding the foreign body sensation. With respect to powders, for which precision of dosage is difficult to achieve, these new nasal systems are able to deliver an exact dose of drug into the nasal cavity. Owing to CH mucoadhesive properties, nasal inserts based on this polymer can adhere to the mucosa and prevent rapid clearance of the drug, thus increasing its residence time. Moreover, good control of drug release can be achieved through the crosslinked CH's ability to form a gelled network in which the drug can diffuse. Finally, there is no need to remove the inserts mechanically from the nasal cavity because, after gel formation, they can be easily eliminated towards the nasopharynx by the mucociliary clearance. As nasal inserts are generally obtained by freeze-drying, which consists of sublimation of the frozen water yielding the formation of pores or channels in the polymer, they are characterized by a sponge-like structure. The spongelike structure of nasal inserts is extremely important to ensure rapid rehydration and gelation at the administration site. Several works have reported the use of nasal inserts based on a well-known mucoadhesive gelling polymer such as hydroxypropyl methylcellulose [101-103]. Bertram and Bodmeier reported the formulation of nasal inserts [104] based on different polymers comprising CH glutamate. They found that the type of polymer chosen for insert preparation influences the mechanical properties of the inserts, their water uptake behaviour and bioadhesion potential and their ability to control drug release. In vitro studies revealed that CH is able to form a thin film on mucosal substrates (agar/mucin gel), owing to its opposite charge to mucin and agar, but it is less efficient at prolonging the contact time with the mucosa with respect to carrageenan,

Carbopol and other negatively charged polymers. The authors suggest that the good bioadhesion ability of these polymers is related to a good balance between available hydrogen bonding sites and an open expanded conformation. In a recent work, Luppi et al. [105] investigated the use of nasal inserts based on CH/hyaluronate complexes for peptide and protein delivery. CH/hyaluronate polyelectrolyte complexes were obtained in different preparative conditions and used for the preparation of lyophilized cone-like shaped inserts loaded with vancomycin or insulin. Drug release from in situ gelling systems is a complex phenomenon of water uptake, polymer chain relaxation, swelling, drug--polymer interactions, drug dissolution and diffusion through the rehydrated insert. The results indicate that the selection of suitable conditions for preparation of the complexes allows modulation of insert functional properties. Moreover, the water uptake ability of the different complexes can be influenced by the presence of insulin or vancomycin in nasal inserts, owing to the possibility of ionic interactions between drugs and polyelectrolyte complexes. On the contrary, insulin and vancomycin release from the gelled inserts seemed to be affected by the molecular mass of the drug but not by the presence of drug--complex interactions. In another work, Luppi [106] described the use of CH/pectin polyelectrolyte complex for the formulation of chlorpromazine-loaded nasal inserts. The results show that higher amounts of pectin in the complexes, with respect to higher amounts of CH, produced a more evident porous structure of the nasal inserts, improving water uptake ability and mucoadhesion capacity. Finally, the presence of increasing amounts of pectin allows interaction with chlorpromazine hydrochloride, inducing the formation of less hydratable inserts, thus prolonging drug release and permeation. These investigations contribute to verifying the formation of polyelectrolyte complexes between CH and anionic polysaccharides (hyaluronic acid and pectin) at pH values in the vicinity of the pKa interval of the two counterions and to confirming their potential use for nasal drug delivery.

## EXPERIMENTAL SECTION



*Removal of the Nasal Mucosa of Sheep (Dr. G. Corvaci, July 2009, Bologna)*

### 3. ALBUMIN NANOPARTICLES CARRYING CYCLODEXTRINS FOR NASAL DELIVERY OF THE ANTI-ALZHEIMER DRUG TACRINE

---



**Fig. 3.1 Graphical Abstract. SEM image of freeze-dried Nanoparticles obtained, on the top left there is an Albumin nanoparticle carrying pure drug, on the top right there is an Albumin nanoparticle carrying pure drug and  $\beta$ -cyclodextrin**

### 3.1. Introduction

Tacrine (1,2,3,4-tetrahydro-9-aminoacridine monohydrochloride) (THA), a potent, centrally active, reversible cholinesterase inhibitor, was the first drug approved by the United States Food and Drug Administration (FDA) in 1993 for treating the symptoms of mild to moderate Alzheimer disease [107]. THA is available in the market as oral capsule dosage forms. Despite the favourable aqueous solubility, peroral administration of THA is associated with low bioavailability due to hepatic first-pass effect, short elimination half-life, gastrointestinal side effect and reversible dose-dependent hepatotoxicity, the major reasons for its withdrawal [108]. Hence the search for alternative routes of THA delivery such as transdermal [109,110] or, more recently, nasal route that deserved attention for rapid drug delivery to the central nervous system (CNS) [111].

Advantages of intranasal administration include a large surface area for drug absorption, rapid achievement of target drug levels and avoidance of first-pass metabolism [112]. Intranasal drug delivery systems should be designed to provide a controlled release and a complete absorption of drug at the mucosal site. In this view, hydrogel based systems and mucoadhesive excipients have been used to modulate drug release and prevent the rapid clearance of the drug formulation from the nasal cavity [113]. Among the various studied nasal formulations, nanoparticles have been found to improve drug transport across the mucosa due to the small particle size and the large total surface area favouring drug transfer from the formulation into the surrounding mucosa [114,115]. In the literature some studies describing the THA delivery in the CNS using intravenous administration of nanoparticles are reported. In particular, chitosan or poly(butylcyanoacrylate) nanoparticles have been evaluated after intravenous injection [116,117]. However, only few studies have been focused on THA delivery by nasal administration of nanosystems. Jogani and coauthors reported a study concerning the use of mucoadhesive microemulsion for targeting THA to the brain after intranasal administration in mice [118]. Their results suggest a possible role of intranasal THA delivery in treating Alzheimer's patients.

The goal of this work was to prepare and evaluate a new intranasal formulation of THA based on albumin nanoparticles. In a previous study, we prepared thermally

cross-linked bovine serum albumin nanoparticles showing good mucoadhesion properties, useful to prolong drug absorption from the applied formulation [119]. Moreover, by virtue of its ability to interact with a wide variety of drugs, albumin was found an interesting material for loading the active ingredient in the delivery system. Finally, the three-dimensional network of cross-linked albumin was found useful to control drug release.

In this study we tested bovine serum albumin nanoparticles carrying  $\beta$ -cyclodextrin and some of its hydrophilic derivatives in order to assess if and how the presence of these cyclic oligosaccharides can modulate drug release, permeation through nasal mucosa and mucoadhesion. In fact, it was recently demonstrated that in addition to improve drug solubility, cyclodextrins added to intranasal formulation can improve drug absorption and allow for targeting to specific brain regions [120,121]. Differential Scanning Calorimetry (DSC) and Thermogravimetric Analysis (TG) with a support by Fourier Transform Infrared spectroscopy (FT-IR) were used for solid-state characterization of nanoparticles. Nanoparticles were evaluated for yield, drug content, morphology, size distribution and surface charge, as well as for mucoadhesion properties, in-vitro drug release and ex-vivo permeation ability.

## **3.2. Materials and Methods**

### **3.2.1. Materials**

Bovine serum albumin, tacrine hydrochloride, mucin (type II: crude from porcine stomach) were purchased from Fluka (Milan, Italy).  $\alpha$ -cyclodextrin and hydroxypropyl  $\alpha$ -cyclodextrin with molar substitution degree MS 0.65 were a gift from Wacker Chemie GmbH (Monach, Germany), sulphobutylether  $\alpha$ -cyclodextrin with substitution degree DS 6.4 were a gift from CyDex Inc. (KS, USA). All the solvents and salts employed were purchased from Carlo Erba (Milan, Italy). Dimensional analysis, mucoadhesion and permeation studies were carried out in pH

6.0 aqueous buffer with the following composition (g/L): 7.97  $\text{KH}_2\text{PO}_4$ , 3.30  $\text{Na}_2\text{HPO}_4 \cdot 12\text{H}_2\text{O}$ .

### 3.2.2. Preparation of bovine serum albumin nanoparticles

Bovine serum albumin nanoparticles (nP) were prepared modifying a previously proposed method [119]. Briefly, 0.50 g of bovine serum albumin (BSA) were dissolved in 100 ml of pH 9.0 aqueous solution (10 mM NaCl) stirred magnetically in the presence of glass beads. Ethanol was added dropwise to this solution at a rate of 1.0 ml/min so as to produce a ratio 1:1 (v/v) ethanol/BSA solution and, after desolvation, the pH of the medium was subsequently adjusted to 9.0. Magnetic stirring (680 rpm) was continued at 75 °C for 60 min to yield an aqueous suspension of thermally cross-linked albumin nanoparticles. After evaporation of the residual

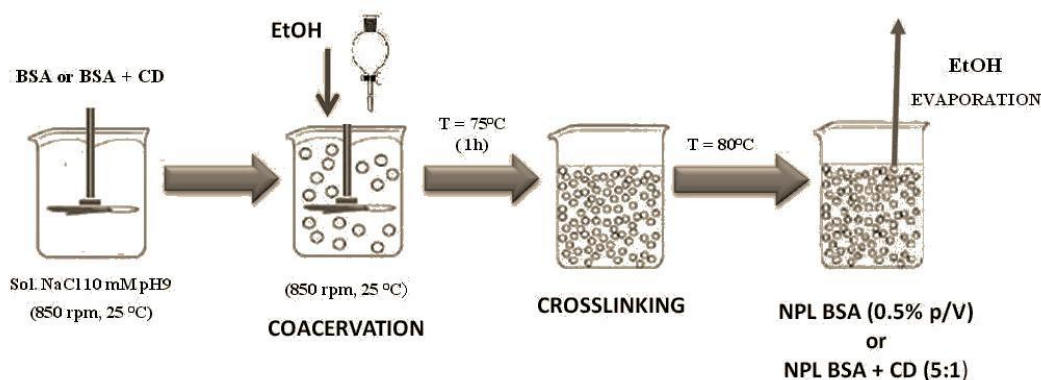


Fig. 3.2 Scheme of preparation of the Nanoparticles

ethanol with a rotavapor, the pH was lowered to 7.0 and the final volume of suspension was exactly adjusted to 100 ml in order to obtain an exact amount of nanoparticles per volume (Fig. 3.2). Then suspensions were lyophilized (Alpha 1-2, Christ, Naples, Italy) and stored in a desiccator until use or employed for the loading process. For the preparation of nanoparticles carrying cyclodextrins (nP<sub>CD</sub>), 100 mg

of  $\beta$ -cyclodextrin ( $\beta$ CD), hydroxypropyl  $\beta$ -cyclodextrin (HP $\beta$ CD) or sulphobutylether  $\beta$ -cyclodextrin (SBE $\beta$ CD) were dissolved in the aqueous albumin solution. The nanoparticles were formed and recovered as previously described.

### 3.2.3. Nanoparticle loading and determination of loading efficiency

THA loading into nanoparticles was achieved by soaking. For drug loading, nanoparticles (100 mg) were added to 20 ml of THA (2 mg/ml) in pH 7.0 aqueous solution (10 mM NaCl). The experiments were performed at room temperature under magnetic stirring. After the equilibrium was attained (24 h) the solvent was removed by ultracentrifugation (12000 rpm, 30 min, 4 °C) and nanoparticles were washed with the same aqueous solution, immediately ultracentrifuged again and finally freeze-dried. After the loading with THA the nanoparticles (THAnP, THAnP $\beta$ CD, THAnP<sub>HP $\beta$ CD</sub>, and THAnP<sub>SBE $\beta$ CD</sub>) were stored in a desiccator until use.

For the determination of loading efficiency an amount of 100 mg of the freeze-dried nanoparticles was weighed and transferred into a 10 ml volumetric flask and brought to volume with HCl 0.1M. The suspension obtained was sonicated for 10 min, left at room temperature for 20 min and then centrifuged at  $3400 \times g$  for 20 min. The supernatant was finally diluted in the mobile phase employed for HPLC analysis. The chromatographic system was composed of a Shimadzu (Milan, Italy) LC-10ATVP chromatographic pump and a Shimadzu SPD-10AVP UV-Vis detector set at 240 nm. Separation was obtained on a Phenomenex (Torrance, CA, USA) Sinergy Fusion-RP 80A (150 x 4.6 mm I.D., 5  $\mu$ m) coupled to a Phenomenex (Torrance, CA, USA) SecurityGuard C18 guard cartridge (4 x 3.0 mm I.D., 5  $\mu$ m). The mobile phase was composed of a mixture of acetonitrile – pH 3.0 solution of triethylamine (0.5%) 20:80 (v/v). The flow rate was 0.4 ml/min and manual injections were made using a Rheodyne 7125 injector with a 20  $\mu$ l sample loop. Data processing was handled by means of a CromatoPlus computerised integration system (Shimadzu Italia, Milan, Italy). A calibration curve was set up in the 0.05–5.00  $\mu$ g ml<sup>-1</sup> range; good linearity was found ( $r^2 = 0.9997$ ).

#### **3.2.4. Particle size, zeta-potential measurements and morphology**

Particle size and size distributions were measured by PCS using an instrument (Brookhaven 90-PLUS) with an He–Ne laser beam at a wavelength of 532 nm (scattering angle of 90°) [122,123]. For measurement, nanoparticles were dispersed in pH 6.0 phosphate buffer at a 1:400 (w/v) ratio. Measurements were carried out at 25 °C without filtering.

Zeta-potential measurements were carried out at 25 °C on a Malvern Zetasizer 3000 HS instrument, after the same dilution. Both average particle size and zeta-potential measurements were run in triplicate.

The morphology of the particles was observed using scanning electron microscopy (SEM) (LEO 420 Electron Microscopy Ltd, Cambridge, England). Lyophilised particles were deposited on aluminium stubs using double-faced adhesive and coated with gold-palladium under an argon atmosphere using a gold sputter module in a high-vacuum evaporator, before observation. Alternatively, nanosphere suspensions were reconstituted in deionised water and drops were placed on aluminium stubs, allowed to dry and finally coated with gold-palladium as described above.

#### **3.2.5. Thermogravimetric analysis (TG), Differential scanning calorimetry (DSC) and Fourier Transform Infrared Spectroscopy (FT-IR)**

Mass losses were recorded with a Mettler TA 4000 (Mettler Toledo, Novate Milanese, MI, Italy) apparatus equipped with a TG 50 cell on 8–10 mg samples in open alumina crucibles ( $\beta = 10 \text{ K min}^{-1}$ , static air atmosphere, 30–400 °C temperature range). Measurements were carried out at least in triplicate (relative standard deviation  $\pm 5\%$ ).

Temperature and enthalpy values were measured with a Mettler STAR<sup>e</sup> system (Mettler Toledo, Novate Milanese, MI, Italy) equipped with a DSC821<sup>e</sup> Module and an Intracooler device for subambient temperature analysis (Julabo FT 900) on 3–5 mg (Mettler M3 Microbalance) samples in sealed aluminium pans with pierced lid ( $\beta$

=10 K min<sup>-1</sup>, nitrogen air atmosphere (flux 50 ml min<sup>-1</sup>), -10 to 350 °C temperature range). The instrument was preventively calibrated with Indium as standard reference. Measurements were carried out at least in triplicate (relative standard deviation ±5%).

Mid-IR (650–4000 cm<sup>-1</sup>) spectra were recorded on powder samples using a Spectrum One Perkin-Elmer FTIR spectrophotometer (resolution 4 cm<sup>-1</sup>) (Perkin Elmer, Wellesley, MA, US) equipped with a MIRacle™ ATR device (Pike Technologies, Madison, WI, US).

### **3.2.6. Mucoadhesion properties**

The mucoadhesion behaviour was performed as described elsewhere [124]. Briefly, 1 ml of a mucin suspension (0.05% w/v) was mixed with 1ml of albumin nanospheres (0.1% w/v) for 1h and for 24 h at pH 6.0 at 37 °C under continuous stirring. Mucin nanoparticles interactions were evaluated by DLS (Dynamic Light Scattering). In addition the mucoadhesion ability was measured in terms of the force needed to pull out freshly excised sheep nasal mucosa (surface area 1 mm<sup>2</sup>) from a tablet (100 mg) with an adapted tensiometer (Krüss 132869; Hamburg, Germany) [125]. For this study tablets (weight of 100 mg) were prepared by direct compression of freeze-dried nanoparticles (compaction force: 18 kN) with a single punch press (type Korsch, Korsch Maschinenfabrik No. 1.0038.86, Berlin, Germany). Sheep nasal mucosa was obtained from local slaughterhouses. The turbinates were fully exposed by a longitudinal incision through the nose and the mucosa was carefully removed from the underlying bone by cutting with haemostatic forceps. To maintain the freshness of the specimen as far as possible, mucoadhesion studies were started immediately after the mucosa samples were excised. The nasal mucosa was fixed to a support with cyanoacrylate adhesive and then suspended from the tensiometer spring. The mucosa was lowered until it just contacted the surface of the tablet, previously immersed in aqueous buffer at pH 6.0 for 15 min. A 90 dyne force, measured by the torsion balance of the instrument as a negative force, was applied to the tablet for 30

s. Then the nasal mucosa was raised until it was separated from the tablet. This point represents the adhesive bond strength between these elements and is expressed as a positive force in dyne.

### **3.2.7. *In-vitro release studies***

In-vitro release studies were carried out as follows: loaded nanoparticles and 1 ml phosphate buffer solution pH 6.0 were put into a dialysis tube (MWCO: 14000) and then the dialysis tube was introduced into vial with 10 ml of the same buffer (sink condition) and the media was stirred at 100 rpm at 37 °C. At specific time intervals, medium was taken and replaced with fresh buffer. The concentration of the released THA was determined by HPLC as previously described.

### **3.2.8. *Ex-vivo permeation studies across sheep nasal mucosa***

The permeation study was conducted using sheep nasal mucosa in a Franz-type permeation cell with a diffusional area of 1.5 cm<sup>2</sup>. At time zero, an exact amount of loaded nanoparticles or an exact amount of THA was placed on the mucosa in the donor compartment. The receiver phase (6.0 ml of a phosphate buffer solution, pH 6.0, maintained at 37 °C by means of a surrounding jacket) was stirred constantly and at predetermined time intervals samples of 100 µl were taken and replaced by fresh medium. The amount of THA in the receiving phase was analysed by HPLC as previously described. The studies were carried on for 420 min.

### **3.2.9. *Statistical analysis***

ANOVA was used to determine statistical significance. Differences were considered to be significant for values of  $P < 0.05$ .

### 3.3. Results

#### 3.3.1. Particle characteristics

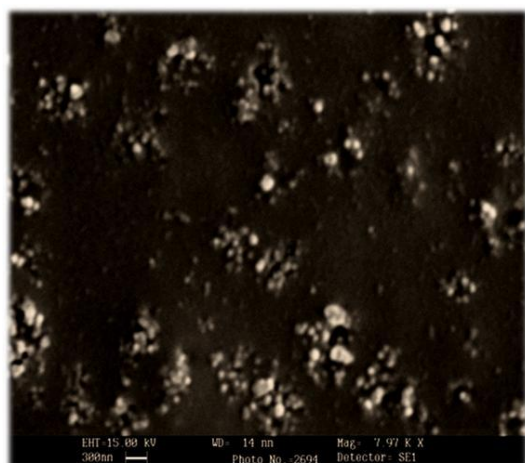
Table 3.1 shows that the % yield (calculated by dividing the dried mass of the particles by the dried weight of used materials and converting the weight ratio into percent) was higher for unloaded nanoparticles than for loaded nanoparticles, according to the mass loose due to ultracentrifugation and washing steps following THA loading into nanoparticles.

Table 3.1 also shows that all the nanoparticles presented quite *polydisperse populations* with a mean diameter lower than 300 nm and negative zeta potential, even after drug loading. The presence of the native and derivatives  $\beta$ CD and the loading of THA provided a significant decrease and increased in particle size, respectively. On the contrary, zeta potential was not significantly influenced.

Fig. 3.3 shows SEM images of freeze-dried THAnP $\beta$ CD. Moreover, SEM image of the same reconstituted sample in deionised water (Fig. 3.4), with a higher magnification, shows individualized spherical shaped particles allowing observing that the mean particles diameter is similar to that reported for PCS data.

**Table 3.1. % Yield (%Y), mean diameter ( $\phi$ ), polydispersity index (PI), zeta potential (Z) and drug loading (%L) of albumin nanoparticles.**

	Unloaded				Loaded			
	nP	nP $\beta$ CD	nP $_{HP\beta}CD$	nP $_{SBE\beta}CD$	THAnP	THAnP $\beta$ CD	THAnP $_{HP\beta}CD$	THAnP $_{SBE\beta}CD$
<b>%Y</b>	98 $\pm$ 5	99 $\pm$ 3	97 $\pm$ 3	97 $\pm$ 5	88 $\pm$ 5	85 $\pm$ 6	91 $\pm$ 6	88 $\pm$ 9
<b><math>\phi</math> (nm)</b>	221.7 $\pm$ 11.0	159.0 $\pm$ 9.1	145.3 $\pm$ 9.3	132.5 $\pm$ 12.4	266.2 $\pm$ 12.2	189.3 $\pm$ 10.0	199.4 $\pm$ 13.1	177.4 $\pm$ 18.0
<b>PI</b>	0.288	0.129	0.184	0.225	0.325	0.228	0.327	0.257
<b>Z (mV)</b>	-11.5 $\pm$ 0.7	-11.6 $\pm$ 0.8	-11.3 $\pm$ 0.7	-12.0 $\pm$ 0.5	-10.9 $\pm$ 0.7	-10.2 $\pm$ 0.6	-10.5 $\pm$ 0.8	-10.0 $\pm$ 0.9
<b>% L</b>	/	/	/	/	14.7 $\pm$ 0.3	12.5 $\pm$ 0.9	14.3 $\pm$ 0.4	22.0 $\pm$ .05



**Fig. 3.3 SEM image of freeze-dried sample of THAnP $\beta$ CD.**

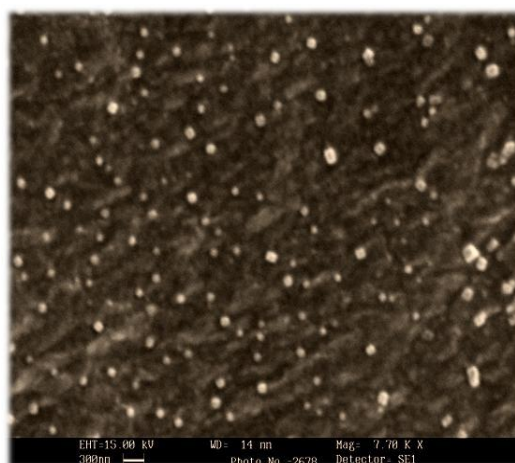


**Fig. 3.4 SEM image of freeze-dried nanoparticles (THAnP $\beta$ CD) after suspension reconstitution.**

### **3.3.2 Nanosphere loading and determination of loading efficiency**

Table 3.1 shows the results of drug loading process. Drug loading recovered for all the samples revealed the affinity of albumin nanoparticles towards THA. The presence of  $\beta$ CD and HP $\beta$ CD in the nanoparticle network did not affect drug loading with respect to nanoparticles based on BSA alone. On the contrary, the presence of SBE $\beta$ CD increased the drug loading.

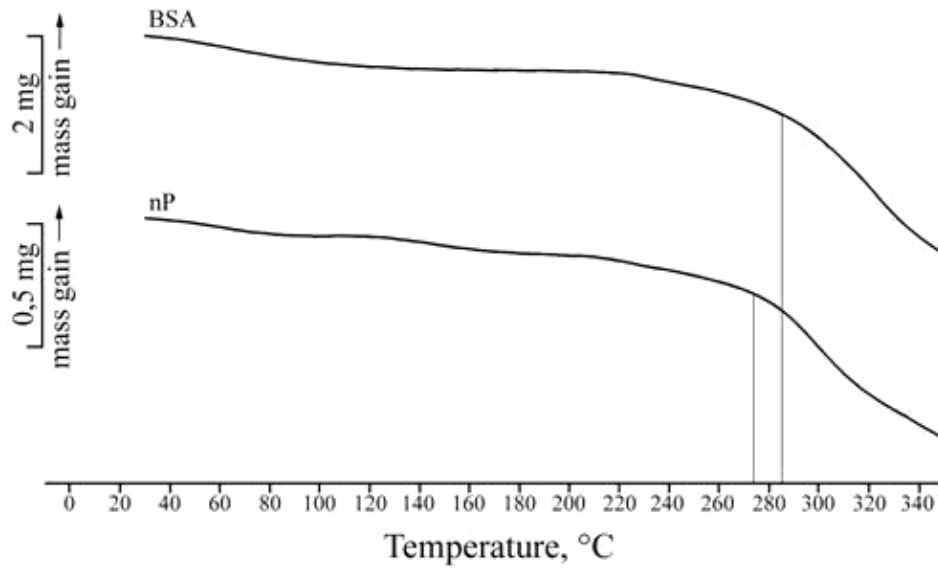
### **3.3.3. Thermogravimetric analysis (TG), Differential scanning calorimetry (DSC) and Fourier transform infrared (FT-IR) spectroscopy**

Fig. 3.5 shows thermogravimetric curves of native albumin (BSA) and nanoparticles prepared with albumin alone (nP). BSA and nP decomposed around 287 and 275 °C, respectively.

In Fig. 3.6 are reported DSC curves of BSA and nP. The characteristic endothermic peak of the protein at 230 °C appeared in both DSC profiles, but the calculated enthalpy was different for the two samples. A decrease in enthalpy value of the

endothermic effect in nP, compared to BSA, is evident indicating a partially loss of protein structure organization during thermal cross-linking.

Accordingly to a previous work [119] FT-IR spectra of BSA and nP were recorded in order to confirm albumin denaturation after ethanol-induced coacervation followed



**Fig. 3.5** TGA curves of native albumin (BSA) and nanoparticles prepared with albumin alone (nP).

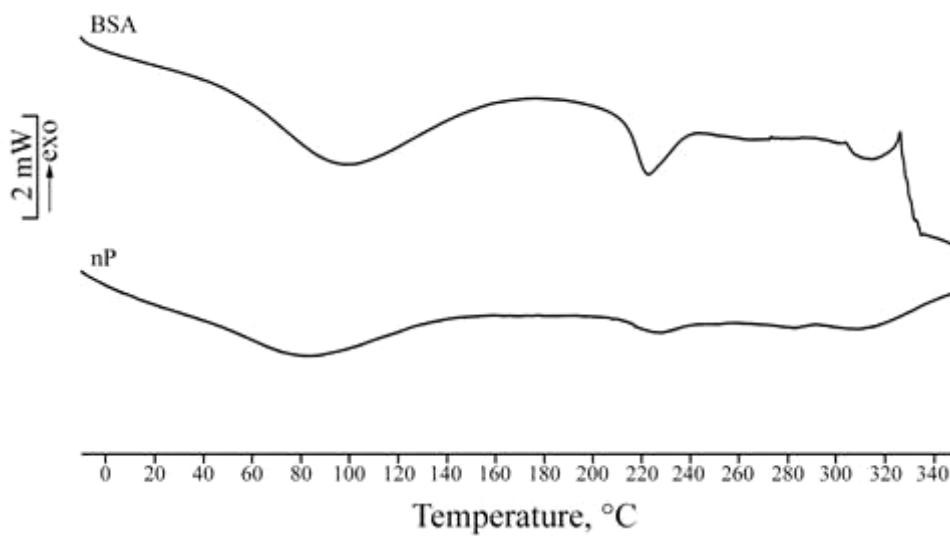


**Fig. 3.6** DSC curves of native albumin (BSA) and nanoparticles prepared with albumin alone (nP).

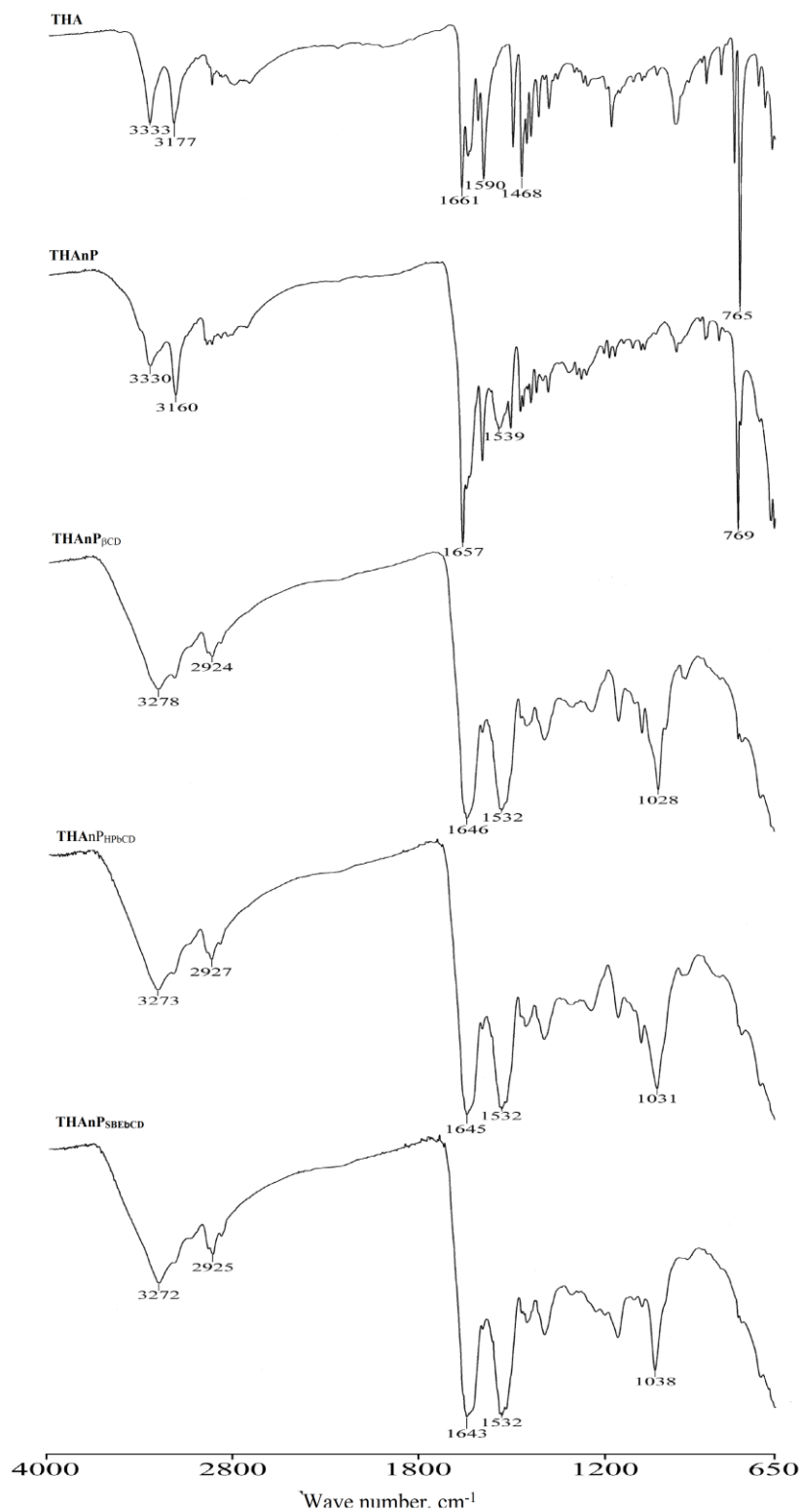


**Fig. 3.7** FT-IR spectra of THA, THAnP, THAnP<sub>β</sub>CD, THAnP<sub>HP</sub>-CD and THAnP<sub>SBE</sub>-CD.

by thermal cross-linking. As in acetone-induced coacervation followed by thermal cross-linking, BSA and nP presented the same protein characteristic peaks relative to C-O stretching vibration (amide I band) and to a mix vibration of N-H bending and C-N stretching (amide II band), but the band intensities and frequencies appeared modified (data not reported).

In Fig. 3.7 are reported the FT-IR spectra of THA, THAnP, THAnP $\beta$ CD, THAnP $_{HP\beta}CD$  and THAnP $_{SBE\beta}CD$ . The THA characteristic band at 765 cm $^{-1}$ , assignable for aromatic C-H, is evident in the THAnP system and disappears in those carrying native and derivatives  $\beta$ CD, probably as a consequence of an interaction between the drug and the albumin/cyclodextrin network.

#### **3.3.4. Mucoadhesion properties**

Mucin/nanosphere aggregates presented higher dimensions than the standard samples (Fig. 3.8). In particular, nanoparticles carrying HP $\beta$ CD increased their mean size of ten times after 24 h showing the best mucodhesion properties. These results were confirmed by experimental detachment forces (n = 5, the SD did not exceed the 5%): nP, 20 dyne; nP $\beta$ CD, 29 dyne; nP $_{HP\beta}CD$ , 65 dyne; nP $_{SBE\beta}CD$ , 30 dyne.

#### **3.3.5. In-vitro release studies**

Table 3.1 shows the fractional amount of THA released from nanoparticles 30, 180 and 400 min after the beginning of the experiment. Data indicated that THA release did not occur immediately but a sustained release was obtained for all nanoparticles. Moreover, nP $_{SBE\beta}CD$  provided lower release than the other particulate systems accordingly to the good THA affinity for these systems as observed during loading experiments.

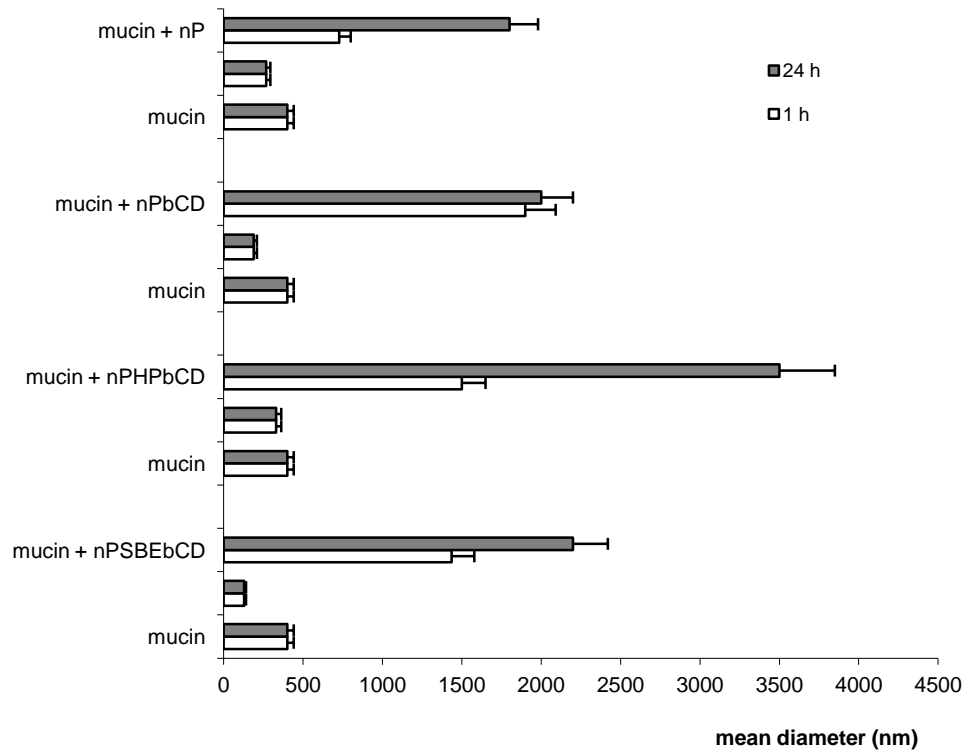


**Fig. 3.8** Mean diameter of mucin (mean  $\pm$  SD, n = 5), nanoparticles and mucin/nanoparticle aggregates measured by Dynamic Light Scattering.

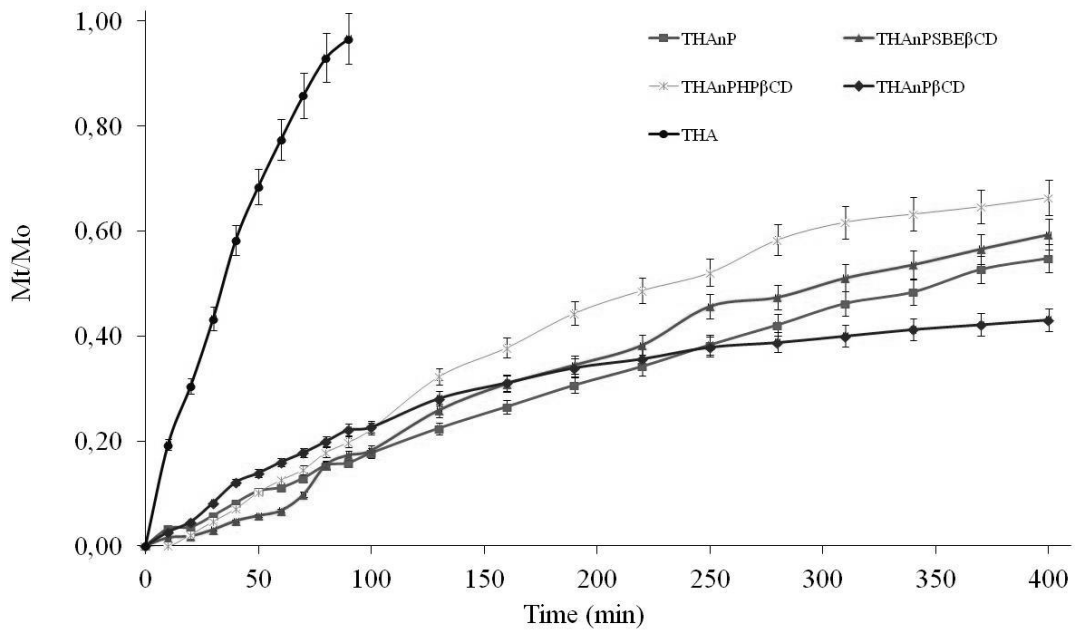


**Fig. 3.9** Permeation profiles profiles (mean  $\pm$  SD, n = 3) of tacrine hydrochloride from loaded nanoparticles.

### **3.3.6. *Ex-vivo permeation studies across sheep nasal mucosa***

Fig. 3.9 shows the permeation profiles of THA after nanoparticles placement on sheep nasal mucosa. THA standard solution presented the best permeation profile, allowing 100% drug permeation in 100 min. Nanoparticles showed sustained permeation profiles and in particular nanoparticles containing the different cyclodextrins revealed enhanced THA permeation with respect to nanoparticles based on albumin alone.

## **3.4. Discussion**

Nanoparticles were obtained modifying a method previously employed [119]. Albumin coacervation with ethanol followed by thermal cross-linking produced albumin nanoparticles with size and polydispersity higher than those obtained by coacervation with acetone. The choice for ethanol-induced coacervation stands in the possibility to reduce particle potential toxicity due to the permanence of solvents. In fact, acetone can damage mucosal epithelia and it has been shown to have anticonvulsant effects in animal models of epilepsy, when administered in very small (millimolar) concentrations [126]. For these reasons the presence of acetone in nasal dosage forms, albeit in small quantities, should be avoided. Moreover, in a recent study Adriaens and co-authors [127] reported that acetone can produce membrane damage at concentrations of 5% (w/v), while ethanol was shown to induce severe irritation (increased mucus production, protein and LDH release) only at concentration of 10% (w/v), whereas concentrations of 5% (w/v) and lower has no effect. Albumin denaturation was confirmed by thermal data supported by FT-IR spectra. In particular, the shift to lower temperature of the thermal degradation of nP indicated a loss of protein organization due to the formation of new bonds between albumin molecules. Moreover, the lowering in the enthalpy values calculated from DSC curves confirmed that albumin lost its native structure during the denaturation process. Finally, FT-IR spectra behaviour could be associated with the destruction of

hydrogen bonds through heat denaturation and reflected a decrease in alfa-helix content of the denaturated protein.

As can be observed in Table 3.1, the presence of the  $\beta$ CD, native and derivatives, in the particle structure influenced their size. As reported by Csaba and co-authors [128] particle size can be correlated to the viscosity of the solution before polymer coacervation. Viscosities of albumin solutions in the presence or in the absence of the different  $\beta$ CDs was measured by means of an Ubbelohde capillary viscometer equipped with an electronic time-measuring unit ViscoClock (Schott, Mainz, Germany) and were found not significantly different ( $0.97 \pm 0.08$  cP for nP,  $0.98 \pm 0.04$  cP for nP $_{\beta$ CD,  $0.98 \pm 0.04$  cP for THAnP $_{HP\beta$ CD and  $0.97 \pm 0.07$  cP for THAnP $_{SBE\beta$ CD). These data confirmed that albumin molecules were greatly solubilised in the solution due to the high repulsive forces existing at pH 9.0 and that cyclodextrins/albumin interactions in the solution did not cause variation of viscosity. However, Ko and Gunasekaran [129] reported that, for preparing nanoparticles of small size, high protein unfolding and low hydrophobic interactions of protein molecules are extremely important. We hypothesize that the presence of the different  $\beta$ CDs in the solution could mask the hydrophobic regions of albumin molecules thus suppressing their interactions and improving protein unfolding. For instance, during albumin coacervation in the presence of the different  $\beta$ CDs, the great protein unfolding favoured the formation of nanoparticles with smaller size.

The increased particle size after drug loading suggests that THA molecules could interact with nP due to physical absorption improved by ionic interactions. In fact, as confirmed by zeta potential measurements, at pH > 6.0 albumin nanoparticles (albumin P.I., 4.6) were negatively charged due to the presence of much more carboxylic groups than amino groups [119], while THA (pKa, 9.85) showed a positive charge.

Shape of the samples was analysed by electron microscopy. In particular, Fig. 3.4 shows individualized particles with mean diameter consistent with that measured by PCS, indicating that nanoparticles were discrete entities and that lyophilisation process produced a reversible aggregation of nanoparticles.

Loading data suggest that THA had great affinity for all albumin-based nanoparticles and the presence of SBE $\beta$ CD allowed entrapping the highest amount of drug. In fact,

SBE $\beta$ CD, due to its negative charges, could increase the charge density on the nanoparticle surface thus improving the absorption of the positive charged THA. This behaviour was also confirmed by the lower in-vitro release of THA from nP<sub>SBE $\beta$ CD</sub> compared to the other nanoparticles.

Only nanoparticles without  $\beta$ CDs showed the characteristic band of THA at 765 cm<sup>-1</sup> in FT-IR spectra. Otherwise the absence of this band in drug/nanoparticle carrying  $\beta$ CDs suggested the presence of interactions between the drug and the albumin/cyclodextrins network.

As described in a previous work [119], nP showed mucoadhesion properties in in-vitro and ex-vivo studies. Also albumin nanoparticles carrying the different  $\beta$ CDs maintained the same characteristics and in particular nP<sub>HP $\beta$ CD</sub> showed the highest mucoadhesive ability. Mucoadhesion is affected by the synergistic action of the properties of the polymeric delivery system and the biological environment. The interactions between mucus and hydrophilic polymers are a result of physical entanglement and secondary bonding related to the chemical groups of the polymeric chain. Moreover, polymers hydration ability, increasing the mobility of molecules, facilitates interpenetration and interaction with the mucus layer [130-132]. We hypothesize that nanoparticles have different ability to hydrate accordingly to the different solubility of the loaded  $\beta$ CDs. In particular,  $\beta$ CD has the lowest solubility (18 mg/ml), while HP $\beta$ CD and SBE $\beta$ CD have higher solubility (>600 mg/ml and >500 mg/ml, respectively) [133]. The lower mucoadhesiveness of nP<sub>SBE $\beta$ CD</sub> with respect to nP<sub>HP $\beta$ CD</sub> could be attributed to the presence of the higher electrostatic repulsive forces arising from the ionized functional groups of SBE $\beta$ CD loaded in the nanoparticles and sialic acid (pKa, 2.6) of the mucus.

Generally, non mucoadhesive formulations can be rapidly cleared from the nasal cavity by mucociliary mechanism, thus providing short residence times and low drug bioavailability. All nanoparticles produced lower drug permeation than THA standard solution (Fig. 3.9), but good adhesion to nasal mucosa. This behaviour suggests that they could be suitable delivery systems for improving nasal drug bioavailability. Moreover, the presence of the different  $\beta$ CDs, particularly HP $\beta$ CD, favoured drug permeation with respect to nanoparticles based on albumin alone. In fact, a decrease in lag time and an increase in the flux could be observed and

correlated to  $\beta$ CDs ability to interact with the lipophilic components of biological membranes changing their permeability.

### **3.5. Conclusions**

The results in this study indicate that albumin nanoparticles carrying native and hydrophilic derivatives  $\beta$ CD can be employed for the formulation of mucoadhesive nasal formulations with interesting drug permeation properties. The selection of suitable CD during particle preparation allows the modulation of their mucoadhesion ability and THA permeation at the administration site. This work will be furthered by performing intranasal absorption studies in animal models.

#### 4. MULTIFUNCTIONAL LIPOSOMES FOR DELIVERY OF THE ANTI-ALZHEIMER DRUG TACRINE HYDROCHLORIDE BY THE NASAL ROUTE. PART 1: FORMULATION, CHARACTERIZATION, IN-VITRO/EX-VIVO PERMEABILITY AND NEURONAL UPTAKE EVALUATION

---

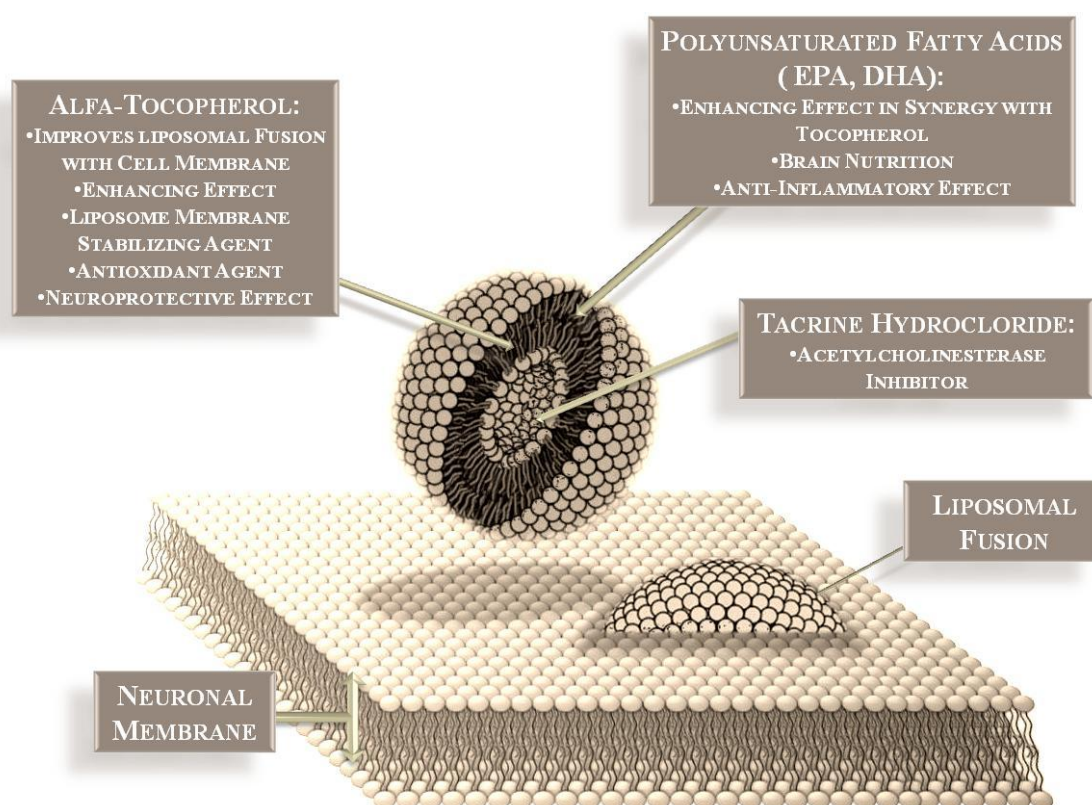


**Fig. 4.1 Graphical Abstract. Improvements achieved by the addition of  $\alpha$ -Tocopherol and Polyunsaturated Fatty Acid ( $\Omega$ 3) in the liposome formulations**

#### 4.1. Introduction

Alzheimer's disease (AD) is a fatal neurodegenerative condition characterized clinically by progressive memory loss and irreversible cognitive deterioration. It has been shown that there is a progressive degeneration of the brain's acetylcholine neurons which leads to the appearance of cognitive symptoms of the disease. At present, there are no therapeutic interventions able to stop the progression or to treat brain degeneration. Treatments are therefore aimed at slowing down the worsening course, maintaining, at least temporarily, the cognitive and behavioural symptoms, thus ensuring patients to have good or decent quality of life. One strategy to combat this disease is to increase cholinergic transmission; therefore acetylcholinesterase inhibitors have been developed including tacrine, rivastigmine and donepezil [134-137]. Although the aetiology is not still understood, it appears that oxidative stress (OS) plays a central role in the pathogenesis and progression of the AD [138] and then it would be desirable to integrate traditional therapeutic strategy, based on the recovery of the acetylcholine deficit, with an antioxidant treatment. In fact, epidemiological investigations have shown an improvement in cognitive activity and a slowing of disease progression following the administration of antioxidants. In addition,  $\alpha$ -tocopherol (Toc) administration has been shown to reduce hepatotoxic effects of the anti-Alzheimer drug tacrine and can be considered a suitable adjunct to tacrine therapy [139]. Moreover, it has recently been shown that when the brain is rich in docosahexaenoic acid (DHA), an omega-3 fatty acid which can also be biosynthesized starting from  $\alpha$ -linolenic acid, production of amyloid plaques is lower, with a decrease of the characteristic symptoms of the disease. Tacrine (1,2,3,4-tetrahydro-9-aminoacridine) (THA), one of the drugs approved by the FDA for the treatment of Alzheimer's disease [140,141], is present in the market only as oral formulation. However, peroral THA administration is associated with low bioavailability, due to the extensive hepatic first-pass effect and the rapid clearance from the systemic circulation, and with a reversible dose-dependent hepatotoxicity and peripheral cholinergic side effect [142,143]. Hence, alternative routes of administration for the centrally active acetylcholinesterase inhibitor THA may offer

distinct advantages. Drug delivery from the nose to the CNS can be achieved via olfactory neuroepithelium and can involve paracellular (inter cellular spaces and tight junction), transcellular (passive diffusion, active transport and transcytosis) and/or neuronal transport [144, 145]. Moreover, the transport via trigeminal nerve system from the nasal cavity to CNS has also been described [146]. THA delivery into CNS through intranasal route has been reported both in humans and in animal models of Alzheimer's disease and its administration by intranasal route not only has been found useful for circumventing the blood-brain barrier, but also for avoiding the hepatic first-pass effect, thus allowing lower dosage and side effects [147]. The current oral dosing regimen for THA is 40 mg/day (10 mg 4 times daily). The possibility to administer a lower THA dosage depends on the formulation ability to interact with the mucus layer and mucosal epithelium, as well as promote drug permeation during their residence in the nasal cavity, thus to their ability to allow complete absorption of the encapsulated drug [148]. In the last few years, different kinds of liposomes have been evaluated as potential intranasal drug delivery systems; moreover, Mahmoud Reza Jaafari et al. have demonstrated that nasal clearance half-lives of liposomes were at least four-fold than normal clearance half-life of human nose (about 20 min), thus suggesting that these particulate systems are highly mucoadhesive [149]. The permeability-enhancing effect of liposomes has also been demonstrated and may be increased by adding to the formulation substances that can promote lipid vesicles fusion with cellular membrane. As reported by Nakagawa H. et al. [150] the presence of isoprenoids, like Toc, in liposome bilayer improves the ability of phospholipid vesicles to fuse with cellular membrane. In addition, Toc in liposomes acts as a membrane stabilizing agent, reducing liposome drug leaking and avoiding lipid oxidation [151].

In this work, the capacity of Toc and polyunsaturated fatty acids ( $\Omega 3$ ) in liposome formulations to influence drug permeability and neuronal uptake was evaluated. The antioxidant and neuroprotective properties of our multifunctional liposomes have been going evaluating and will be reported in details in the chapter 5.

## 4.2. Materials and Methods

### 4.2.1. Materials

Tacrine hydrochloride (THA),  $\alpha$ -tocopherol, L- $\alpha$ -phosphatidylcholine from egg yolk and cholesterol were purchased from Fluka (Milan, Italy). Eicosapentaenoic acid and docosahexaenoic acid were obtained from Doosan Serdary Research Laboratories (Englewood Cliffs, NJ). Egg phosphatidylcholine, Lipoid E-80, was kindly provided by Lipoid GmbH (Ludwigshafen, Germany). Triton X-100, calcein and Dulbecco's modified Eagle's medium (DMEM), fetal calf serum (FCS), penicillin/streptomycin, were purchased from Sigma-Aldrich (Milan, Italy). Clear culture Transwell inserts (diameter 6.5 mm) and plates were obtained from Corning GmbH, Life Sciences (Wiesbaden, Germany). Clear Millicell cell culture plates (24 well) were purchased from Millipore A/S (Copenhagen, Denmark). All the solvents and salts were purchased from Carlo Erba (Milan, Italy). Phosphate buffer pH 6.0 and pH 7.4 had the following composition (g/L): 7.97  $\text{KH}_2\text{PO}_4$ , 3.30  $\text{Na}_2\text{HPO}_4 \cdot 12\text{H}_2\text{O}$  and 0.60  $\text{KH}_2\text{PO}_4$ , 6.40  $\text{Na}_2\text{HPO}_4 \cdot 12\text{H}_2\text{O}$ , 7.42 NaCl respectively.

### 4.2.2. Determination of THA octanol/phosphate buffer solution PBS (pH 7.4 and 6.0) distribution coefficient (LogD)

LogD [152] values at pH 6.0 and 7.4 were determined using a new method, based on Nuclear Magnetic Resonance (NMR) spectroscopy. In particular, the method is based on localized  $^1\text{H}$  NMR spectroscopy, measuring simultaneously, in situ, the concentration of THA in both phosphate buffer (PBS) and octanol phases, without disturbing the interface [153]. Briefly, 300  $\mu\text{L}$  of THA solution (5mg/mL in PBS pH 6.0 or 7.4) were placed on the bottom of a standard 5 mm od NMR tube. 300  $\mu\text{L}$  of 1-Octanol were placed above the THA solution. After 72 hours (time required for equilibration [153]) spectra of the two phases were recorded simultaneously and

analyzed. The experiments were carried out on a Varian INNOVA 500 spectrometer operating at a proton frequency of 499.845 MHz and equipped with performax II gradient amplifiers. The water signal was suppressed using presaturation. The experiments were performed without deuterium lock, as no  $^2\text{H}$  was present in the solvents. A standard sample containing PBS and 10%  $\text{D}_2\text{O}$  was used for shimming and referencing purpose. The experiments were performed at 25 °C.

#### **4.2.3. Preparation of liposomes**

Liposomes were prepared by a modified Reverse-Phase Evaporation Vesicles technique [154-156]. Different unloaded ( $\alpha$ ,  $\beta$ ,  $\gamma$  and  $\delta$ ) and THA loaded (A, B, C and D) liposome formulations were prepared according to the following lipid compositions (molar percentage): L- $\alpha$ -phosphatidylcholine from egg yolk (EPC) 60% and cholesterol (CHO) 40% for Lipo A and Lipo  $\alpha$ ; EPC 60%, Toc 13% and CHO 27% for Lipo B and Lipo  $\beta$ ; EPC 60%,  $\Omega 3$  13% and CHO 27% for Lipo C and Lipo  $\gamma$ ; EPC 60%, Toc 13%,  $\Omega 3$  13% and CHO 14% for Lipo D and Lipo  $\delta$ . Briefly, lipid mixture (800  $\mu\text{mol}$  in total) was dissolved in 75 mL of diethyl ether; 25 mL of physiological buffered solution (0.9% NaCl, pH 6.0 and 295 mOsm/L) of THA (0.45 mg/mL) were then added to the organic solution and the resulting biphasic system was emulsified by sonication at 4 °C in a bath-type ultrasonic cleaner, until the water/oil emulsion became clear. Finally, the organic solvent was removed under reduced pressure (Buchi Rotavapor R-200, Flawil, CH; 400 bar, 15°C, 210 rpm). When the majority of the solvent was removed, a significant increase in viscosity (gel-like) appeared and the emulsion subsequently converted into an aqueous liposomal dispersion. The time needed to achieve this conversion was dependent on the lipid composition; in fact, a more rapid inversion was obtained for formulations Lipo A and Lipo  $\alpha$  (20 min) with respect to the other formulations (60 min); all liposomal dispersions were diluted 1:1 with physiological buffer solution. In order to obtain small and homogeneous liposomes, all the suspensions were sequentially extruded through 800 nm, 400 nm, 200 nm and 100 nm pore size polycarbonate filter

**Table 4.1 Final lipid concentrations in liposome formulations**

LIPOSOMES	EPC (mM)	$\Omega$ -3 <sup>a</sup> (mM)	Toc (mM)	CHO (mM)
Lipo A	9.60			6.40
Lipo $\alpha$	9.60			6.40
Lipo B	9.60		2.08	4.32
Lipo $\beta$	9.60		2.08	4.32
Lipo C	9.60	2.08		4.32
Lipo $\gamma$	9.60	2.08		4.32
Lipo D	9.60	2.08	2.08	2.24
Lipo $\delta$	9.60	2.08	2.08	2.24

<sup>a</sup> $\Omega$ 3 = 60% eicosapentaenoic acid (EPA), 40% docosahexaenoic acid (DHA)

(Nucleopore, Pleasanton, CA), by using an extruder (DE; Liposo-Fast<sup>TM</sup>-Basic, Avestin Inc., Ottawa, Canada). For all the extruded liposomes the encapsulation efficiency was evaluated (see section 2.4). The free THA was removed from loaded liposomes by ultracentrifugation (4 hours, 42029 g and 4°C). The liposomal fractions were washed twice and then diluted to 50 mL with fresh physiological buffer solution. Final lipid concentration is reported in Table 4.1. These liposomes were used for the subsequent experiments.

#### **4.2.4. Liposome size distribution and zeta-potential measurements**

Liposome size distribution was measured by PCS (Photon-Correlation Spectroscopy) using an instrument (Brookhaven 90-PLUS) with He–Ne laser beam at a wavelength of 532 nm (scattering angle of 90°). For size measurements, liposome suspensions were diluted (1:400; v/v) in ultra-filtered physiological buffer solution. The dispersions were stirred at 25°C for 30 min and then analyzed without filtering. Zeta-potential measurements were carried out at 25°C on a Malvern Zetasizer 3000 HS

instrument, after the same dilution. Both liposome average size and zeta-potential measurements were run six times.

#### 4.2.5. Determination of encapsulation efficiency

Encapsulation efficiency was determined after liposome extrusion. Separation technique of liposomal and non-liposomal THA is based upon the property of liposomes to cross reversed-phase C18 silica gel cartridges without being retained,

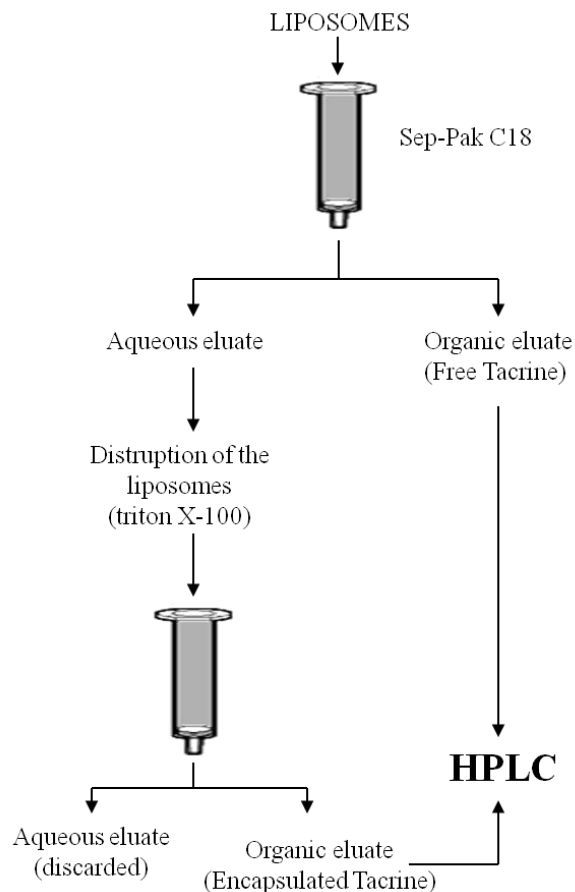


**Fig. 4.2 Solid Phase Extraction (SPE) diagram used to separate liposomal and non-liposomal encapsulated THA**

while THA retained on the stationary phase can be eluted with methanol as illustrated in Fig. 4.2 [157]. Briefly, liposome suspension (50  $\mu\text{L}$ ) was passed through a Sep-Pak  $\text{C}_{18}$  cartridge (Waters Corporation, Milford, Massachusetts, USA) conditioned with 3 mL methanol and 6 mL physiological buffer solution at pH 9.5. The eluate containing liposomal THA was collected in a 10-mL tube containing 100  $\mu\text{L}$  of 20% (v/v) Triton X-100 in water; then 4 mL of physiological buffer solution at pH 9.5 was finally passed through the cartridge and all eluates were collected together in the Triton X-100-containing tube. Finally, the non-liposomal THA was eluted with two portions of 1.5 mL of methanol and recovered by evaporation in a rotavapor. The liposome-associated THA-fraction recovered in Triton X-100 was vortex-mixed vigorously, sonicated for 30 minutes at 60°C in a bath-type cleaner and slowly passed through a new conditioned Sep-Pak  $\text{C}_{18}$  cartridge. The aqueous eluate was discarded, while THA was eluted with two portions of 1.5 mL of methanol. The methanol eluate was collected in a tube and recovered by evaporation in a rotavapor. The two dried residues were reconstituted with 10 mL of mobile phase and liposomal and non-liposomal THA was determined by HPLC analysis using Shimadzu (Milan, Italy) LC-10ATVP chromatographic pump and a Shimadzu SPD-10AVP UV-Vis detector set at 240 nm. Separation was obtained on a Phenomenex (Torrance, CA, USA) Sinergy Fusion-RP 80A (150 x 4.6 mm I.D., 5  $\mu\text{m}$ ) coupled to a Phenomenex (Torrance, CA, USA) SecurityGuard C18 guard cartridge (4 x 3.0 mm I.D., 5  $\mu\text{m}$ ). The mobile phase was composed of a mixture of acetonitrile - methanol - pH 6.5 solution of triethylamine (1.4%) 20:10:70 (v/v). The flow rate was 0.4 mL/min and manual injections were made using a Rheodyne 7125 injector with a 20  $\mu\text{L}$  sample loop. A calibration curve was set up in the 0.05–5.00  $\mu\text{g ml}^{-1}$  range; good linearity was found ( $r^2 = 0.9998$ ).

Encapsulation Efficiency % was calculated according to the following equation:

$$\text{EE\%} = [(\text{THA}_{\text{in}} / \text{THA}_{\text{in}} + \text{THA}_{\text{out}})] \times 100 \quad (1)$$

where  $\text{THA}_{\text{in}}$  and  $\text{THA}_{\text{out}}$  are the amount of liposomal and non-liposomal THA, respectively.

#### **4.2.6. *Ex-vivo Mucoadhesion Studies***

The mucoadhesion behaviour was tested determining the residence time on sheep nasal mucosa as described elsewhere [158]. Briefly, sheep nasal mucosa was obtained from local slaughterhouses and the time from slaughter to removal of the nose was 5 min maximum. The excised tissue was stored directly on ice during transportation to the laboratory, where turbinates were fully exposed by a longitudinal incision through the nose and the mucosa carefully removed from the underlying bone [159]. To maintain the freshness of the specimen as far as possible, mucoadhesion studies were started immediately after the mucosa samples were excised and carried out within 3 hours of procurement of the mucosa; in addition, to ensure the tissue viability, experiments were conducted in oxygen-enriched atmosphere, blowing on the nasal mucosa a gas mixture composed by 95% of O<sub>2</sub> and 5% of CO<sub>2</sub>. An exact amount of liposome dispersions (200 µL) were placed on the mucosal surface (2.0 cm<sup>2</sup>), which was attached, with cyanoacrylate glue, over a polyethylene support fixed in an angle of 30° relative to the horizontal plane. Immediately after liposomes placement on mucosal surface, the mucosa was thoroughly washed with physiological buffered solution pH 6.0, at the rate of 0.5 ml/min using a peristaltic pump. At predetermined time intervals, samples of 100 µl were taken and replaced by fresh medium. Then, samples were treated with Triton X-100 and the amount of THA was analysed by HPLC, using the same conditions previously employed.

Mucoadhesion (%) was calculated according to the following equation:

$$\text{Mucoadhesion (\%)} = [(M_0 - M_p) / M_0] \times 100 \quad (2)$$

Where M<sub>0</sub> is the total drug and M<sub>p</sub> is the drug recovered in the perfusate at each time.

#### **4.2.7. Evaluation of THA apparent permeability ( $P_{APP}$ ) using the Phospholipid Vesicle-based Permeation Assay (PVPA)**

PVPA is a technique based on deposited liposomes on filter supports in culture inserts, forming a barrier for transport studies. Phospholipid vesicle based barriers were prepared according to the protocol developed by Flaten GE. et al. [160,161]. Briefly, mixed cellulose ester filters (pore size 0.6  $\mu\text{m}$ , Millipore A/S, Copenhagen, Denmark) were sealed by heat (150°C, 25s) on Millicell filter holders (custom-produced by Millipore A/S, Copenhagen, Denmark) using custom-made sealing machine (IBR-Ingenieurbüro, Waldkirch, Germany). Liposomes were prepared by film hydration/filter extrusion using egg phosphatidylcholine Lipoid E80 (Lipoid GmbH, Ludwigshafen, Germany). Liposome dispersion was extruded through 0.8 and 0.4  $\mu\text{m}$  polycarbonate membrane filters (Millipore) to obtain liposomes with two different mean sizes, which were subsequently spun down (first the liposomes with size of 0.4  $\mu\text{m}$  and subsequently those with size of 0.8  $\mu\text{m}$ ) on filter inserts. Finally, to promote the liposome fusion and obtain tight barriers, inserts were frozen at -80°C and thawed at 65°C. Permeation studies were performed over 200 min. Briefly, phospholipid vesicle based barriers were pre-incubated with phosphate buffer pH 6.0 for 60 min. Subsequently, inserts were moved to a new plate with the wells filled (acceptor chambers) with 600  $\mu\text{L}$  phosphate buffer pH 6.0; at time zero 400  $\mu\text{L}$  of THA solution (65 $\mu\text{g}/\text{mL}$ , 0.9% NaCl) or 400  $\mu\text{L}$  of loaded liposomes (A, B, C and D) were added to each insert (donor chamber). At predetermined time intervals (30, 60, 80, 100, 120, 140, 160, 180 and 200 min) inserts were moved to a new plate in order to assure sink condition. Samples of 300  $\mu\text{L}$  were taken from each acceptor chamber and the amount of permeated THA was analyzed by HPLC as previously described. The cumulative amount of permeated THA was plotted against the time obtaining a curve. The slope of the linear part, representing steady state flux (J), was used to calculate the apparent permeability coefficient ( $P_{APP}$ ) according to the following equation:

$$P_{APP} (\text{cm/s}) = J / Cd \times A \quad (3)$$

where  $A$  is the area of the insert used and  $C_d$  is the initial donor concentration. Electrical resistance (ER) across the barrier and the calcein flux were measured in order to test the integrity of the membrane. The ER of the lipid barriers was measured using a Millicell-ERS (Millipore GmbH, Schwalbach, Germany) immediately after completion of the permeation studies. Calcein flux was also evaluated as a parameter to define the integrity of the barriers; in fact, calcein at pH 7.4 is charged, so its  $P_{APP}$  should be very low. Barriers were considered tight when the ER values at the end of permeation experiment were between 100% and 90% of the initial ER values and the calcein  $P_{APP}$  values were lower than  $0.1 \times 10^{-6}$  cm/s. The experiments were performed in six parallels for each liposome formulation and THA solution.

#### ***4.2.8. Evaluation of THA permeability (P) using Ex-vivo Sheep Nasal mucosa Permeation Assay (ENSPA)***

Permeation studies were conducted using sheep nasal mucosa obtained as previously described. The excised nasal mucosa was put between the donor and receptor compartments of the Franz diffusion cell with a diffusional area of  $1.5 \text{ cm}^2$ . The mucosal surface of the nasal mucosa faced the donor compartment and the serosal surface faced the receptor compartment. At time zero, 150  $\mu\text{L}$  of loaded liposomes (A, B, C and D) or 150  $\mu\text{L}$  of THA solution (65  $\mu\text{g}/\text{mL}$ , 0.9% NaCl) were placed on the mucosa in the donor compartment. The receiver phase (6.0 mL of PBS pH 6.0, maintained at  $37^\circ \text{C}$  by means of a surrounding jacket and oxygen-enriched by bubbling a mixture of  $\text{O}_2\text{-CO}_2$  (95-5%) for 15 minutes before being inserted in the receiver compartment), was stirred constantly and at predetermined time intervals (10 minutes) samples of 100  $\mu\text{l}$  were taken and replaced by fresh medium. The amount of THA in the receiving phase was analysed by HPLC as previously described. The studies were carried on for 80 minutes. Flux data were plotted as the cumulative amount of drug diffused from the mucosal to the serosal side of epithelium versus time. The permeability coefficient (P) was calculated using the equation (3) previously described.

#### **4.2.9. Assessment of tacrine uptake/association in SH-SY5Y cell line**

Human neuroblastoma SH-SY5Y cell line was routinely grown at 37°C in a humidified incubator with 5% CO<sub>2</sub> in DMEM supplemented with 10% FCS, 2 mM glutamine, 100 U/ml penicillin and 100 µg/ml streptomycin as previously reported [162]. Cells with 15–20 passages were used. SH-SY5Y cells were seeded in culture dishes (size 100 mm) at 1.0 10<sup>6</sup> cells/dish. To evaluate the cell-associated levels of THA, SH-SY5Y cells were treated with 35 µL of loaded liposomes (Lipo A, Lipo B, Lipo C and Lipo D) / mL of medium (corresponding at a final THA concentration of 10 µM) or THA solution 10 µM for 24 h. Cells were washed four times with ice-cold PBS to ensure not associated THA removal and rapidly lysed on ice using aqueous methanol (50% v/v) containing HCl (0.1%). SH-SY5Y cells were scraped off and left on ice to solubilize for 45 min, then centrifuged at 2000 g for 5 min at 4 °C to remove unbroken cell debris and nuclei. THA contained in the supernatants was determined by HPLC analysis using Beckman Coulter (Milan, Italy) 125 S pump Solvent Module and a Shimadzu Fluorescence Detector Model RF-551 (excitation: 330nm and emission: 365nm). Separation was obtained on Beckman Coulter (Milan, Italy) Ultrasphere ODS (4.6 mm x 25 cm, 5 µm). The mobile phase used was the same as previously described (section 2.4). The protein concentration in the supernatants was determined by the Bio-Rad Bradford protein assay (Bio-Rad Laboratories, Hercules, CA, USA).

#### **4.2.10. Statistical analysis**

Each experiment was performed at least six times, and all values are represented as means ± standard error of the mean (SEM). One-way analysis of variance (ANOVA) was used to compare differences among data sets. Generally, values P < 0.05 were considered to be statistically significant.

### 4.3. Results and discussion

#### 4.3.1. Evaluation of THA LogD

The distribution coefficients (LogD) of THA were calculated by dividing the total area underneath THA aromatic hydrogen peaks in the spectrum recorded in the octanol phase with those recorded in the PBS phase (Fig. 4.3). As expected, LogD values were negative suggesting that THA can locate mainly in the aqueous phase of a liposome system. Moreover, the LogD value obtained with pH 7.4 was higher (-0.617) than pH 6.0 (-0.978) accordingly to the higher ionization degree of THA in the acidic environment. On this basis, the Reverse-Phase Evaporation Vesicles technique followed by extrusion (French press) was chosen for liposome preparation obtaining unilamellar vesicles characterized by an increased trapped aqueous volume (LUV) and thus increased encapsulation efficiency. In addition, aqueous solution (0.9% NaCl, pH 5.95 and 295 mOsm/L) was used for liposome preparation in order to favour drug-phospholipids ionic interaction and greater drug loading.

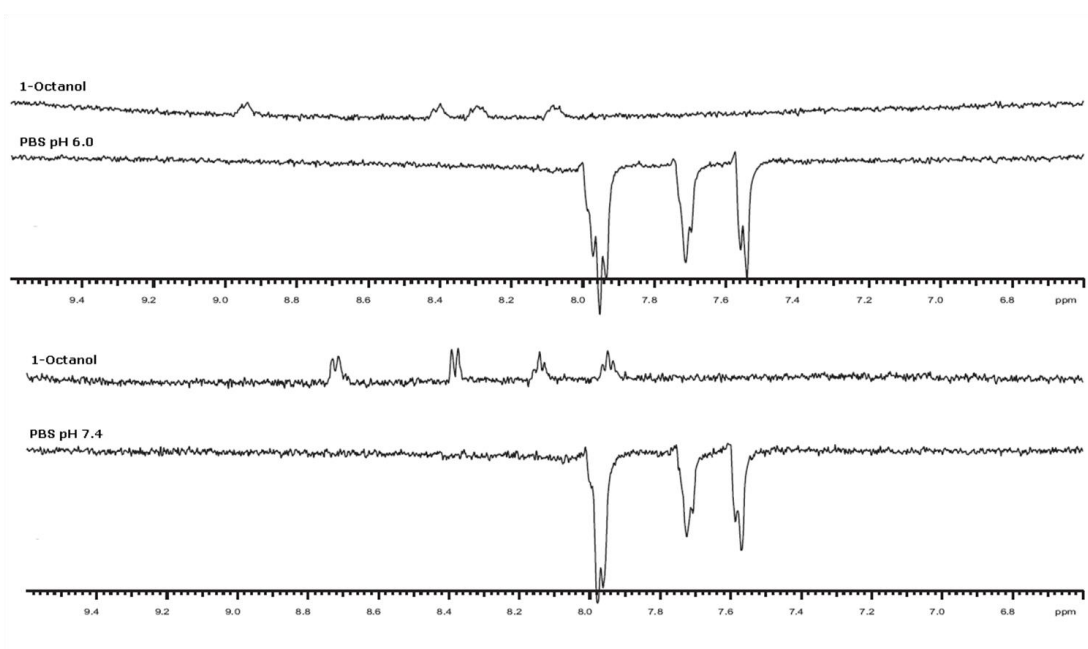


**Fig. 4.3**  $^1\text{H}$  NMR spectra of the aromatic protons of THA in 1-octanol and in phosphate buffer solution (PBS) at pH 7.4 and 6.0. The phase change is for display purposes only.

#### ***4.3.2. Physical properties of liposomes***

Size and charge of THA loaded and unloaded liposomes were investigated by measuring their mean size and polydispersity index (PI) as well as zeta potential (Z) and compared with THA encapsulation efficiency (EE%). The results are summarized in Table 4.2. After mechanical extrusion, all liposomal formulations showed low PI values below 0.25, which indicates good size homogeneity. No significant difference in mean size was seen between loaded and unloaded liposomes, while there were minor, yet significant, differences between the different formulations. The mean diameters of conventional liposome formulation (Lipo A and Lipo  $\alpha$ ) were lower than the mean diameters of liposomes containing Toc (Lipo B and Lipo  $\beta$ ) or Toc and  $\Omega 3$  (Lipo D and Lipo  $\delta$ ). We hypothesize that the presence of Toc could slightly increase liposome size due to an increased flexibility of the vesicles which could more easily cross the polycarbonate filter without being broken [163].

Zeta potential was negative for all studied liposomal formulations. In particular, Lipo  $\gamma$  and Lipo  $\delta$  which contain  $\Omega 3$  presented lower Z potential values than Lipo  $\alpha$  and Lipo  $\beta$ . This could also explain the increased encapsulation efficiency (Table 4.2) detected for Lipo C and Lipo D. The positively charged THA is expected to interact to a higher extent with a more negative liposome system.

Encapsulation efficiency values (Table 4.2) highlight that the technique and operating parameters used for liposome preparation were promising; in fact, the EE% (about 30% for all liposome formulations) was particularly high compared to others liposome formulations encapsulating drug with similar Log D and prepared with different techniques [164]. On the basis of EE% data and liposome dilution (50 mL), the final THA concentration in the liposomes formulation was 285.36  $\mu\text{M}$ , 304.91  $\mu\text{M}$ , 308.84  $\mu\text{M}$  and 313.35  $\mu\text{M}$  for Lipo A, B, C and D, respectively.

**Table 4.2 Mean Diameter ( $\phi$ ), Polydispersity Index (PI), Zeta Potential (Z) and Encapsulation Efficiency (EE%).**

	Unloaded				Loaded			
	Lipo $\alpha$	Lipo $\beta$	Lipo $\gamma$	Lipo $\delta$	Lipo A	Lipo B	Lipo C	Lipo D
$\phi$ (nm)	175.7 $\pm$ 0.7	197.2 $\pm$ 4.7	208.8 $\pm$ 4.5	190.6 $\pm$ 3.8	181.8 $\pm$ 3.0	192.4 $\pm$ 2.9	179.3 $\pm$ 8.1	219.3 $\pm$ 4.2
PI	0.146	0.194	0.203	0.185	0.225	0.186	0.215	0.213
Z (mV)	-12.9 $\pm$ 0.8	-13.3 $\pm$ 1.9	-16.8 $\pm$ 0.2	-17.0 $\pm$ 1.3	-14.0 $\pm$ 1.1	-14.5 $\pm$ 0.6	-16.2 $\pm$ 1.7	-16.8 $\pm$ 0.9
EE%	/	/	/	/	29.77 $\pm$ 1.32	31.81 $\pm$ 1.62	32.22 $\pm$ 1.05	32.69 $\pm$ 1.39

Mean  $\pm$  SEM, n = 6

#### 4.3.3. *Ex-Vivo mucoadhesion study*

Mucoadhesion is an important property for a system which has to be administered by nasal route; it provides information on the permanence of a formulation on the nasal mucosa, contrasting the high mucociliary clearance, which has a speed of 5 mm/min in healthy humans (15-20 min to cross human nasal cavity) [165, 166]. Fig. 4.4 shows THA solution and loaded liposome (A, B, C and D) residence times on excised sheep nasal mucosa. After 30 minutes from application, only 19.41  $\pm$  1.45% of THA remained on nasal mucosa, highlighting poor mucoadhesivity of the free drug and the need to encapsulate THA in a system able to increase residence time and, therefore, favour its permeation. Moreover, all liposome formulations presented higher mucoadhesion ability than THA solution ( $p < 0.001$ ), confirming the results obtained by Quinn PJ [151]. Particularly, after 30 minutes from application of Lipo A, Lipo B, Lipo C and Lipo D on the mucosa, the percentage of THA that remained adhered on nasal mucosa was 68.54  $\pm$  2.07 %, 72.85  $\pm$  1.95 %, 67.91  $\pm$  3.24 % and 71.23  $\pm$  2.49 %, respectively. In comparison to others liposome formulations Lipo A showed lower mucoadhesion ability, which became significant after 90 minutes ( $p < 0.05$ ), suggesting that the presence of Toc and/or  $\Omega 3$  in the phospholipid vesicles can improve their interaction with the cell surface.

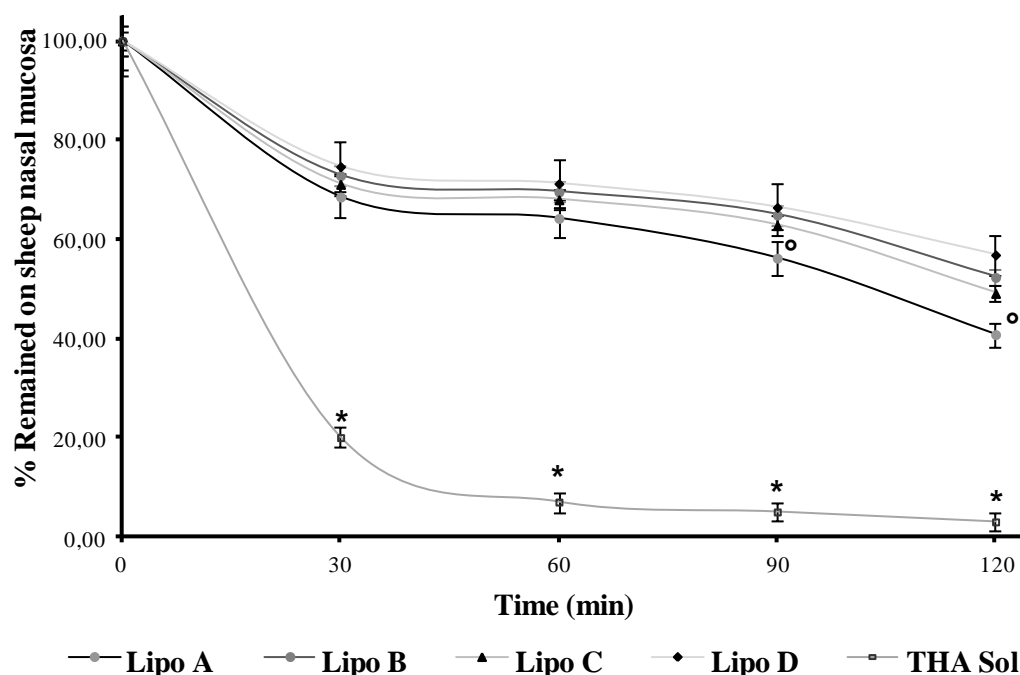


**Fig. 4.4** Percentage of THA remained on nasal mucosa after the application of THA solution, Lipo A, Lipo B, Lipo C and Lipo D at 30, 60, 90 and 120 minutes. Data are means  $\pm$  SEM of four independent experiments. \* $p < 0.001$  with respect to others liposome formulations,  $^{\circ}p < 0.05$  with respect to others liposome formulations.

#### 4.3.4. THA permeability

With regard to in-vitro permeation assay (PVPA), the trans-barrier electrical resistance (ER) was evaluated in order to assess the phospholipid vesicles barrier integrity in presence of the formulations. The electrical resistance after the permeation assay (data not shown) was in all cases found slightly lower (by about 10%) as compared to the one before, so the barriers could be considered intact. In addition, the apparent permeability ( $P_{APP}$ ) of the hydrophilic marker calcein across phospholipid vesicles barrier was  $0.07 \pm 0.01 \times 10^{-6}$  cm/s, further confirming the barrier integrity. Fig. 4.5 shows the permeability values ( $P_{APP}$  and  $P$ ) of THA in solution and THA encapsulated in the different liposomal formulations, obtained using in-vitro (PVPA) and ex-vivo (ENSPA) assays. These data show that THA encapsulation in liposomal formulations improved drug permeability. As can be observed in Figure 4.5, the presence of Toc in Lipo B and  $\Omega 3$  in Lipo C further

significantly improved THA permeability ( $p < 0.05$ ) with respect to Lipo A. This behaviour suggests an enhancing effect of both tocopherol and poly-unsaturated fatty acids, when incorporated in the liposomal formulations. Moreover, this effect seems to be synergistic; in fact the best permeation profile and consequently the best  $P_{APP}$  was owned by Lipo D.

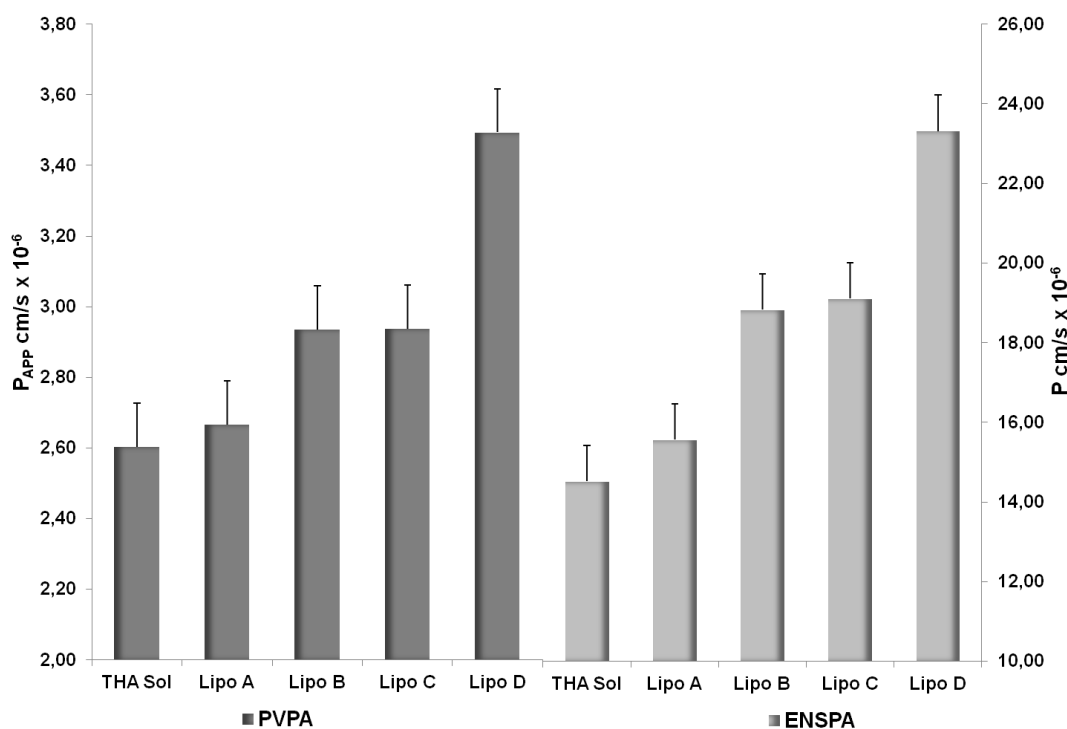


**Fig. 4.5** THA apparent permeability ( $P_{APP}$ ,  $\text{cm/s} \times 10^{-6}$ ) and THA permeability ( $P$ ,  $\text{cm/s} \times 10^{-6}$ ) evaluated using (PVPA) Phospholipid Vesicle based Permeation Assay and (ENSPA) Ex-vivo Sheep Nasal Permeation Assay, respectively. Data are means  $\pm$  SEM of six independent experiments. \* $p < 0.05$  vs THA solution, ° $p < 0.05$  vs Lipo A, # $p < 0.05$  vs Lipo C and Lipo B.

THA permeability values obtained using ENSPA are reported in Fig. 4.5. These values were higher than those obtained with PVPA accordingly to the structural and functional differences between the barriers used in the two permeation assays. In fact, the phospholipid vesicle barriers used for PVPA consist of a stack of multiple bilayers, where drugs permeate exclusively via passive diffusion. On the contrary, the sheep nasal mucosa employed for ENSPA, represents a cellular barrier composed, which allows to measure not only transcellular passive diffusion but also

paracellular passive diffusion and active transport. Although, the absolute permeability values were different for the two assays employed, permeability trend was very similar following the order: Lipo D > Lipo C ~ Lipo B > Lipo A ~ THA solution. Plotting the two data sets in a graph a good linear correlation ( $R^2 = 0.9715$ ) was obtained, indicating good comparability between the two methods (not shown). Furthermore, this behaviour indicates that THA permeability differences between the various liposomal formulations most likely are due to changes in the passive diffusion and the enhancing effect of Toc and/or  $\Omega 3$  might be due to a modulation of barrier characteristics.

#### **4.3.5. THA neuronal uptake/association**

The main assumption for the direct transport across olfactory nerve to the central nervous system is drug absorption into olfactory neurons [167, 168]. This study was thus performed using neuronal cells with the aim to evaluate liposome ability to promote THA uptake/association.

Fig. 4.6 shows THA associated level in human neuroblastoma SH-SY5Y cell line, after incubation with THA solution or with loaded liposomes. In particular, the amount of THA (expressed as nmol of THA recovered for mg of cellular protein) associated to neurons after treatment with THA solution, Lipo A, Lipo B, Lipo C and Lipo D, was:  $0.42 \pm 0.02$  nmol/mg protein,  $0.74 \pm 0.04$  nmol/mg protein,  $0.93 \pm 0.04$  nmol/mg protein,  $0.82 \pm 0.05$  nmol/mg protein and  $1.08 \pm 0.05$  nmol/mg protein, respectively. Data highlight that drug uptake/association was greater for THA loaded liposomes compared to THA solution ( $p < 0.001$ ), confirming the results obtained with permeability studies and emphasizing the benefits to include drug in liposomal vesicles. Significant difference in THA uptake/association is also present between the various liposomal formulations. Particularly, liposomes enriched with Toc (Lipo B and Lipo D) presented a greater uptake/association compared to Lipo A and Lipo C ( $p < 0.05$ ). Furthermore, it is possible to note that the concomitant presence of Toc

and  $\Omega 3$  in Lipo D allowed obtaining the best uptake performance, confirming once again the synergistic enhancing effect of the two substances.

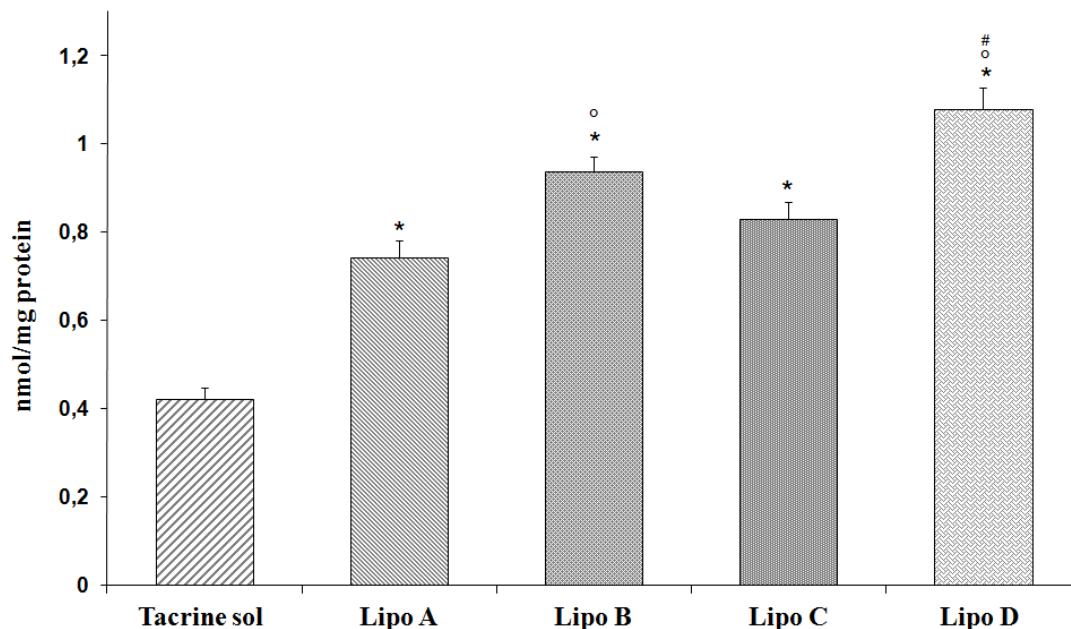


**Fig. 4.6** THA uptake in human neuroblastoma SH-SY5Y cell line. Data are reported as nmol of THA per mg of protein recovered in the supernatant of lysed cells and are means  $\pm$  SEM of six independent experiments. \* $p < 0.001$  vs THA solution, ° $p < 0.05$  vs Lipo A and Lipo C, # $p < 0.05$  vs Lipo B.

#### 4.4. Conclusions

In summary, the presented data allow us to conclude that the inclusion of THA within liposomal formulations as well as the incorporation of Toc and/or  $\Omega 3$  in the liposomal formulation enhances the permeability both across a phospholipid vesicle-based permeation barrier and ex-vivo sheep nasal mucosa. Furthermore, the liposome formulation strategy resulted in enhanced mucoadhesion, making it promising for nasal administration. In addition to these features, Toc has promising antioxidant and neuroprotective effect (studied in detail in chapter 5). For these reasons, we can conclude that these new multifunctional liposomes may be potentially useful in AD treatment.

**5. MULTIFUNCTIONAL LIPOSOMES FOR DELIVERY OF THE ANTI-ALZHEIMER DRUG TACRINE HYDROCHLORIDE BY THE NASAL ROUTE. PART 2: TOCOPHEROL LATERAL DIFFUSION AND NEUROPROTECTIVE EFFECT EVALUATION**

---

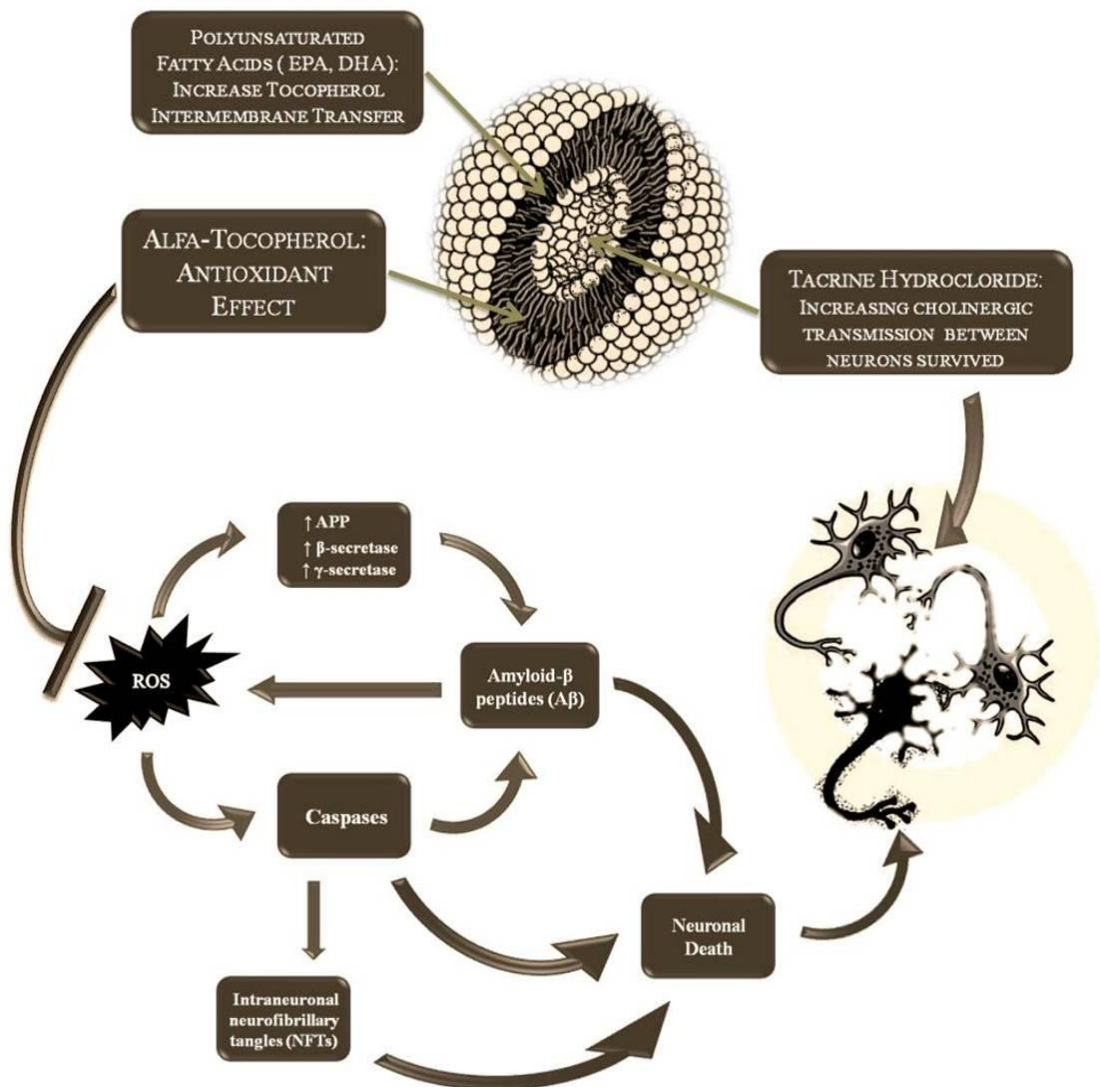


**Fig. 5.1 Graphical Abstract. Multifunctional liposomes convey Tacrine Hydrochloride and also have an antioxidant effect due to the presence of Tocopherol between their excipients.**

## 5.1. Introduction

Alzheimer's disease (AD) the most common form of dementia among older people, is characterized by the breakdown of connections between neurons and their eventual death [169]. Neuropathological examination of the AD brain shows the presence of characteristic markers such as intraneuronal neurofibrillary tangles (NFTs) composed of hyperphosphorylated tau protein and senile plaques, which are due to the deposition of amyloid- $\beta$  peptides ( $A\beta$ ), derived from the altered cleavage, operated by  $\beta$ -secretases (BACE1) and  $\gamma$ -secretases (proteic complex composed by Presenilin 1 (PS1) and 2 (PS2), and mature Nicastrin (APH-1)), on the  $A\beta$  precursor protein (APP), resulting in over production and aggregation of neurotoxic forms of  $A\beta$ . The relationships between  $A\beta$  and the pathogenesis of the disease seems well established. In fact,  $A\beta$  aggregates are neurotoxic and also promote the hyperphosphorylation of tau protein, thus causing before neuronal dysfunction and subsequently neuron death [170-172]. Moreover, the possibility that soluble forms of  $A\beta$ , including profibrils and oligomers, may also be more toxic than  $A\beta$ , has recently been taken into account. In fact, the presence of soluble  $A\beta$  increases the caspases activation [173]. Caspases are a family of serine-aspartyl proteases whose activation normally leads to cell apoptosis. Caspases are involved in the cleavage of numerous proteins, including APP, presenilin (PS1, PS2) and tau [174, 175], which, as mentioned above, are involved in AD. Recently, has been shown that their activation does not necessarily conduct neurons to the apoptosis process; in fact, caspases can be activated for long time without neuronal death [176] carrying out their deleterious actions on neurons and promoting the AD progression [177].

Based on these notions, oxidative stress (OS) is increasingly taking a key role in the pathogenesis and progression of several neurodegenerative disorders including AD. OS and  $A\beta$  are closely intertwined; particularly, OS increases the production of  $A\beta$  [178], due to the increase of BACE1 and PS1 expression and activity [179], and  $A\beta$  promotes OS in-vivo and in-vitro [180], creating a vicious cycle that forwards the disease. In addition, is well known that reactive oxygen species (ROS) activate the caspases with everything that goes with it.

Nowadays, the approved AD therapy is based on the administration of acetylcholinesterase (AChE) inhibitors (tacrine hydrochloride, rivastigmine and

donepezil) able to increase acetylcholine (ACh) levels in the cholinergic synapses [181]. Indeed, knowing the multifactorial nature of AD, would be desirable to combine the approved AD therapy with the treatment of the OS, which is one of the most critical factor for the AD progression.

Alpha-Tocopherol (Toc) is the primary form of vitamin E, one of the earliest-known and best-studied vitamins, which its major role is regarded to be as an antioxidant acting to prevent free radical damage to tissues and specifically to unsaturated lipids, which are particularly abundant in the brain [182-184]. In fact, brain is very vulnerable to OS due to its high oxygen consumption, high polyunsaturated fatty acids concentration and relatively low levels of antioxidants; this condition is much more pronounced in the elderly and in AD patients [178, 185].

The inclusion of Toc in the liposome phospholipid bilayer has been extensively studied. Peter J. Quinn [186] has highlighted as Toc influences the stability reducing the drug leaking from liposomes. We reported in the first part of this article that liposomes encapsulating Toc can improve the mucoadhesion properties and permeability of THA, also increasing neuronal uptake. In addition to these vesicle structural improvements, the inclusion of Toc can enriches the function of liposomes, which would no longer be only a drug's carrier but also antioxidant liposomes able to carry out a more protective action. This is extremely important, especially in those diseases where the OS is strongly implicated and where the reduction of drug toxicity is needed, such as in the AD [187-190].

Another important factor for the brain health is its content in docosahexaenoic acid (DHA). Researcher have established that when the brain is rich in DHA, production of senile plaques is lower, with a decrease of characteristic symptoms of the disease [191]. Other studies have highlighted that in the AD patients the DHA concentration in blood cell is very low, on the contrary was seen that the DHA breakdown products in the blood were very high, concluding that in AD, DHA is being destroyed, realising inflammatory breakdown products and consequently decreasing its concentration in the brain [192]. It has been reported that encapsulating marine phospholipids, which are rich in DHA and eicosapentaenoic acid (EPA), in liposomes their oxidation is reduced and their biocompatibility is increased [193].

We suggest that antioxidant liposomes encapsulating a classical (AChE) inhibitors such as tacrine hydrochloride THA and enriched with DHA and EPA ( $\Omega 3$ ) could be useful as a multifunctional therapy for the AD, increasing THA bioavailability and performing a neuroprotective action. In the present study we tested the neuroprotection ability of several liposome formulations, in particular, the ability to protect the neuroblastoma SH-SY5Y cell line against  $H_2O_2$ -induced oxidative injury was evaluated, measuring the reduction of intraneuronal ROS production and the inhibition of Caspase-3 activation, following liposomes treatment.

The liposomes used have been previously prepared and characterized as regards drug loading, particle size, Z-potenzial, mucoadhesion to nasal mucosa, permeability and neuronal uptake. the results are reported in the chapter 4 of the thesis.

## 5.2. Materials and Methods

### 5.2.1. Materials

Tacrine hydrochloride (THA),  $\alpha$ -tocopherol, L- $\alpha$ -phosphatidylcholine from egg yolk and cholesterol were purchased from Fluka (Milan, Italy). Eicosapentaenoic acid and docosahexaenoic acid were obtained from Doosan Serdary Research Laboratories (Englewood Cliffs, NJ). Egg phosphatidylcholine, Lipoid E-80, was kindly provided by Lipoid GmbH (Ludwigshafen, Germany). Triton X-100, calcein, CellLytic M, 3-(4,5-dimethylthiazol-2-yl)-2,5-diphenyltetrazolium bromide (MTT), 20,70 dichlorodihydrofluorescein diacetate (DCFH-DA), H<sub>2</sub>O<sub>2</sub>, bovine serum albumin (BSA), dimethyl sulfoxide (DMSO), Dulbecco's modified Eagle's medium (DMEM), fetal calf serum (FCS), penicillin/streptomycin, were purchased from Sigma-Aldrich (Milan, Italy). Clear culture Transwell inserts (diameter 6.5 mm) and plates were obtained from Corning GmbH, Life Sciences (Wiesbaden, Germany). Clear Millicell cell culture plates (24 well) were purchased from Millipore A/S (Copenhagen, Denmark). All the solvents and salts were purchased from Carlo Erba (Milan, Italy). Phosphate buffer pH 6.0 and pH 7.4 had the following composition (g/L): 7.97 KH<sub>2</sub>PO<sub>4</sub>, 3.30 Na<sub>2</sub>HPO<sub>4</sub>\*12H<sub>2</sub>O and 0.60 KH<sub>2</sub>PO<sub>4</sub>, 6.40 Na<sub>2</sub>HPO<sub>4</sub>\*12H<sub>2</sub>O, 7.42 NaCl respectively.

### 5.2.2. Liposome Formulations and characterization

The composition of liposome formulations investigated in this part of the study (Lipo A, Lipo B, Lipo C and Lipo D) is summarized in Table 1. These were prepared by a modified Reverse-Phase Evaporation Vesicles technique; preparation and characterization are described in detail in Part 1 of this study. In particular, liposomes presented a mean diameter of approximately 200 nm and a slightly negative Z potential; not significant difference was found between the different liposome

formulations. The functional properties of the liposome formulation are reported in Table 5.1 Data highlighted the advantages of THA encapsulation liposomes compared to THA solution; in fact, an improvement in terms of permeability, mucoadhesion and neuronal uptake/association can be noted.

**Table 5.1 Liposome formulations, Mean Diameter ( $\phi$ ), Zeta Potential (Z), THA Permeability (P), Mucoadhesion and Neuronal uptake/association (N)**

	Lipid Concentration (mM)				THA Conc. ( $\mu$ M)	$\phi$ (nm)	Z (mV)	P (cm/s x 10 <sup>-6</sup> )	M	N (nmol/mg protein)
	EPC	$\Omega$ -3 <sup>a</sup>	Toc	CHO						
<b>Lipo A</b>	9.60			6.40	285.3	181.8 $\pm$ 3.0	-14.0 $\pm$ 1.1	15.56 $\pm$ 0.6	++	0.74 $\pm$ 0.04
<b>Lipo B</b>	9.60		2.08	4.32	304.9	192.4 $\pm$ 2.9	-14.5 $\pm$ 0.6	18.82 $\pm$ 1.0	+++	0.93 $\pm$ 0.04
<b>Lipo C</b>	9.60	2.08		4.32	308.8	179.3 $\pm$ 8.1	-16.2 $\pm$ 1.7	19.10 $\pm$ 0.9	+++	0.82 $\pm$ 0.05
<b>Lipo D</b>	9.60	2.08	2.08	2.24	313.3	219.3 $\pm$ 4.2	-16.8 $\pm$ 0.9	23.31 $\pm$ 0.8	+++	1.08 $\pm$ 0.05
<b>THA Sol</b>	/	/	/	/	/	/	/	14.51 $\pm$ 0.9	+/-	0.42 $\pm$ 0.02

<sup>a</sup> $\Omega$ 3 = 60% eicosapentaenoic acid (EPA), 40% docosahexaenoic acid (DHA); +++ excellent mucoadhesion, ++ good mucoadhesion and +/- poor mucoadhesion

### 5.2.3. Cell culture and treatments

Human neuronal-like SH-SY5Y cells were routinely grown at 37°C in a humidified incubator with 5% CO<sub>2</sub> in Dulbecco's modified Eagle's medium (DMEM) supplemented with 10% fetal bovine serum (FCS), 2mM glutamine, 100 U/ml penicillin and 100 mg/ml streptomycin, as previously reported [194]. Cells with 15–

20 passages were used. To evaluate neuronal viability and ROS formation, the SH-SY5Y cells were seeded in culture dishes (size 100 mm) at  $1.0 \times 10^6$  cells/dish. Experiments were carried out 24 h after cells seeding. SH-SY5Y cells were incubated for 24 h with different concentration of THA ( 0.01  $\mu$ M, 0.1 $\mu$ M, 1 $\mu$ M and 10 $\mu$ M) or with different volumes of loaded liposomes (Lipo A, Lipo B, Lipo C and Lipo D)/ml of medium (corresponding at a final THA concentration of 0.01  $\mu$ M, 0.1 $\mu$ M, 1 $\mu$ M and 10  $\mu$ M).

#### **5.2.4. Determination of neuronal viability**

Neuronal viability in terms of mitochondrial activity was evaluated with the colorimetric MTT assay, as previously described [195]. MTT is a substrate for intracellular and plasma membrane oxidoreductase, and its reduction is an indication of cellular metabolic activity. Active mitochondria of living cells can cleave MTT to produce formazan, whose amount is directly related to the number of living cells. Briefly, after SH-SY5Y cells incubation for 24 h with THA solution or loaded liposomes (detail are reported in the paragraph 2.3), the SH-SY5Y cells were washed with Hank's Buffered Salt Solution (HBSS) and then incubated with MTT (0.5 mg/mL) in HBBS for 30 minutes. After removal of MTT and further washing, the formazan crystals were dissolved in DMSO. The amount of formazan was measured at  $\lambda = 595$  nm with a microplate spectrophotometer (VICTOR3 V Multilabel Counter, Perkin-Elmer Wellesley, MA, USA). The mitochondrial activity as well the neuronal viability are expressed as percentage of control cells and calculated by the formula:

(absorbance of treated neurons/absorbance of untreated neurons) x 100.

### **5.2.5. Intracellular ROS formation**

The intraneuronal ROS generation measurement was quantified with the fluorescent probe DCFH-DA as a well-established compound to detect and quantify intracellular produced  $H_2O_2$ . The test is based on the conversion, in several steps, of the nonfluorescent DCFH-DA to the highly fluorescent compound 2',7'-dichlorofluorescein (DCF). First, DCFH-DA is transported across the cell membrane and deacetylated by esterases to form the non-fluorescent 2',7'-dichlorofluorescein (DCFH). This compound is trapped inside of the cells. Next, DCFH is converted to DCF through the action of peroxidase catalyzed by the presence of peroxidase [196]. Briefly, after SH-SY5Y cells incubation for 24 h with THA solution or loaded liposomes (detail are reported in the paragraph 2.3), cells were incubated with 5 mM DCFH-DA in HBSS for 30 min in the dark. After DCFH-DA removal and further washing, the cells were treated with  $H_2O_2$  200  $\mu$ M for 30 min and fluorescence was measured using a microplate spectrofluorometer (VICTOR3 V Multilabel Counter, Perkin-Elmer) ( $\text{exc} = 485 \text{ nm}$  and  $\lambda_{\text{em}} = 535 \text{ nm}$ ). Data are expressed as percent of cells exposed only to  $H_2O_2$ , calculated by the formula:

$(\text{Fluorescence of treated neurons} / \text{Fluorescence of untreated neurons}) \times 100$ .

### **5.2.6. Assessment of Neuroprotection**

Neuroprotection was qualitatively measured by the inhibition of Caspase-3 activation; in fact, the activation of this enzyme is closely linked to apoptosis, and then to cell (neuron) death. Briefly, SH-SY5Y cells were seeded on 15 mm diameter glass cover-slips and were treated with 35  $\mu$ L of loaded liposomes (Lipo A, Lipo B, Lipo C and Lipo D) / mL of medium (corresponding at a final THA concentration of 10  $\mu$ M) or THA solution (10  $\mu$ M) for 24 h. Then, cells were treated with  $H_2O_2$  200  $\mu$ M for 30 min and subsequently were fixed with 4% paraformaldehyde (PFA) in PBS, permeabilized for 5 min in 0.1% Triton X-100 (Sigma) in PBS and incubated overnight in 3% bovine serum albumin (BSA) in PBS containing the primary

antibody rabbit anti-activated caspase-3 1:500 (Chemicon, Millipore). Cells were then incubated for 2 h at room temperature with a secondary antibody conjugated with Alexa 546 (Invitrogen), mounted in Aqua Poly/Mount (Polysciences, Inc.), and analyzed by fluorescence microscopy. DAPI was used to visualize nuclei.

### ***5.2.7. Evaluation of $\alpha$ -Tocopherol intermembrane transfer***

Tocopherol intermembrane transfer was evaluated quantifying the amount of tocopherol diffused from the liposome formulation (A, B, C and D) to an acceptor system represented by Phospholipid Vesicle barrier (PVb) (barriers used for the in-vitro permeability assay reported in detail in the Part 1 of this study). The permeation of free THA was used as negative control. Briefly, after phospholipid vesicle based permeation assay (PVPA), barriers were carefully washed, three times, with phosphate buffer pH 7.4; subsequently they were treated with 1 mL of 1% v/v triton X100 methanolic solution to break and to solubilize lipid vesicles. Finally, the amount of transferred tocopherol was determined by HPLC analysis [197] using a Waters 2695 HPLC with UV detection set at 295 nm (Waters 2487 Dual  $\lambda$  Absorbance Detector). Separation was performed by an Acclaim 120 (C18, 5  $\mu$ m particle size, 120 Å, 4.6 mm  $\times$  250 mm) column. The mobile phase was composed of a mixture of methanol-water 98:2 (v/v) and the flow rate was 1.5 mL/min. The phospholipid concentration in the barrier was determined by colorimetric phospholipase D-based serum-phospholipid assay [198]. The experiments were performed six times for each loaded liposome formulation and THA solution.

### 5.3. Results and discussion

#### 5.3.1. Effect of THA and loaded liposomes on neuronal viability

SH-SY5Y cells were treated with increasing concentration of THA in solution or loaded in liposomes ( 0.01  $\mu\text{M}$ , 0.1 $\mu\text{M}$ , 1 $\mu\text{M}$  and 10 $\mu\text{M}$ ) for 24 h to investigate their effect on neuronal viability. In Fig. 5.2 (.1, .2, .3, .4 and .5) data obtained by the MTT viability test are reported. From the data it can be deduced that THA solution, in the range of concentrations used in the test, was not neurotoxic. In fact, the neuronal viability, expressed as percentage of control cells (untreated) at different THA concentration, was always close to 100%, without significant difference. Also the loaded liposomes (Lipo A, LipoB, Lipo C and Lipo D) at the same THA concentrations used for the test with THA solution, were not neurotoxic being neuronal viability close to 100%.

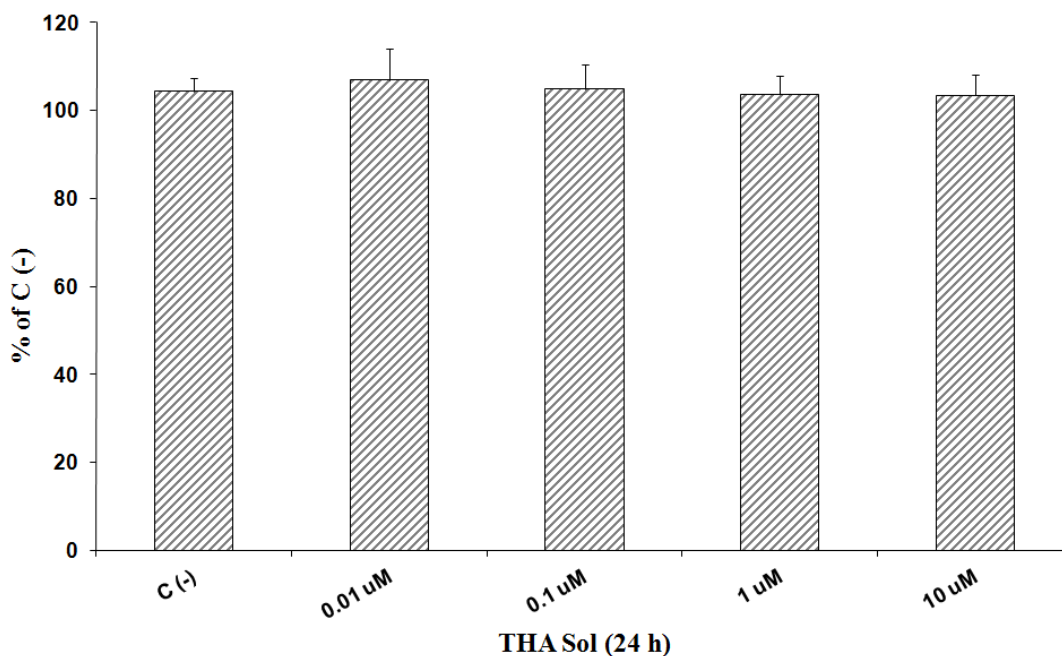


Fig. 5.2.1 MTT assay of THA sol. Cells were exposed to different THA concentrations (0-10  $\mu\text{M}$ ) for 24 h. Cell viability was assessed by MTT reduction. Cell viability is comparable to control cells C(-). Data are means  $\pm$  SEM of six independent experiments.

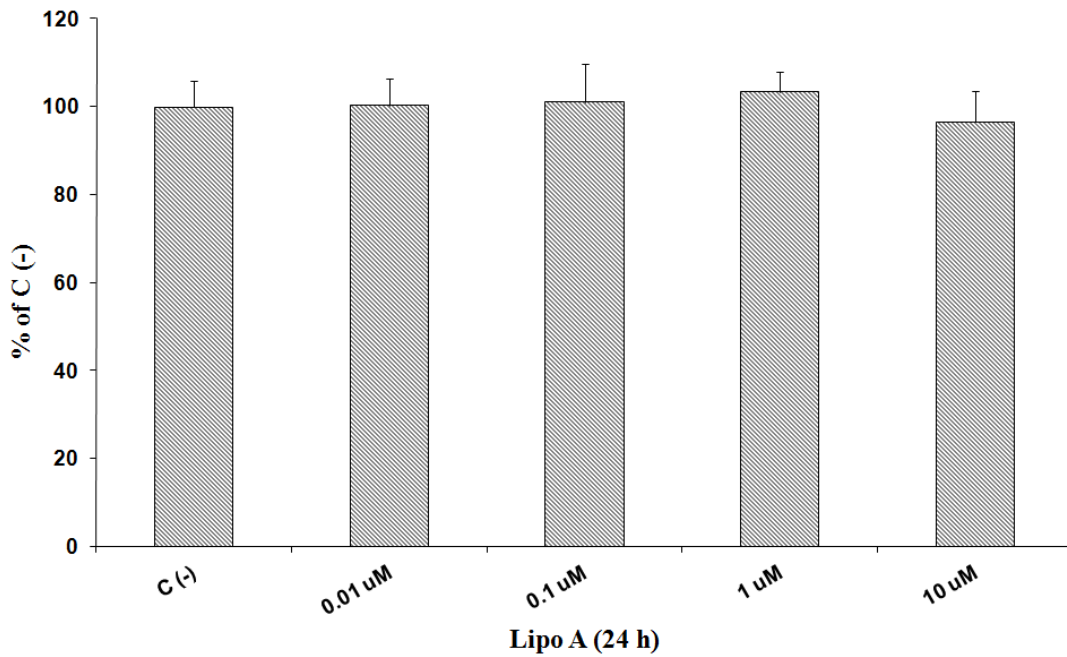


Fig. 5.2.2 MTT assay of Lipo A. Cells were exposed to Lipo A with the same content in THA (0-10  $\mu$ M) for 24 h. Cell viability was assessed by MTT reduction. Cell viability is comparable to control cells C(-). Data are means  $\pm$  SEM of six independent experiments.

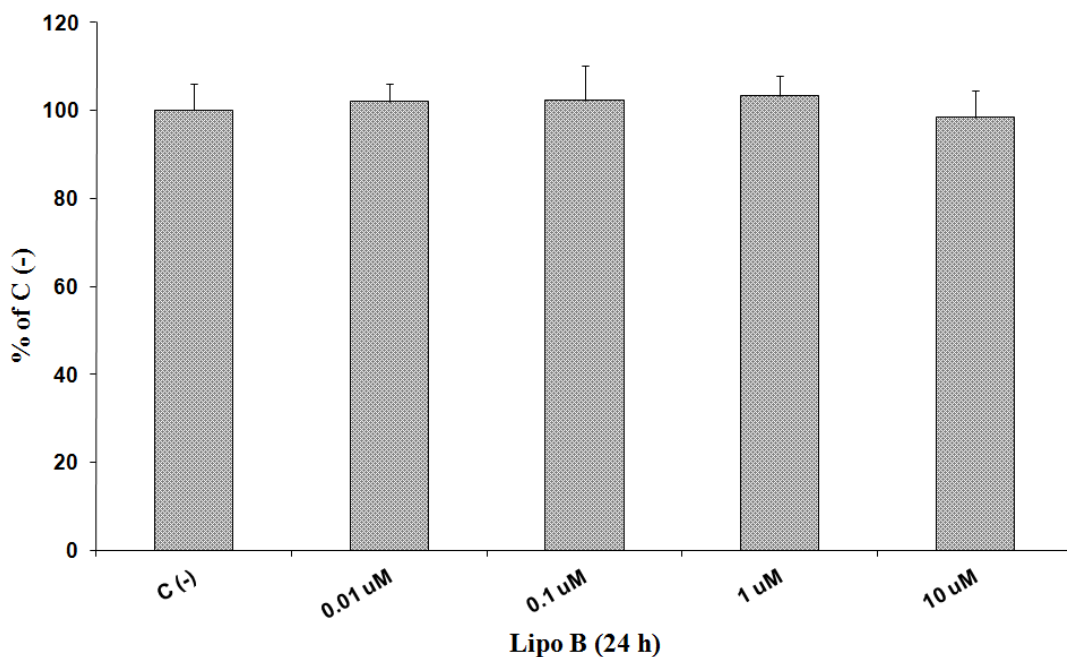


Fig. 5.2.3 MTT assay of Lipo B. Cells were exposed to Lipo B with the same content in THA (0-10  $\mu$ M) for 24 h. Cell viability was assessed by MTT reduction. Cell viability is comparable to control cells C(-). Data are means  $\pm$  SEM of six independent experiments.

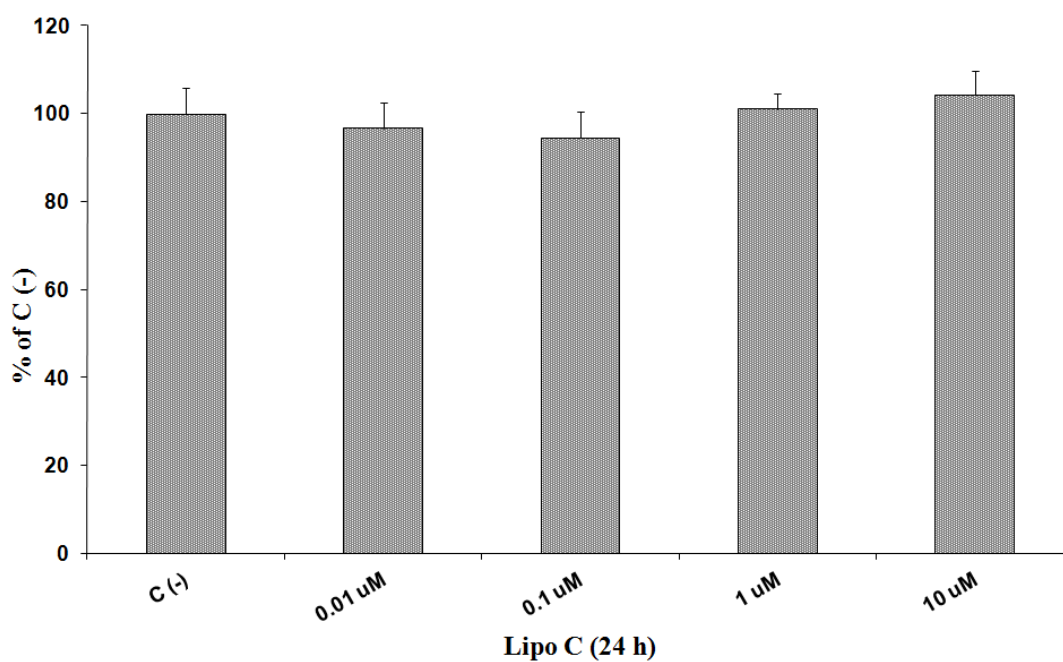


Fig. 5.2.4 MTT assay of Lipo C. Cells were exposed to Lipo C with the same content in THA (0-10  $\mu$ M) for 24 h. Cell viability was assessed by MTT reduction. Cell viability is comparable to control cells C(-). Data are means  $\pm$  SEM of six independent experiments.

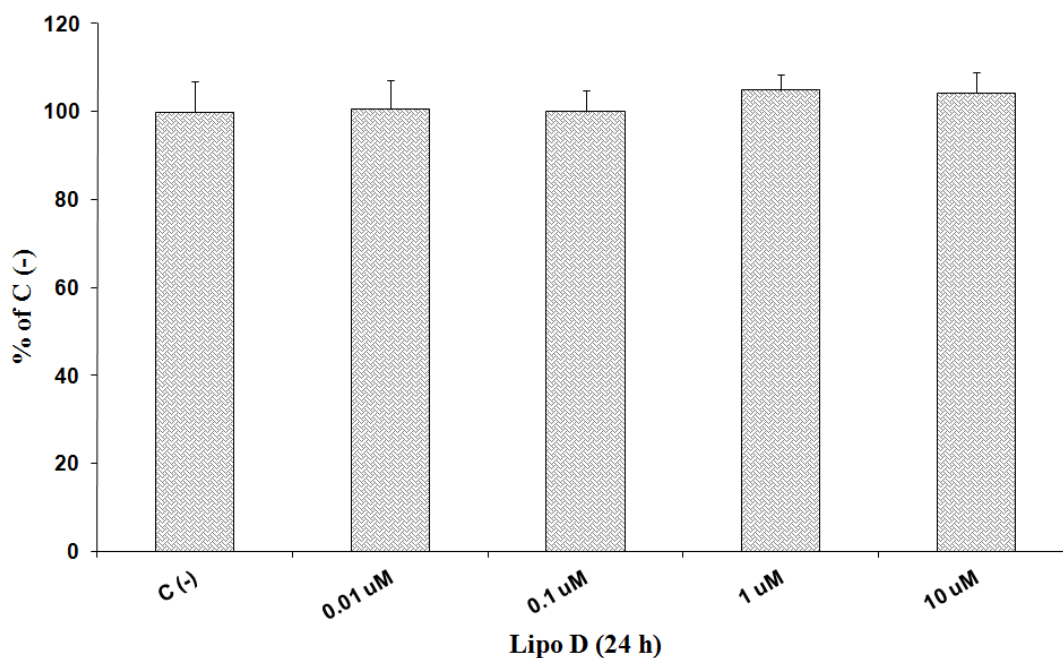


Fig. 5.2.5 MTT assay of Lipo D. Cells were exposed to Lipo D with the same content in THA (0-10  $\mu$ M) for 24 h. Cell viability was assessed by MTT reduction. Cell viability is comparable to control cells C(-). Data are means  $\pm$  SEM of six independent experiments.

In addition to the non toxicity of the excipient used to prepare liposome, preparation techniques and operating parameters appear suitable; in fact usually, one of the main issues concerning liposomes is their toxicity due to the residues of organic solvent used during preparation steps [199]. These solvents not only affect the chemical structure of the entrapped substance but can also remain in the final liposome formulation and contribute to toxicity and influence the stability of the vesicles [200-202]. On this basis, we can suppose that the operating parameter adopted during liposome preparation, allowed to completely remove the organic solvent (diethyl ether) from the formulation.

### ***5.3.2. Effect of THA solution and loaded liposomes on intracellular ROS production***

Liposomes were enriched with Toc for its antioxidant properties and in general to produce a vesicle system capable non only to convey THA to CNS but also characterized by additional function such as antioxidant and neuroprotective effect, thus obtaining multifunctional liposomes. To investigate the ability of our liposome formulation to reduce intracellular oxidative stress, SH-SY5Y cells were pre-treated with THA solution or loaded liposomes (THA concentration = 0.01  $\mu$ M, 0.1 $\mu$ M, 1 $\mu$ M and 10 $\mu$ M) for 24 h, prior to the addition of H<sub>2</sub>O<sub>2</sub> (200 mM, 30 min) and the level of intracellular ROS was determined using the peroxide-sensitive fluorescent probe DCFH-DA. As expected, THA solution at different concentration, Lipo A (classical liposome formulation) and Lipo C (Liposome formulation enriched with  $\Omega$ 3) pre-treatment not reduced the intracellular ROS production following exposure to peroxide Fig. 5.3 (.1, .2, .3, .4 and .5). Indeed, with high concentration of liposomes a non significant increase of ROS generation was observed, which might be due to the phospholipids peroxidation by H<sub>2</sub>O<sub>2</sub>. On the contrary, pre-treatment with Lipo B and especially LipoD promoted a statistically significant decreases of intracellular ROS production induced by H<sub>2</sub>O<sub>2</sub>. This effect was strictly linked to the amount of liposomes used; particularly, for a THA concentration of 10 $\mu$ M corresponding to lipid concentration of 0.56 mM, the reduction due to pre-treating

with Lipo B and Lipo D was 35% and 50%, respectively. Data highlighted that Lipo D had a significant higher antioxidant activity than Lipo B, although the Toc concentration in both liposome formulation was the same. The reasons for this unexpected result might be due to a different Toc intermembrane transfer (see paragraph 5.3.4.).

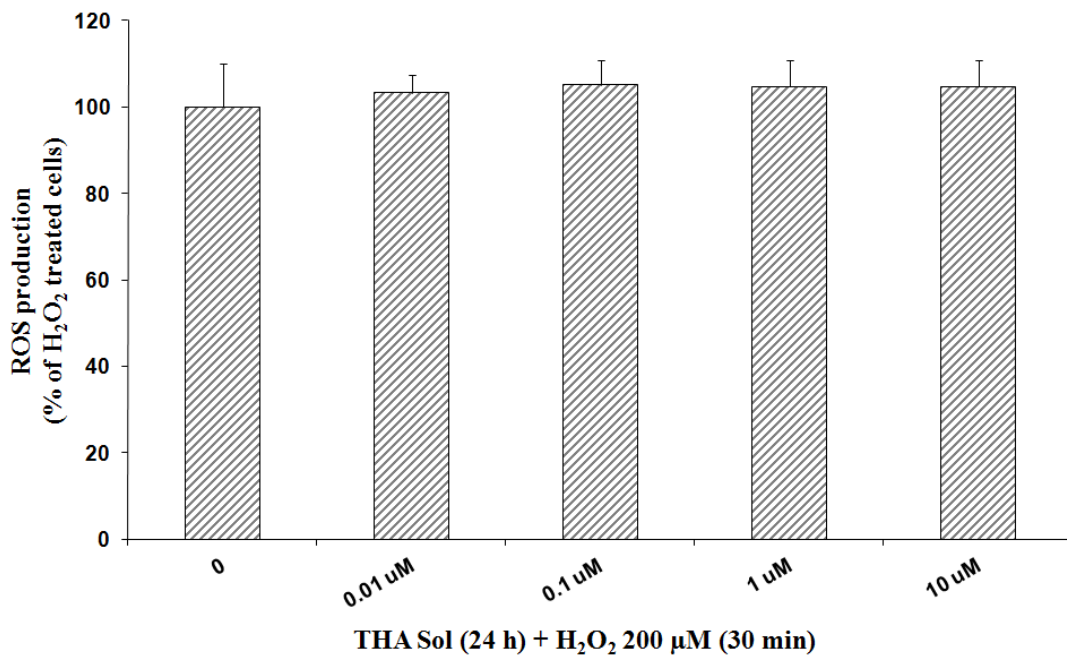


**Fig. 5.3.1.** ROS production (DCFH-DA assay) THA Sol. Cells were exposed to different THA concentrations (0-10 μM). After 24 cells were stressed with H<sub>2</sub>O<sub>2</sub> 200 μM (30 min). ROS production is expressed as percentage of H<sub>2</sub>O<sub>2</sub> treated (0) cells. THA pretreatment is not able to reduce ROS production. Data are means ± SEM of six independent experiments.

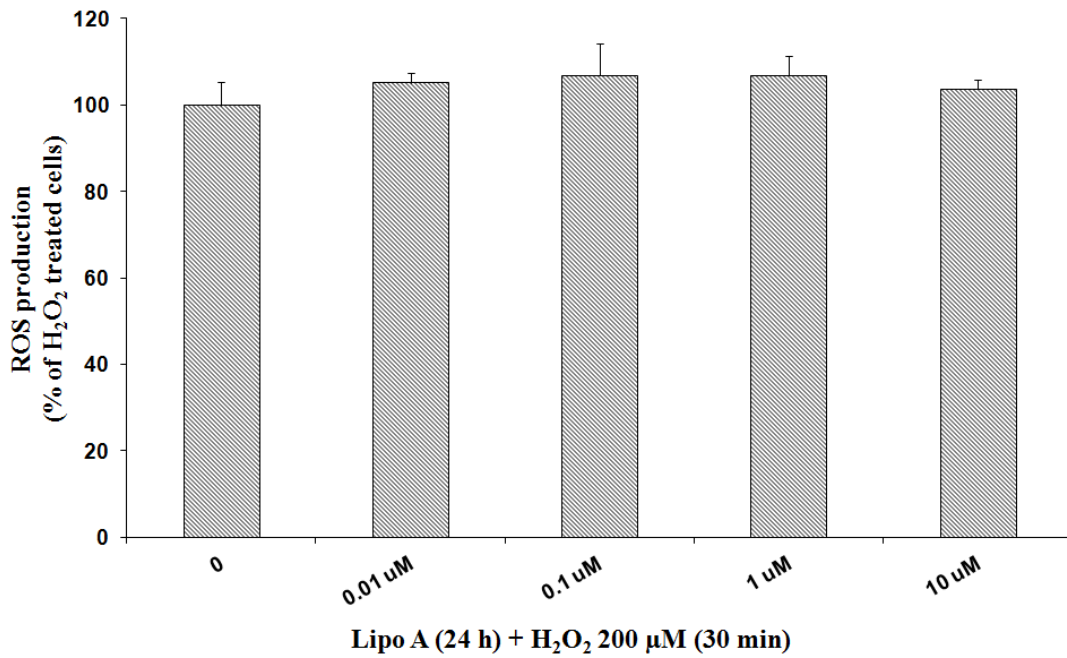


Fig. 5.3.2 ROS production (DCFH-DA assay) Lipo A. Cells were exposed to Lipo A with the same content in THA (0-10 μM). After 24 cells were stressed with H<sub>2</sub>O<sub>2</sub> 200 μM (30 min). ROS production is expressed as percentage of H<sub>2</sub>O<sub>2</sub> treated (0) cells. Lipo A pretreatment is not able to reduce ROS production. Data are means ± SEM of six independent experiments.

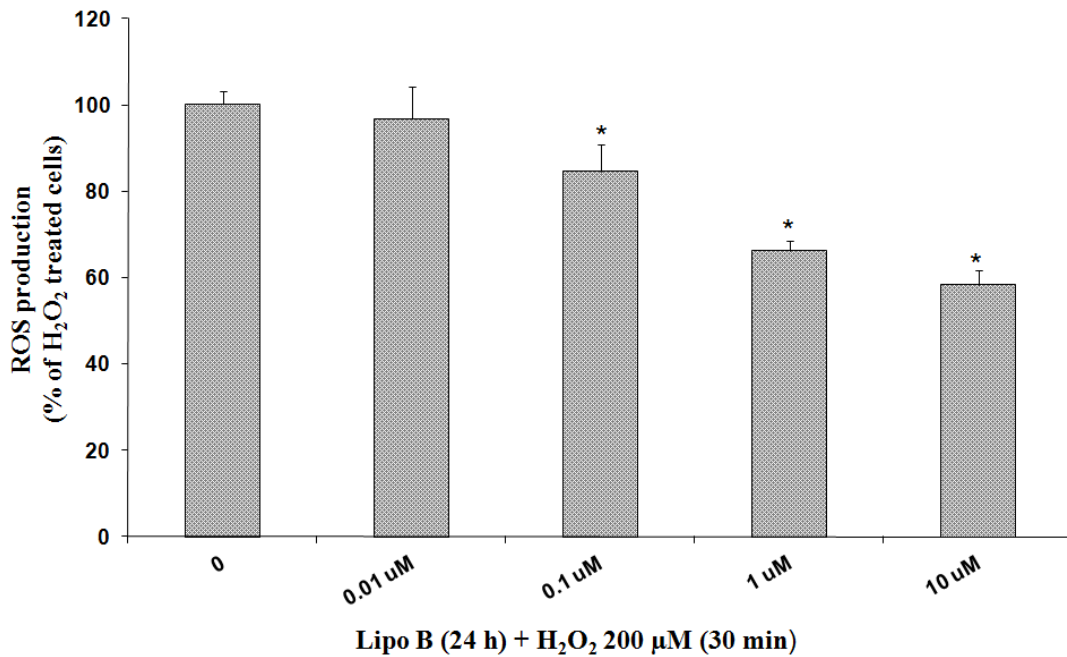


Fig. 5.3.3 ROS production (DCFH-DA assay) Lipo B. Cells were exposed to Lipo B with the same content in THA (0-10 μM). After 24 cells were stressed with H<sub>2</sub>O<sub>2</sub> 200 μM (30 min). ROS production is expressed as percentage of H<sub>2</sub>O<sub>2</sub> treated (0) cells. Lipo B significantly reduce the ROS formation induced by H<sub>2</sub>O<sub>2</sub>. Data are means ± SEM of six independent experiments. \*p < 0.001 vs H<sub>2</sub>O<sub>2</sub> treated (0) cells

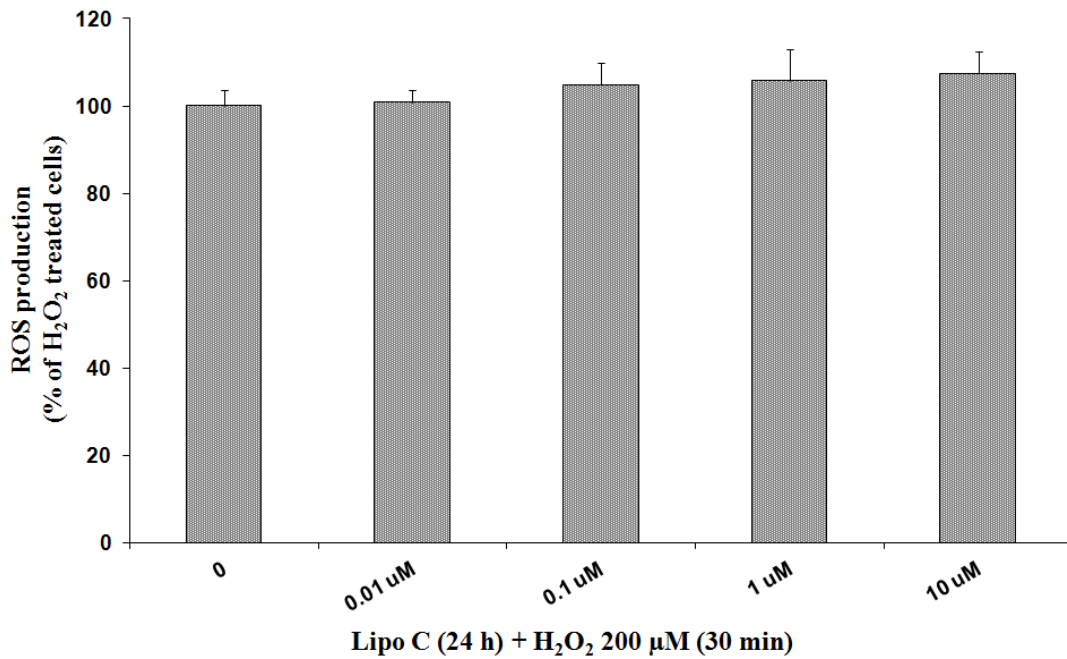


Fig. 5.3.4 ROS production (DCFH-DA assay) Lipo C. Cells were exposed to Lipo C with the same content in THA (0-10 μM). After 24 cells were stressed with H<sub>2</sub>O<sub>2</sub> 200 μM (30 min). ROS production is expressed as percentage of H<sub>2</sub>O<sub>2</sub> treated (0) cells. Lipo C pretreatment is not able to reduce ROS production. Data are means ± SEM of six independent experiments.

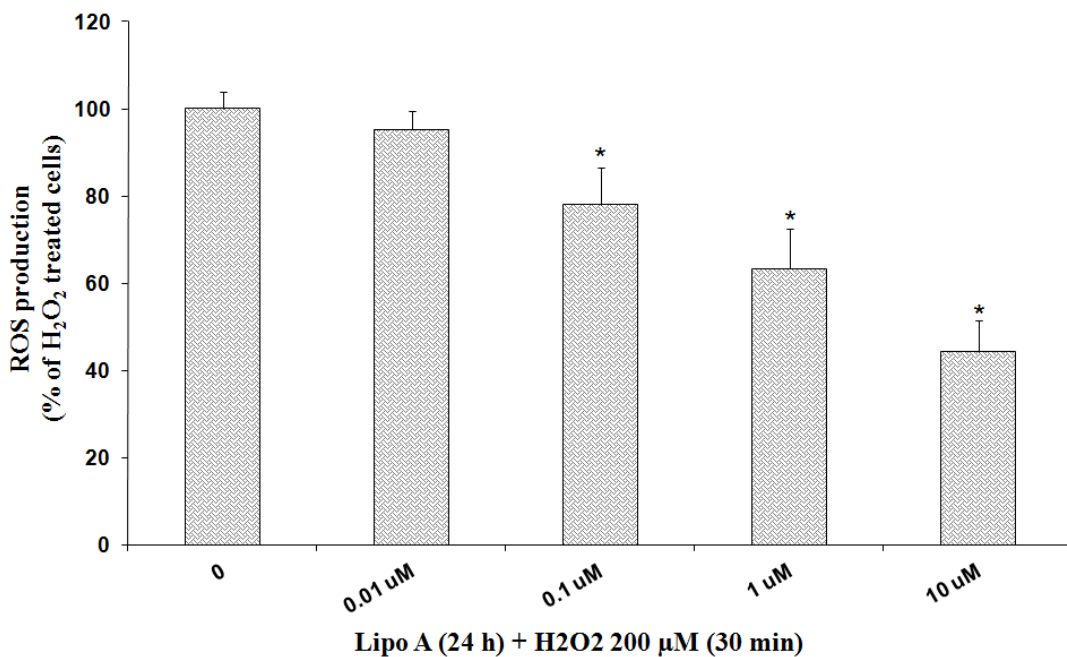


Fig. 5.3.5 ROS production (DCFH-DA assay) Lipo D. Cells were exposed to Lipo D with the same content in THA (0-10 μM). After 24 cells were stressed with H<sub>2</sub>O<sub>2</sub> 200 μM (30 min). ROS production is expressed as percentage of H<sub>2</sub>O<sub>2</sub> treated (0) cells. Lipo D significantly reduce the ROS formation induced by H<sub>2</sub>O<sub>2</sub>. Data are means ± SEM of six independent experiments. \*p < 0.001 vs H<sub>2</sub>O<sub>2</sub> treated (0) cells

### 5.3.3. Assessment of Neuroprotection

Caspase-3 protein is a member of the cystein-aspartic acid protease family. Sequential activation of caspases plays a central role in the execution-phase of cell apoptosis. It is the predominant caspase involved in the cleavage of amyloid-beta 4a precursor protein, which is associated with neuronal death in Alzheimer's disease. Since many studies have established the involvement of hydrogen peroxide in apoptotic SH-SY5Y cell death [203-205]. We investigated qualitatively whether loaded liposomes (Lipo A, LipoB, Lipo C and Lipo D) were able to reduce peroxide-induced caspase-3 activation in SH-SY5Y cells [Fig. 5.4 (.1, .2, .3, .4, .5 and .6)]. In Fig. 5.4.1 can be noted that in the absence of oxidative stress, the enzyme was not activated, while after treatment with H<sub>2</sub>O<sub>2</sub> (200 mM), a strong activation was observed (Fig. 5.4.2). Lipo A and Lipo B pre-treatment not reduced significantly the caspase-3 activation (Fig. 5.4.3, Fig. 5.4.4), while Lipo B and especially Lipo D almost completely reduced the enzyme activation; in fact, in Fig. 5.4.5 and Fig. 5.4.6 is possible to note that red halo, corresponding to caspase-3 active, is almost absent as in the control (Fig. 5.4.1), highlighting the neuroprotective effect possessed by the two liposomes formulation. Should also be noted that Lipo D showed a higher neuroprotective activity compared to Lipo B, probably due to a higher antioxidant action performed by Lipo D (see paragraph 5.3.4.).

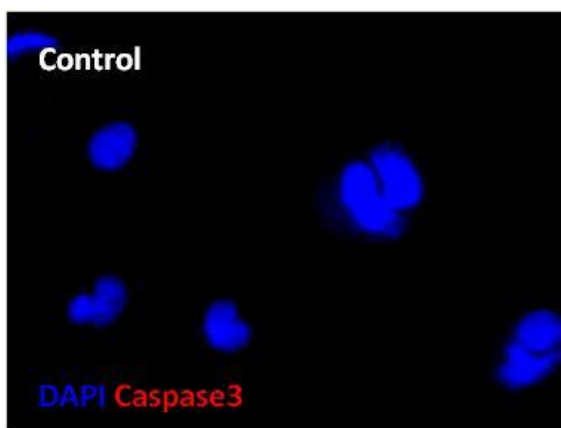


Fig. 5.4.1 SH-SY5Y cells no stressed with H<sub>2</sub>O<sub>2</sub>. Caspase-3 no activated.

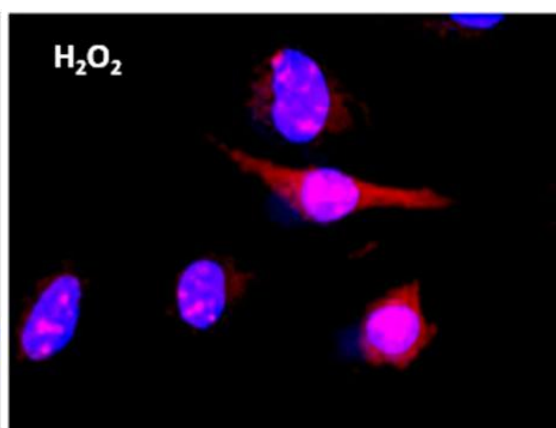
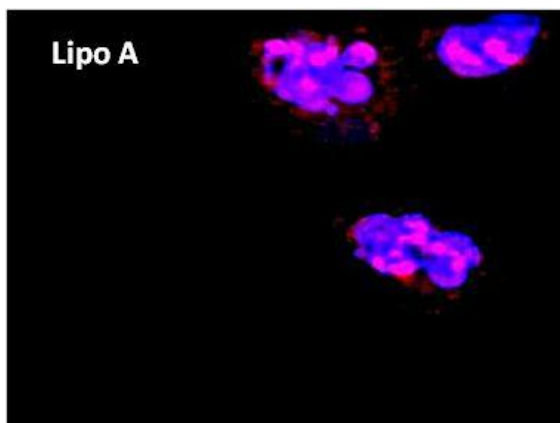
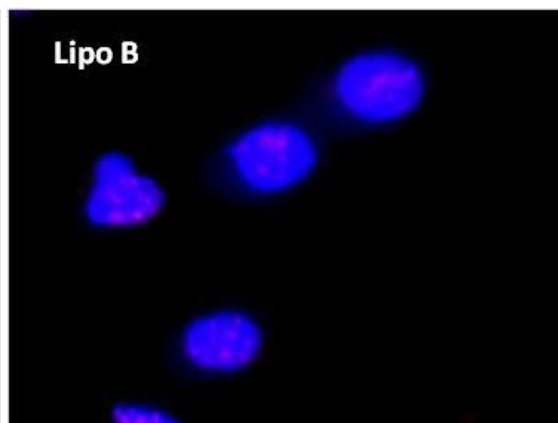


Fig. 5.4.2 SH-SY5Y cells, stressed with H<sub>2</sub>O<sub>2</sub>. Caspase-3 activated. (Red Halo)



**Fig. 5.4.3** SH-SY5Y cells pre-treated with Lipo A (24 h) and after stressed with  $H_2O_2$ . Lipo A pretreatment is not able to reduce Caspase-3 activation



**Fig. 5.4.4** SH-SY5Y cells pre-treated with Lipo B (24 h) and after stressed with  $H_2O_2$ . Lipo B pretreatment significantly reduces Caspase-3 activation

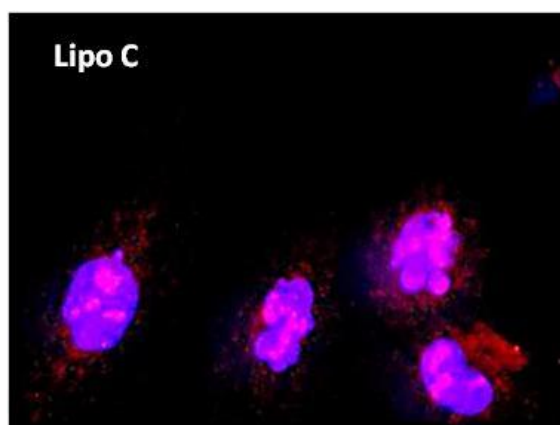


**Fig. 5.4.5** SH-SY5Y cells pre-treated with Lipo C (24 h) and after stressed with  $H_2O_2$ . Lipo C pretreatment is not able to reduce Caspase-3 activation

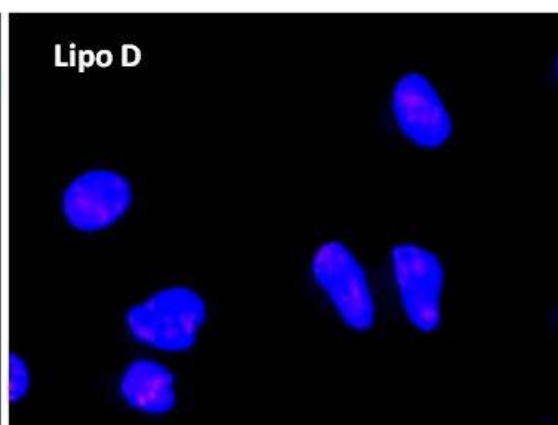


**Fig. 5.4.6** SH-SY5Y cells pre-treated with Lipo D (24 h) and after stressed with  $H_2O_2$ . Lipo D pretreatment significantly reduces Caspase-3 activation

#### 5.3.4. Evaluation of Toc intermembrane transfer

The intermembrane transfer of Toc was evaluated to explain the antioxidant and neuroprotective properties of liposome formulations (Lipo A, Lipo B, Lipo C and Lipo D). In particular, this study was done to explain why Lipo D and Lipo B had different antioxidant activity, even if the amount of Toc contained in the two liposome formulations was the same.

Fig. 5.5 shows the amount of Toc associated to the Phospholipid Vesicle barrier (PVb) after permeation assay “acceptor liposome”. In particular, the amount of Toc (expressed as nmol of Toc recovered for mg of phospholipids) associated to PVb after treatment with THA solution, Lipo A, Lipo B, Lipo C and Lipo D, was:  $0.45 \pm 0.03$  ng/mg phospholipids,  $0.59 \pm 0.01$  ng/mg phospholipids,  $1.37 \pm 0.03$  ng/mg phospholipids,  $0.69 \pm 0.02$  ng/mg phospholipids and  $2.03 \pm 0.06$  ng/mg phospholipids, respectively. The amount of Toc recovered after THA permeation was considered as negative control; in fact, Toc contained as preservative in Lipoid E80 used to prepare the PVb. Moreover, the Toc recovered after Lipo A and Lipo C permeations was that contained in the manufacturing excipients as preservative (L- $\alpha$ -phosphatidylcholine from egg yolk, Fluka; Eicosapentaenoic acid and docosahexaenoic acid, Doosan Serdary Research Laboratories), in addition to that contained in the PVb. Indeed, the amount of Toc recovered after Lipo B and Lipo D permeations, correspond to that added in the liposome formulations (“donor liposomes”) during liposome preparation, in addition to that contained in the PVb and in the manufacturing excipients. Data highlight that Toc intermembrane transfer was greater for Toc encapsulated in Lipo D compared to that in Lipo B ( $p < 0.001$ ), confirming the results obtained by Kagan, V.E. et al., which found that Toc intermembrane transfer efficiency was greater when “donor liposomes” contained unsaturated phospholipids [206].

This effective transfer of Toc explains why Lipo D presented the best antioxidant and neuroprotective activity. Practically,  $\Omega 3$  increase the Toc transfer, thereby improving antioxidant effectiveness.

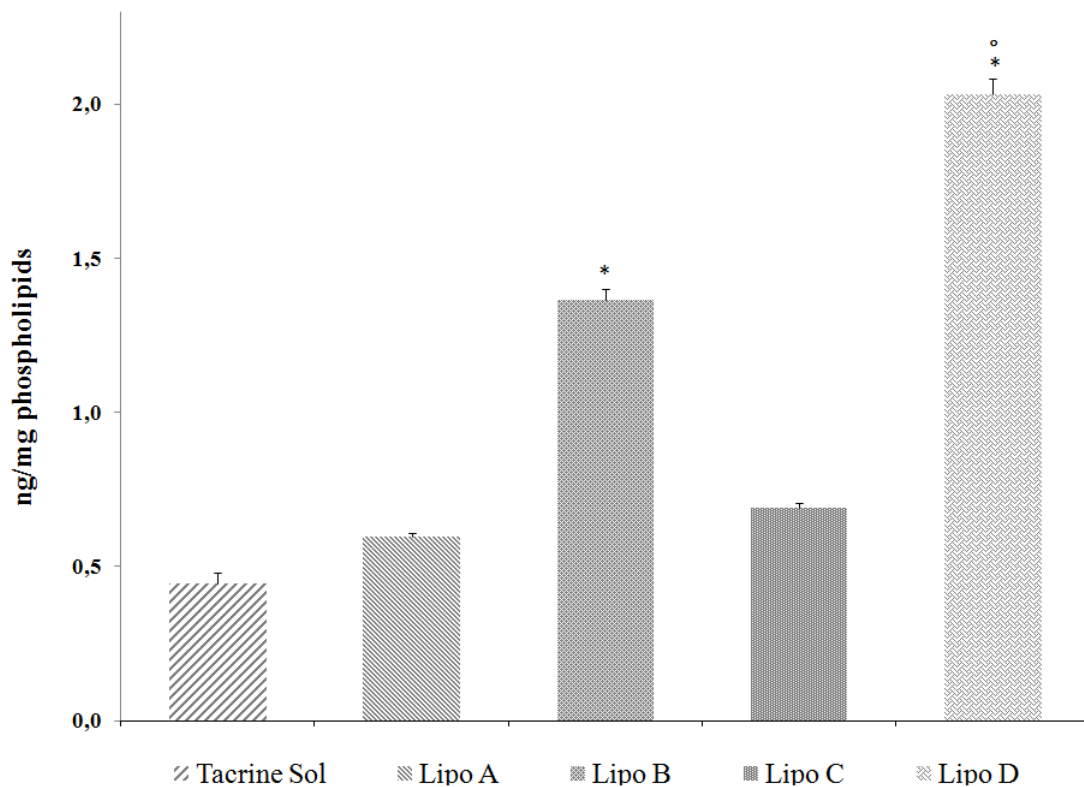


**Fig. 5.5** Toc intermembrane transfer. Amount of Toc transferred to Phospholipid Vesicles barrier (PVb) as a result of THA Sol or Lipo (A, B, C and D) permeations, expressed as nmol of Toc recovered for mg of phospholipids. Data are means  $\pm$  SEM of six independent experiments. \* $p < 0.001$  vs THA solution, ° $p < 0.001$  vs Lipo B

#### 5.4. Conclusion

As general sum up, all these data allow us to conclude that the inclusion of Toc (Lipo B) and especially of Toc and  $\Omega 3$  (Lipo D) in the liposomal formulation provided several advantages. These formulation strategy permitted to obtain liposomes with excellent antioxidant and neuroprotective activity. These properties have to be added to those relating to the conveyance to the CSN through the nasal mucosa, reported in the chapter 4. In conclusion, we can say that these new multifunctional liposomes are potentially useful in AD treatment, combining the traditional therapies strategy based on administration of acetylcholinesterase inhibitors (Tacrine hydrochloride) with the treatment of oxidative stress.

## 6. CONCLUDING REMARKS

---

Alzheimer's disease is multifactorial and heterogeneous neurodegenerative disease, involves several etiopathogenic mechanisms. It is irreversible disorder clinically characterized by abnormal memory loss along with deterioration of other cognitive abilities as well as motor capacities. AD is a progressive and disabling disorder, which affects particularly the elderly population and is the fourth main cause of death among people over 65 years old in industrialized countries. At present, there are no therapeutic interventions able to stop the progression nor to treat brain degeneration. The only marginal beneficial treatment currently achievable involves the enhancement of cholinergic neurotransmission, while the neurodegenerative process continues unabated. This is despite thousands of research articles and copious knowledge of molecular cascades that are presumed pathogenic. On the basis of its multifactorial nature, it seems likely that the next major advance will occur either as a multidisciplinary multimodality approach, attacking every conceivable facet of neurodegeneration.

One of the main limitations of the new active molecules synthesized against AD is their poor bioavailability and especially their inability to cross the BBB. To overcome these limitation a new route of administration was taken in account in this thesis, the nasal route, which present numerous advantages compared to traditional oral route. In addition nasal route allows to convey drug administered directly in the CNS through the olfactory region. On the other hand this alternative route of administration present some limitations relative to physio-anatomical characteristics of the nose such as the high mucociliary clearance that removes in a few minutes the particulates, which are deposited on the mucosa. For this reasons, a drug to be administered by the nasal route has to be inserted in a particular formulation, capable of prolonge residence time of the drug by means of mucoadhesive properties and at same time enhance drug permeability. In this thesis two formulations were produced

and analyzed. The first project was to produce *Albumin nanoparticles carrying cyclodextrin*. The results obtained highlighted that these nanoparticles carrying native and hydrophilic derivatives  $\beta$ CD can be employed for the formulation of mucoadhesive nasal formulations with interesting drug permeation properties. The selection of suitable CD during particle preparation allows the modulation of their mucoadhesion ability and THA permeation at the administration site.

The second project was to produce *Multifunctional liposomes*. These liposome formulation was conceived on the basis of the AD multifactorial nature; in particular, on the basis of the knowledge that oxidative stress plays a key role in the pathogenesis of AD. So liposomes were produced combining the traditional therapies strategy based on administration of acetylcholinesterase inhibitors (Tacrine hydrochloride) with the treatment of oxidative stress. Results were very interesting; in fact, these new nanocarriers were found not only to improve mucoadhesion on the nasal mucosa but also to increase THA permeability. In addition, studies conducted on neuronal cell showed an excellent antioxidant and neuroprotective effect.

Finally, it is very important to note the new “formulative philosophy”, adopted to produce these liposomes; practically, the antioxidant effect is due to the Tocopherol, which was added as excipient in the formulation. This upsets the classical concept of excipient which is no more a simple envelope of the drug but becomes itself an active molecule contributing with the drug to achieve the therapeutic effect.

## 7. REFERENCES

---

- 1 E. Giacobini, Pharmacotherapy of Alzheimer's disease: new drugs and novel therapy. In: Corain B, Iqbal K, Nicolini M, et al, eds. Alzheimer's Disease: Advances in Clinical and Basic Research. Wiley, New York, 1993, pp. 529–538
- 2 C. Reitz, C. Brayne and R. Mayeux. Epidemiology of Alzheimer disease. *Nat. Rev. Neurol.* 7 (2011) 137–152
- 3 Alzheimer's Association. Alzheimer's Association Report 2011 Alzheimer's disease facts and figures. *Alzheimer's & Dementia* 7 (2011) 208–244
- 4 B. A. Yankner, Mechanism of neuronal degeneration in Alzheimer's disease. *Neuron.* 16 (1996) 921-932
- 5 J. Hardy, A hundred years of Alzheimer's disease research, *Neuron* 52 (2006) 3-13
- 6 JJ. Cook, Acute gamma-secretase inhibition of nonhuman primate CNS shifts amyloid precursor protein (APP) metabolism from amyloid-beta production to alternative APP fragments without amyloid-beta rebound, *Journal of Neuroscience* 30(19) (2010) 6743-6750
- 7 B. T. Hyman, Caspase activation without apoptosis: insight into A $\beta$  initiation of neurodegeneration, *Nature Neuroscience* 14 (2011) 5-6
- 8 T. W. kim, W. H. Pettingell, Y.K. Jung, Alternative cleavage of Alzheimer-associated presenilins during apoptosis by caspase-family protease, *Science* 277 (1997) 73-76
- 9 S.J. Martin, Proteolysis of fodrin (non erythroid spectrin) during apoptosis, *J Biol Chem* 270 (1995) 6425-28
- 10 B. McLaughlin, K. A. Hartnett, Caspase 3 activation is essential for neuroprotection in preconditioning, *Proc Natl Acad Sci USA* 100 (2003) 715-20

- 11 Y. Tong, Oxidative stress potentiates BACE1 gene expression and Abeta generation, *J. Neural trasm.* 112 (2005) 455-469
- 12 M. Guglielmotto, L. Gilberto, E. Tamagno, M. Tabaton, Oxidative stress mediates the pathogenic effect of different Alzheimer's disease risk factors, *Frontier in Aging neurosc.* 2 (2010) 1-8
- 13 K. A. Hensley, Model for beta-amyloid aggregation and neurotoxicity based on free radical generation by the peptide, *Proc. natl. acad. Sci.* 91 (1994) 3270-3274
- 14 D. Harman, Alzheimer's Disease Pathogenesis Role of Aging, *Ann. N.Y. Acad. Sci.* 1067 (2006) 454-460
- 15 R. A.. Hansen, G. Gartlehner, D. J. Kaufer , K. N. Lohr, T. Carey, Drug Class Review on Alzheimer's Drugs, Oregon Health & Science University (2006)
- 16 M. E. Bodor Brewster, Problems of delivery of drug to the brain, *Pharmac. Ther.* 19 (1983) 337-386
- 17 X. Lataste, The Blood-Brain Barrier in Hypoxia, *Int. J. Sports Med.* 13 (1992) 45-47
- 18 C. L. Graff, R. Zhao, G. M. Pollack, Pharmacokinetics of substrate uptake and distribution in murine brain after nainstillation. *Pharm Res.* 22 (2005) 235-244
- 19 A. Pires, A. Fortuna, G. Alves, A. Falcão, Intranasal Drug Delivery: How, Why and What for?, *J Pharm Pharmaceut Sc.* 12(3) (2009) 288 - 311
- 20 V. D. Romeo, J. Meireles, A. P. Sileno, H. K. Pimplaskar, C. R. Behl, Effects of physicochemical properties and other factors on systemic nasal delivery, *Adv Drug Deliv Rev* 29 (1998) 89-116
- 21 A. K. Leonard, A. P. Sileno, G. C. Brandt, C. A. Foerder, S. C. Quay, H. R. Costantino, In vitro formulation optimization of intranasal galantamine leading to enhanced bioavailability and reduced emetic response in vivo. *Int J Pharm* 335 (2007) 138-146
- 22 H. R. Costantino, L. Illum, G. Brandt, P. H. Johnson, S. C. Quay, Intranasal delivery: Physicochemical and therapeutic aspects, *Int. J. Pharm.* 337 (2007) 1-24
- 23 H. R. Costantino, A. K. Leonard, G. Brandt, P. H. Johnson, S. C. Quay, Intranasal administration of acetylcholinesteraseinhibitors, *BMC Neurosci.* 9 (2008) S3-S6

- 24 S. Upadhyay, A. Parikh, P. Joshi, U. M. Upadhyay, N. P. Chotai, Intranasal drug delivery system- A glimpse to become Maestro, *Journal of Applied Pharmaceutical Science* 01(03) (2011) 34-44
- 25 C. Shoshkes Reiss, I. V. Plakhov, T. Komatsu, Viral replication in olfactory receptor neurons and entry into the olfactory bulb and brain, *Ann NY Acad Sci.* 855 (1998) 751-761
- 26 H. H. Chow, N. Anavy, A. Villalobos, Direct Nose-Brain Transport of benzoylecgonine following intranasal administration in rats, *J Pharm Sci.* 90 (2001) 1729-1735
- 27 C. Dufes, J. C. Olivier, F. Gaillard, A. Gaillard, W. Couet, J. M. Muller, Brain delivery of vasoactive intestinal peptide (VIP) following nasal administration to rats, *Int J Pharm* 255 (2003) 87-97
- 28 Q. Z. Zhang, X. G. Jiang, C. H. Wu, Distribution of nimodipine in brain following intranasal administration in rats, *Acta Pharmacol Sin* 25 (2004) 522-527
- 29 K. P. Doyle, T. Yang, N. S. Lessov, T. M. Ciesielski, S. L. Stevens, R. P. Simon, J. S. King, M. P. Stenzel-Poore, Nasal administration of osteopontin peptide mimetics confers neuroprotection in stroke, *J Cereb Blood Flow Metab* 28 (2008) 1235-1248
- 30 V.V. Jogani, P. J. Shah, P. Mishra, A. K. Mishra, A. R. Misra, Nose-to-brain delivery of tacrine, *J Pharm Pharmacol* 59 (2007) 1199-1205
- 31 V. V. Jogani, P. J. Shah, P. Mishra, A. K. Mishra, A. R. Misra, Intranasal mucoadhesive microemulsion of tacrine to improve brain targeting, *Alzheimer Dis Assoc Disord.* 22 (2008) 116-124
- 32 R. Hashizume, T. Ozawa, S. M. Gryaznov, A. W. Bollen, K. R. Lamborn, W. H. Frey 2nd, D. F. Deen, New therapeutic approach for brain tumors: Intranasal delivery of telomerase inhibitor GRN163, *Neuro Oncol.* 10 (2008) 112-120
- 33 T. Sakane, S. Yamashita, N. Yata, H. Sezaki, Transnasal delivery of 5-fluorouracil to the brain in the rat, *J. Drug Target* 7 (1999) 233-240
- 34 N. S. Barakat, S. A. Omar, A. A. Ahmed, Carbamazepine uptake into rat brain following intra-olfactory transport, *J. Pharm. Pharmacol.* 58 (2006) 63-72
- 35 U. Westin, E. Piras, B. Jansson, U. Bergström, M. Dahlin, E. Brittebo, E. Björk, Transfer of morphine along the olfactory pathway to the central

- nervous system after nasal administration to rodents, *Eur. J. Pharm. Sci.* 24 (2005) 565-573
- 36 K. Yamada, M. Hasegawa, S. Kametani, S. Ito, Nose-to-brain delivery of TS-002, prostaglandin D2 analogue, *J. Drug. Target* 15 (2007) 59-66
- 37 L. Illum, Transport of drugs from the nasal cavity to the central nervous system. *Eur. J. Pharm. Sci.* 11 (2000) 1–18
- 38 Y. W. Chien, K. S. E. Su, Chang, Anatomy and physiology of the nose, In: Swarbrick, J, (eds.), *Nasal systemic drug delivery; Drugs and pharmaceutical science*, v. 39, Marcel Dekker, New York, 1989, pp, 1-19
- 39 V. Jogani, Recent patents review on intranasal administration for CNS drug delivery. *Recent Patents on Drug Delivery e Formulation* 2 (2008) 25-40
- 40 L. Illum, Transport of drug from the nasal cavity to central nervous system, *Eur. J. Pharm. Sci.* 11 (2000) 1-18
- 41 L. Illum, Nasal drug delivery – possibilities, problem and solutions, *J. Control. Rel.* 87 (2003) 187-198
- 42 L. Illum, P. Watts, A. N. Fisher, M. Hinchcliffe, H. Norbury, I. Jabbal-Gill, R., Nankervis, S. S. Daviss, Intranasal delivery of morphine, *J. Pharmacol. Exp. Ther.* 301 (2002) 391-400
- 43 A. Anwar Hussain, Intranasal drug delivery, *Advanced Drug Delivery Reviews* 29 (1998) 39–49
- 44 R. G. Thorne, Delivery of Neurotrophic Factors to the brain: Pharmacokinetic consideration, *Clinical Pharmacokinetics* 40(12) (2001) 907-946
- 45 H. Chow, Z. Chen, G.T. Matsuura, Direct transport of cocaine from the nasal cavity to brain following intranasal cocaine administration in rats, *J. Pharm. Sci.* 88 (1999) 754-758
- 46 H. L. Fehm, B. Perras, R. Smolink, W. Kern, J. Born, Manipulating neuropeptidergic pathways in humans: A novel approach in neuropharmacology? *Eur. J. Pharmacol.* 405 (2000) 43-54
- 47 C. R. Behl, H. K. Pimplaskar, A. P. Sileno, J. Demeireles, V. D. Remo, Effect of physiochemical properties and other factors on systemic nasal drug delivery, *Adv. Drug Deliv. Rev.* 29 a (1998) 89-116
- 48 M. I. Lethem, The role of trachealbronchial mucus in drug administration to the airway, *Adv. Drug Deliv. Rev.* 11 (1993) 19-27

- 49 M. I. Ugwoke, R. U. Agu, N. Verbeke, R. Kinget, Nasal mucoadhesive drug delivery: Background, applications, trends and future perspectives, *Adv. Drug Deliv. Rev.* 57 (2005) 1640-1665
- 50 N. Washington, Determination of baseline human pH and the effect of intranasally administered buffers, *Int. J. Pharm.* 198 (2000) 139-146
- 51 K. Morimoto, H. Tabata, K. Morisaka, Nasal absorption of nifedipine from gel preparations in rats, *Chem. Pharm. Bull.* 35 (1987) 3041-3044
- 52 C. Wadell, Nasal drug delivery. Ph D thesis, Uppsala University, Sweden, (2002)
- 53 F. W. Merkus, Nasal mucociliary clearance as a factor in nasal drug delivery, *Adv Drug Deliv Rev.* 29(1-2) (1998) 13-38
- 54 E. Marttin, G. M. Nicolass, J. Schipper, C. Verhoef, F.W.H. M. Merkus, Nasal mucociliary clearance as a factor in nasal drug delivery, *Adv. Drug Deliv. Rev.* 29 (1998) 13-38
- 55 M. N. Zaki, G. A. Awad, N. D. Mortada, S. S. Abd ElHady, Enhanced bioavailability of metoclopramide HCl by intranasal administration of a mucoadhesive in situ gel with modulated rheological and mucociliary transport properties, *Eur. J. Pharm. Sci.* 32 (2007) 296-307
- 56 F. Y. Chung, M. D. Donovan, Nasal pre-systemic metabolism of peptide drugs: substance P metabolism in the sheep nasal cavity, *Int. J. Pharm.* 128 (1996) 229-237
- 57 R. Alan, Nasal Cavity Enzymes Involved in Xenobiotic Metabolism: Effects on the Toxicity of Inhalants, *Critical Reviews in Toxicology* (1991) Volume 21, issue 5
- 58 M.A. Sarkar, Drug metabolism in nasal mucosa, *Pharm. Res.* 9 (1992) 1-9
- 59 A. Bernkop-schnurch, Use of inhibitory agents to overcome the enzymatic barrier to perorally administered therapeutic peptides and proteins, *J. Control. Rel.* 52 (1998) 1-16
- 60 F. Y. Chung, M. D. Donovan, Large molecule and particulate uptake in nasal cavity: the effect of size on nasal absorption, *Adv. Drug Deliv. Rev.* 29 (1998) 147-155
- 61 T. Ohwaki, M. Ishii, S. Aoki, K. Tatsushi, M. Kayano, Effect of dose, pH and osmolarity on nasal absorption of secretin in rats III: in vivo membrane permeation test and determination of apparent partition coefficient of secretin, *Chem. Pharm. Bull.* 37 (1989) 3359-3362

- 62 D. C. Corbo, J. C. Liu, Y. W. Chien, Characterization of the barrier properties of mucosal membrane, *J. Pharm. Sci.* 79 (1990) 202-206
- 63 T. J. Aspden, L. Illum, Ø. Skaugrud, Chitosan as a nasal delivery system: evaluation of insulin absorption enhancement and effect on nasal membrane integrity using rat models, *Eur. J. Pharm. Sci.* 4 (1996) 23-31
- 64 S. G. Chandler, N. W. Thomas, L. Illum, Nasal absorption in the rat. IV. Membrane activity of absorption enhancer, *Int. J. Pharm.* 117(1995)139-146
- 65 M.A. Deli, Potential use of tight junction modulators to reversibly open membranous barriers and improve drug delivery, *Biochim. Biophys. Acta* 1788 (2009) 892-910
- 66 F. G. Gu, F. D. Cui, Y. D. Gao, Preparation of prostaglandin E1-hydroxypropyl-cyclodextrincomplex and its nasal delivery in rats, *Int. J. Pharm.* 290 (2005) 101-108
- 67 N. G. M. Schipper, J. C. Verhoef, S. G. Romeijn, F. W. H. M. Merkus, Methylated  $\beta$ -cyclodextrins are able to improve the nasal absorption of salmon calcitonin, *Calcifi. Tissue Int.* 56 (1995) 280-282
- 68 A. P. Sayani, Y. W. Chien, Systemic delivery of peptides and proteins across absorptive mucosae, *Crit Rev Ther Drug Carrier Syst* 13 (1996) 85-184
- 69 R. P. Ramesh, C. Mahesh, O. Patil, Nasal Drug delivery in Pharmaceutical and biotechnology: present and future, *e-Journal of Science & Technology* 3 (2009) 1-21
- 70 S. A. Sajadi Tabassi, H. Hosseinzadeh, M. Ramezani, E. Moghimipour, S. A. Mohajeri, Isolation, characterization and study of enhancing effects on nasal absorption of insulin in rat of the total saponin from *Acanthophyllum squarrosum*, *Indian J Pharmacol* 39(2007) 226-30
- 71 K. Ikeda, K. Murata, M. Kobayashi, K. Noda, Enhancement of bioavailability of dopamine via nasal route in beagle dogs *Chem. Pharm. Bull.* 40 (1992) 2155-2158
- 72 M. J. Deurloo, W. A. Hermens, S. G. Romeyn, J. C. Verhoef, F. W. Merkus, Absorption enhancement of intranasally administered insulin by sodium taurodihydrofusidate (STDHF) in rabbits and rats, *Pharm Res.* 6(10) (1989) 853-6
- 73 Z. Shao, A. K. Mitra, Nasal Membrane and Intracellular Protein and Enzyme Release by Bile Salts and Bile Salt-Fatty Acid Mixed Micelles:

- Correlation with Facilitated Drug Transport, *Pharmaceutical Research* 9(9) (1992) 1184-1189
- 74 M. A. El-Shafy, I. W. Kellaway, G. Taylor, P. A., Dickinson, Improved nasal bioavailability of FITC-dextrin (Mw 4300) from mucoadhesive microspheres in rabbits, *J. Drug Target.* 7 (2000) 355-61
- 75 T. Tugrul, Kararli, E. Thomas, D, A. Baron, R. E. Schmidt, B. Katz and B. Belonio, Enhancement of Nasal Delivery of a Renin Inhibitor in the Rat Using Emulsion Formulations, *Pharmaceutical Research.* 9(8) (1992) 1024-1028
- 76 C. Agerholm, L. Bastholm, P. B. Johansen, M. H. Nielsen, F. Elling, Epithelial transport and bioavailability of intranasal growth hormone formulated with the absorption enhancers didecanoyl-L- $\alpha$ -phosphatidylcholine and  $\alpha$ -cyclodextrin in rabbit, *J. Pharmaceut. Sci.* 83 (1994) 1706–1711
- 77 T. Loftsson, P. Jarho, M. Másson, T. Järvinen, Cyclodextrins in drug delivery, *Expert Opin. Drug Deliv.* 2(2) (2005) 335-351
- 78 D. Duchene, G. Ponchel, D. Wouessidjewe, Cyclodextrins in targeting. Application to nanoparticles, *Adv. Drug Deliv. Rev.* 36 (1999) 29-40
- 79 F. W. Merkus, J. C. Verhoef, S. G. Romeijn, N. G. Schipper, Absorption enhancing effect of cyclodextrins on intranasally administered insulin in rats, *Pharm Res.* 8(5) (1991) 588-92
- 80 E. Björk, U. Issksson, P. Edman, P. Artursson, Starch microspheres induce pulsatile delivery of drugs and peptides across the epithelial barrier by reversible separation of the tight junctions., *J. Drug Target.* 2 (1995) 501-507
- 81 J. T. Kelly, B. Asgharian, J.S. Kimbell, Particle deposition in human nasal airway replicas manufactured by different methods. Part 1: Inertial regime particles, *Aerosol Sci. Technol.* 38 (2004) 1063-1071
- 82 J. D. Schroeter, J. S. Kimbell, B. Asgharian, Analysis of particle deposition in the turbinate and olfactory regions using a human nasal computational fluid dynamics model, *J. Aerosol Med.* 19 (2006) 301-313
- 83 M. Rathananand, D. S. Kumar, A. Shirwaikar, R. Kumar, D. Sampath Kumar, R. S. Prasad, Preparation of mucoadhesive microspheres for nasal delivery by spray drying, *Indian J Pharm Sci* 69 (2007) 651-7
- 84 S. B. Patil, A. Kaul, A. Babbar, R. Mathur, A. Mishra, K. K. Sawant, In vivo evaluation of alginate microspheres of carvedilol for nasal delivery, *Journal of Biomedical Materials Research Part B: Applied Biomaterials,* 100B (2012) 249–255

- 85 L. Illum, N. F. Farraj, S. S. Davis, B. R. Johansen, D. T. O' Hagan, Investigation of the nasal absorption of biosynthetic human growth hormone in sheep-use of a bioadhesive microspheres delivery system, *Int. J. Pharm.* 63 (1990) 207-211
- 86 S.S.D. Critchley, D. Farraj, L. Illum, Nasal absorption of desmopressin in rats and in sheep. Effect of bioadhesive microspheres delivery system, *J. Pharm. Pharmacol.* 46 (1994) 651-656
- 87 Encyclopedia of Controlled Drug Delivery, P. Colombo. Mucosal Drug Delivery, Nasal. Editor: Edith Mathiowitz. ISBN: 0-471-14828-8
- 88 A. Mistry, S. Stolnik, L. Illum, Nanoparticles for direct nose-to-brain delivery of drugs, *Int. J. Pharm.* 379 (2009) 146–157
- 89 A. M. Dyer, M. Hinchcliffe, P. Watts, J. Castile, I. Jabbal-Gill, R. Nankervis, A. Smith, L. Illum, Nasal delivery of insulin using novel chitosan based formulations: A comparative study in two animal models between simple chitosan formulations and chitosan nanoparticles, *Pharm. Res.* 19 (2002) 998–1008
- 90 U. Seju, A. Kumar, K. K. Sawant, Development and evaluation of olanzapine-loaded PLGA nanoparticles for nose-to-brain delivery: in vitro and in vivo studies, *Acta Biomater.* 7(12) (2011) 4169-76
- 91 D. Lichtenberg, Y. Barenholz, In *Methods of Biological Analysis*, Vol. 33, D. Glick, ed., John Wiley & Sons, Inc., New York, 1988, pp. 337-461
- 92 H. Talsma, M. J. van Steenberg, J. C. Borchert, D. J. Crommelin, A novel technique for the one-step preparation of liposomes and nonionic surfactant vesicles without the use of organic solvents. Liposome formation in a continuous gas stream: the 'bubble' method, *J Pharm Sci.* 83(3) (1994) 276-80
- 93 Y. Maitani, S. Asano, S. Takahashi, M. Nasayuki, T. Nagai, Permeability of insulin in liposomes through the nasal mucosa of rabbits, *Chem Pharm Bull* 40 (1992) 1569–1572
- 94 A. K. Jain, K. B. Chalasani, R. K. Khar, F. J. Ahamed, P. V. Diwan, Mucoadhesive multivesicular liposomes as an effective carrier for transmucosal insulin delivery, *J Drug Target* 15 (2007) 417–427
- 95 I. A. Alsarra, A. Y. Hamed, F. K. Alanazi, Acyclovir liposomes for intranasal systemic delivery: development and pharmacokinetics evaluation, *Drug Deliv* 15 (2008) 313–321

- 96 S. L. Law, K. J. Huang, H. Y. Chou, J. Y. Cherng, Enhancement of nasal absorption of calcitonin in liposomes, *J Liposome Res* 11 (2001) 165–174
- 97 K. Arumugam, G. S. Subramanian, S. R. Mallayasamy, R. K. Averineni, M. S. Reddy, and N. Udupa, A study of rivastigmine liposomes for delivery into the brain through intranasal route, *Acta Pharm* 58 (2008) 287–297
- 98 M. M. Migliore, T. K. Vyas, R. B. Campbell, M. M. Amiji, B. L. Waszczak, Brain delivery of proteins by the intranasal route of administration: A comparison of cationic liposomes versus aqueous solution formulations, *Journal of Pharmaceutical Sciences* 99 (2010) 1745–1761
- 99 F. J. McInnes, B. O'Mahony, B. Lindsay, Nasal residence of insulin containing lyophilised nasal insert formulations, using gamma scintigraphy, *Eur J Pharm Sci* 31 (2007) 25-31
- 100 F. J. McInnes, A. J. Baillie, H. N.E. Stevens, The use of simple dynamic mucosal models and confocal microscopy for the evaluation of lyophilised nasal formulations, *J Pharm Pharmacol* 59 (2007) 759-67
- 101 F. J. McInnes, P. Thapa, A. J. Baillie, In vivo evaluation of nicotine lyophilised nasal insert in sheep, *Int J Pharm* 304(1-2) (2005) 72-82
- 102 P. Thapa, H. N. E. Stevens, A. J. Baillie, In vitro drug release studies from a novel lyophilised nasal dosage form, *Kathmandu Univ J Sci Eng Technol* 5 (2009) 71-86
- 103 U. Bertram, M. C. Bernard, J. Haensler, In situ gelling nasal inserts for influenza vaccine delivery, *Drug Dev Ind Pharm* 2009: published online 3 December 2009, doi:10.3109/03639040903382673
- 104 U. Bertram, R. Bodmeier, In situ gelling, bioadhesive nasal inserts for extended drug delivery: in vitro characterization of a new nasal dosage form, *Eur J Pharm Sci* 27(1) (2006) 62-71
- 105 B. Luppi, F. Bigucci, L. Mercolini, Novel mucoadhesive nasal inserts based on chitosan/hyaluronate polyelectrolyte complexes for peptide and protein delivery, *J Pharm Pharmacol* 61(2) (2009) 151-7
- 106 B. Luppi, Chitosan/pectin polyelectrolyte complexes for nasal delivery of antipsychotic drugs, 9th International Conference of the European Chitin Society; Venice; (2009)
- 107 W.K. Summers, Tacrine and Alzheimer's treatments, *J. Alzheimers Dis.* 9 (2006) 439-445

- 108 A. J. Wagstaff, D. McTavish, Tacrine. A review of its pharmacodynamic and pharmacokinetic properties, and therapeutic efficacy in Alzheimer's disease, *Drugs and Aging* 4 (1994) 510-554
- 109 G. Sathyan, W. A. Ritschel, A. S. Hussain, Transdermal delivery of tacrine: identification of suitable delivery vehicle, *Int. J. Pharm.* 114 (1995) 75-83
- 110 T. Kankkunen, R. Sulkava, M. Vuorio, K. Kontturi, J. Hirvonen, Transdermal iontophoresis of tacrine in vivo, *Pharm. Res.* 19 (2002) 705-708
- 111 V. V. Jogani, P. J. Shah, P. Mishra, A. K. Mishra, A. R. Misra, Nose-to-brain delivery of tacrine, *J. Pharm. Pharmacol.* 59 (2007) 1199-1205
- 112 H. R. Costantino, A. K. Leonard, G. Brandt, P. H. Johnson, S. C. Quay, Intranasal administration of acetylcholinesterase inhibitors, *BMC Neurosci.* 9 (2008) S6
- 113 M. I. Ugwoke, N. Verbeke, R. Kinget, The biopharmaceutical aspects of nasal mucoadhesive drug delivery, *J. Pharm. Pharmacol.* 53 (2001) 3-21
- 114 P. Arbòs, M. A. Campanero, M. A. Arangoa, M. J. Renedo, J. M. Irache, Influence of the surface characteristics of PVM/MA nanoparticles on their bioadhesive properties, *J. Control. Release* 89 (2003) 19-30
- 115 L. Illum, Nanoparticulate systems for nasal delivery of drugs: A real improvement over simple systems, *J. Pharm. Sci.* 96 (2007) 473-483
- 116 B. Wilson, M. K. Samanta, K. Santhi, K. P. Sampath Kumar, N. Paramakrishnan, B. Suresh, Targeted delivery of tacrine into the brain with polysorbate 80-coated poly(n-butylcyanoacrylate) nanoparticles, *Eur. J. Pharm. Biopharm.* 70 (2008) 75-84
- 117 B. Wilson, M. K. Samanta, K. Santhi, K. P. Sampath Kumar, M. Ramasamy, B. Suresh, Chitosan nanoparticles as a new delivery system for the anti-Alzheimer drug tacrine, *Nanomedicine* 6 (2010) 144-152
- 118 V. V. Jogani, P. J. Shah, P. Mishra, A. K. Mishra, A. R. Misra, Intranasal mucoadhesive microemulsion of tacrine to improve brain targeting, *Alzheimer Dis. Assoc. Disord.* 22 (2008) 116-124
- 119 B. Luppi, F. Bigucci, T. Cerchiara, R. Mandrioli, A. M. Di Pietra, V. Zecchi, New environmental sensitive system for colon-specific delivery of peptidic drugs, *Int. J. Pharm.* 358 (2008) 44-49
- 120 D. Duchene, G. Ponchel, D. Wouessidjewe, Cyclodextrins in targeting. Application to nanoparticles, *Adv. Drug Deliv. Rev.* 36 (1999) 29-40

- 121 S. V. Dhuria, L. R. Hanson, W. H. Frey II, Intranasal delivery to the central nervous system: mechanisms and experimental considerations, *J. Pharm. Sci.* 99 (2010) 1654-1673
- 122 B. J. Berne, R. Pecora, *Dynamic Light Scattering with Application to Chemistry Biology and Physics*, Wiley-Interscience, New York, (1976)
- 123 B. Chu, *Laser Light Scattering*, Academic Press, New York (1974)
- 124 T. Cerchiara, B. Luppi, F. Bigucci, V. Zecchi, Chitosan salts as nasal sustained delivery systems for peptidic drugs, *J. Pharm. Pharmacol.* 55 (2003) 1623-1627
- 125 F. Bigucci, B. Luppi, T. Cerchiara, M. Sorrenti, G. Bettinetti, L. Rodriguez, V. Zecchi, Chitosan/pectin polyelectrolyte complexes: selection of suitable preparative conditions for colon-specific delivery of vancomycin, *Eur. J. Pharm. Sci.* 35 (2008) 435-441
- 126 S.S. Likhodii, I. Serbanescu, M. A. Cortez, P. Murphy, O. C. 3rd Snead, W. M. Burnham, Anticonvulsant properties of acetone, a brain ketone elevated by the ketogenic diet, *Ann. Neurol.* 54 (2003) 219-226
- 127 E. Adriaens, M. M. M. Dhondt, J. P. Remon, Refinement of the Slug Mucosal Irritation test as an alternative screening test for eye irritation, *Toxicol. in vitro* 19 (2005) 79-89
- 128 N. Csaba, M. Köping-Höggård, M. J. Alonso, Ionically crosslinked chitosan/tripolyphosphate nanoparticles for oligonucleotide and plasmid DNA delivery, *Int. J. Pharm.* 382 (2009) 205-214
- 129 S. Ko, S. Gunasekaran, Preparation of sub-100-nm beta-lactoglobulin (BLG) nanoparticles, *J. Microencapsul.* 23 (2006) 887-898
- 130 D. Duchene, F. Touchard, N. A. Peppas, Pharmaceutical and medical aspects of bioadhesive systems for drug administration, *Drug Dev. Ind. Pharm.* 14 (1988) 283-318
- 131 R. Gurny, J. M. Meyer, N. A. Peppas, Bioadhesive intraoral release systems: design, testing and analysis, *Biomaterials* 5 (1984) 336-340
- 132 N. A. Peppas, P. A. Buri, Surface, interfacial and molecular aspects of polymer bioadhesion on soft tissues, *J. Control. Release* 2 (1985) 257-275
- 133 T. Loftsson, P. Jarho, M. Másson, T. Järvinen, Cyclodextrins in drug delivery, *Expert Opin. Drug Deliv.* 2(2) (2005) 335-351

- 134 E. Giacobini, Pharmacotherapy of Alzheimer's disease: new drugs and novel therapy, in: B. Corain, K. Iqbal, M. Nicolini, B. Winblad, H. Wisniewski, P. Zatta (Eds.) *Alzheimer's Disease: Advances in Clinical and Basic Research*. Wiley, New York, 1993, pp. 529–538
- 135 J. Marx, Alzheimer's research moves to mice. *Science* 253 (1991) 266–267
- 136 J.L. Cummings, G. Cole, Alzheimer disease, *JAMA* 287 (2002) 2335–2338
- 137 R.J. Polinsky, Clinical pharmacology of rivastigmine: A new generation acetyl choline esterase inhibitor for the treatment of Alzheimer's disease, *Clin. Ther.* 20 (1998) 634–637
- 138 M. Guglielmo, L. Gilberto, E. Tamagno, M. Tabaton, Oxidative stress mediates the pathogenic effect of different Alzheimer's disease risk factors. *Front. Aging Neurosci.* 2 (2010) 1-8
- 139 P. Dogterom, J.F. Nagelkerke, G.J. Mulder, Hepatotoxicity of tetrahydroaminoacridine in isolated rat hepatocytes: Effect of Glutathione and Vitamin E, *Biochem. Pharmacol.* 7 (1988) 2311-2313
- 140 W.K. Summers, Tacrine, and Alzheimer's treatments, *J. Alzheimers Dis.* 9(3) (2006) 439-445
- 141 K.L. Davis, P. Powchik, Tacrine, *Lancet* 345 (1995) 625–630
- 142 P. Hartvig, H. Askmark, S.M. Aquilonius, L. Wiklund, B. Lindström, Clinical pharmacokinetics of intravenous and oral 9-amino-1,2,3,4-tetrahydroacridine, tacrine, *Eur. J. Clin. Pharmacol.* 38 (1990) 259–263
- 143 A.J. Wagstaff, D. McTavish, Tacrine. A review of its pharmacodynamic and pharmacokinetic properties, and therapeutic efficacy in Alzheimer's disease, *Drugs Aging.* 4 (1994) 510–554
- 144 L. Illum, Transport of drugs from the nasal cavity to the central nervous system, *Eur. J. Pharm. Sci.* 11 (2000) 1-18
- 145 L. Illum, Nasal drug delivery: possibilities, problems and solutions, *J. Control. Release* 87 (2003) 187-198
- 146 R.G. Thorne, G.J. Pronk, V. Padmanabhan, W.H. Frey 2nd, Delivery of insulin-like growth factor- I to the rat brain and spinal cord along olfactory and trigeminal pathways following intranasal administration, *Neuroscience* 127 (2005) 481-496
- 147 B. Luppi, F. Bigucci, G. Corace, A. Delucca, T. Cerchiara, M. Sorrenti, L. Catenacci, A.M. Di Pietra, V. Zecchi, Albumin nanoparticles carrying

- cyclodextrins for nasal delivery of the anti-Alzheimer drug tacrine, *Eur. J. Pharm. Sci.* 44(4) (2011) 559-65
- 148 V.V. Jogani, P.J. Shah, P. Mishra, A.K. Mishra, A.R. Misra, Nose-to-brain delivery of tacrine, *J. Pharm. Pharmacol.* 59 (2007)1199-1205
- 149 M. R. Jaafari, M. Tafaghodi, S. Abolghassem Sajadi Tabassi, Evaluation of the clearance characteristics of liposomes in the human nose by gamma-scintigraphy, *Iran. J. Pharm. Res.* 1 (2005) 3-11
- 150 H. Nakagawa, T. Shiina, M. Sekino, M. Kotani, S. Ueno, Fusion and molecular aspects of liposomal nanocarriers incorporated with isoprenoids, *IEEE Trans Nanobioscience* 6(3) (2007) 219-22
- 151 P.J. Quinn, The effect of tocopherol on the structure and permeability of phosphatidylcholine liposomes, *J. Control. Release* (2012), doi:10.1016/j.jconrel.201112.029
- 152 Leo, C. Hansch, D. Elkins, Partition coefficients and their uses, *Chem. Rev.* 71 (1971) 525–616
- 153 P.C. Stein, M.P. di Cagno, A. Bauer-Brandl, A Novel Method for the Investigation of Liquid/Liquid Distribution Coefficients and Interface Permeabilities Applied to the Water-Octanol-Drug System, *Pharm. Res.* 28 (2011) 2140–2146
- 154 F. Szoka Jr, D. Papahadjopoulos, Procedure for preparation of liposomes with large internal aqueous space and high capture by reverse-phase evaporation. *Proc. Natl. Acad. Sci. U S A* 75(9) (1978) 4194–4198
- 155 C. Pidgeon, S. McNeely, T. Schmidt, J.E. Johnson, Multilayered vesicles prepared by reverse-phase evaporation: liposome structure and optimum solute entrapment, *Biochemistry* 26(1) (1987) 17-29
- 156 N. Li, L.H. Peng, X. Chen, S. Nakagawa, J.Q. Gao, Effective transcutaneous immunization by antigen-loaded flexible liposome in vivo, *Int. J. Nanomedicine* 6 (2011) 3241-3250
- 157 R. Bellott, A. Auvrignon, T. Leblanc, Y. Pérel, V. Gandemer, Y. Bertrand, F. Méchinaud, P. Bellenger, J. Vernois, G. Leverger, A. Baruchel, J. Robert, Pharmacokinetics of liposomal daunorubicin (DaunoXome) during a phase I-II study in children with relapsed acute lymphoblastic leukaemia, *Cancer Chemother. Pharmacol.* 47(1) (2001) 15-21
- 158 T. Cerchiara, B. Luppi, G. Chidichimo, F. Bigucci, V. Zecchi, Chitosan and poly(methyl vinyl ether-co-maleic anhydride) microparticles as nasal sustained delivery systems, *Eur. J. Pharm. Biopharm.* 61(3) (2005) 195-200

- 159 E. Gavini, G. Rassa, V. Sanna, M. Cossu, P. Giunchedi, Mucoadhesive microspheres for nasal administration of an antiemetic drug, metoclopramide: in-vitro/ex-vivo studies, *J. Pharm. Pharmacol.* 57(3) (2005) 287-94
- 160 G.E. Flaten, A.B. Dhanikula, K. Luthman, M. Brandl, Drug permeability across a phospholipid vesicle based barrier: a novel approach for studying passive diffusion, *Eur. J. Pharm. Sci.* 27(1) (2006) 80-90
- 161 S.M. Fischer, G.E. Flaten, E. Hagesæther, G. Fricker, M. Brandl, In-vitro permeability of poorly water soluble drugs in the phospholipid vesicle-based permeation assay: the influence of nonionic surfactants, *J. Pharm. Pharmacol.* 63(8) (2011) 1022-1030
- 162 Tarozzi, F. Morroni, A. Merlicco, S. Hrelia, C. Angeloni, G. Cantelli-Forti, P. Hrelia, Sulforaphane as an inducer of glutathione prevents oxidative stress-induced cell death in a dopaminergic-like neuroblastoma cell line, *J. Neurochem.* 111 (2009) 1161-1171
- 163 M. Gallarate, D. Chirio, M. Trotta, E. Carlotti, Deformable liposomes as topical formulations containing  $\alpha$ -Tocopherol, *J. Dispers. Sci. Technol.* 27 (2006) 703-713
- 164 T. Nii, F. Ishii, Encapsulation efficiency of water-soluble and insoluble drugs in liposomes prepared by the microencapsulation vesicle method, *Int. J. Pharm.* 298(1) (2005) 198-205
- 165 L. Illum, Nasal drug delivery: possibilities, problems and solutions, *J. Control. Release* 87 (2003) 187-198
- 166 K. Dae-Duk, *Drug Absorption Studies: In situ, In vitro and In silico models*, chapter 9, Springer, USA, 2007
- 167 S. Mathison, R. Nagilla, U.B. Kompella, Nasal route for direct delivery of solutes to the central nervous system: fact or fiction?, *J. Drug Target* 5(6) (1998) 415-441
- 168 U. Westin, E. Piras, B. Jansson, U. Bergström, M. Dahlin, E. Brittebo, E. Björk, Transfer of morphine along the olfactory pathway to the central nervous system after nasal administration to rodents, *Eur. J. Pharm. Sci.* 24(5) (2005) 565-573
- 169 M. M. Corrada, R. Brookmeyer, A. Paganini-Hill, D. Berlau, C. H. Kawas, Dementia incidence continues to increase with age in the oldest old: the 90+ study, *Annals of Neurology* 67(1) (2010) 114-121
- 170 B. A. Yankner, Mechanism of neuronal degeneration in Alzheimer's disease, *Neuron* 16 (199) 6921-6932

- 171 J. Hardy A, hundred years of Alzheimer's disease research, *Neuron* 52 (2006) 3-13
- 172 J. J. Cook, Acute gamma-secretase inhibition of nonhuman primate CNS shifts amyloid precursor protein (APP) metabolism from amyloid-beta production to alternative APP fragments without amyloid-beta rebound, *Journal of Neuroscience* 30(19) (2010) 6743-6750
- 173 B. T. Hyman, Caspase activation without apoptosis: insight into A $\beta$  initiation of neurodegeneration, *Nature Neuroscience* 14 (2011) 5-6
- 174 T. W. kim, W. H. Pettingell, Y.K. Jung, Alternative cleavage of Alzheimer-associated presenilins during apoptosis by caspase-family protease, *Science* 277 (1997) 73-76
- 175 S.J. Martin, Proteolysis of fodrin (non erythroid spectrin) during apoptosis, *J Biol Chem* 270 (1995) 6425-28
- 176 B. McLaughlin, K. A. Hartnett, Caspase 3 activation is essential for neuroprotection in preconditioning, *Proc Natl Acad Sci USA* 100 (2003) 715-20
- 177 Y. Tong, Oxidative stress potentiates BACE1 gene expression and A $\beta$  generation, *J. Neural trasm.* 112 (2005) 455-469
- 178 M. Guglielmotto, L. Gilberto, E. Tamagno, M. Tabaton, Oxidative stress mediates the pathogenic effect of different Alzheimer's disease risk factors, *Frontier in Aging neurosc.* 2 (2010) 1-8
- 179 K. A. Hensley, Model for beta-amyloid aggregation and neurotoxicity based on free radical generation by the peptide, *Proc. natl. acad. Sci.* 91 (1994) 3270-3274
- 180 T. Gura, Hope in Alzheimer's fight emerges from unexpected places, *Nat. Med* 14 (2008) 894-899
- 181 A. Kamal-Eldin, L. A. Appelqvist, The chemistry and antioxidant properties of tocopherols and tocotrienols, *Lipids* 31 (1996) 671-701
- 182 Y. Saito, Y. Yoshida, T. Akazawa, K. Takahashi, E. Niki, Cell death caused by selenium deficiency and protective effect of antioxidants, *J. Biol. Chem.* 278 (2003) 39428-39434
- 183 E. Serbinova, V. Kagan, D. Han, L. Packer, Free radical recycling and intramembrane mobility in the antioxidant properties of alpha-tocopherol and alpha-tocotrienol, *Free Radic. Biol. Med.* 10 (1991) 263-275

- 184 K. H. Masaki, Association of vitamins E and C supplement use with cognitive function and dementia in elderly men, *Neur.* 54 (2000) 1265-1272
- 185 P. J. Quinn, The effect of tocopherol on the structure and permeability of phosphatidylcholine liposomes, *J. Control. Release.* (2012), doi:10.1016/j.jconrel.201112.029
- 186 W. L. Stone, Therapeutic uses of antioxidant liposomes, *Methods Mol. Biol.* 199 (2002) 145-161
- 187 W. L. Stone, M. Smith, Therapeutic uses of antioxidant liposomes, *Mol. Biotechnol.* 27 (2004) 217-230
- 188 J. Fan, Liposomal antioxidant provide prolonged protection against acute respiratory distress syndrome, *Surgery* 128 (2000) 332-338
- 189 M. Halks-Miller, Tocopherol-phospholipid liposomes: maximum content and stability to serum proteins, *Lipids* 20 (1985) 195-200
- 190 E. Zacharias, Liposomal Antioxidants for Protection against Oxidant-Induced Damage, *Journal of Toxicology* 201 (2011) 1-16
- 191 K. Yazawa, DHA supplementation in dementia. Presented at international Society for the study of Fatty Acids and Lipids, Barcelona, Spain (1996)
- 192 R. Jr. Abel, The DHA story: how nature's super nutrient can save your life, *Read How You Want* 2011 Chapter 6.
- 193 FS. Lu, Oxidative stability of marine phospholipids in the liposomal form and their applications, *Lipids* 46(1) (2011) 3-23
- 194 A. Tarozzi, F. Morroni, S. Hrelia, C. Angeloni, A. Marchesi, G. Cantelli-Forti, P. Hrelia, Neuroprotective effects of anthocyanins and their in vivo metabolites in SH-SY5Y cells, *Neurosci Lett.* 424(1) (2007) 36-40
- 195 C. Angeloni, E. Leoncini, M. Malaguti, S. Angelini, P. Hrelia, S. Hrelia, Role of quercetin in modulating rat cardiomyocyte gene expression profile, *Am. J. Physiol. Heart Circ. Physiol.* 294 (2008)1233-1243
- 196 H. Wang, J.A. Joseph, Quantifying cellular oxidative stress by dichlorofluorescein assay using microplate reader, *Free Radic. Biol. Med.* 27 (1999) 612-616
- 197 B. Edison, Analysis of Tocopherols by High Performance Liquid Chromatography, *E-Journal of Chemistry* 6(2) 2009 395-398

- 198 Grohganz, H., Ziroli, V., Massing, U., Brandl, M., 2003. Quantification of various phosphatidylcholines in liposomes by enzymatic assay. *AAPS Pharm. Sci. Tech.* 4, E63
- 199 Ivanov, I.T. Rapid method for comparing the cytotoxicity of organic solvents and their ability to destabilize proteins of the erythrocytemembrane. *Pharmazie* 56 (2001) 808-809
- 200 Cortesi, R., Esposito, E., Gambarin, S., Telloli, P., Menegatti, E. and Nastruzzi, C. Preparation of liposomes by reverse-phase evaporation using alternative organic solvents. *J. Microencapsul.* 16 (1999) 251-256
- 201 Vemuri, S. and Rhodes, C.T. Preparation and characterization of liposomes as therapeutic delivery systems: A review. *Pharm. Acta Helv.* 70 (1995) 95-111
- 202 Deamer, D.W. and Uster, P.S. Liposome preparation: Methods and mechanism. in: *Liposomes*, (Ostro, M.J. Ed.), Marcel Dekker, New York, 1983, 27-51
- 203 L. Zhang, H. Yu, Y. Sun, X. Lin, B. Chen, C. Tan, G. Cao, Z. Wang, Protective effects of salidroside on hydrogen peroxide-induced apoptosis in SH-SY5Y human neuroblastoma cells, *European Journal of Pharmacology* 564(1-3) ( 2007) 18-25
- 204 S. S. Kang, J. Yeon Lee, Y. Keum Choi, G. Seok Kim, B. Hee Han, Neuroprotective effects of flavones on hydrogen peroxide-induced apoptosis in SH-SY5Y neuroblastoma cells, *Bioorganic & Medicinal Chemistry Letters* 14(9) (2004) 2261-2264
- 205 Y. Lin, Y. Huang, S. Chen, C. Liaw, S. Kuo, L. Huang, P. Gean, Death in Human Neuroblastoma SH-SY5Y Cells Neuroprotective Effects of Ugonin K on Hydrogen Peroxide-Induced Cell Death in Human Neuroblastoma SH-SY5Y Cells, *Neurochemical Research* 34(5) (2008) 923-930
- 206 V. E. Kagan, R. A. Bakalova, Z. Zhelev, D. S. Rangelova, E. A. Serbinova, V. A. Tyurin, N. K. Denisova, L. Packer, Intermembrane transfer and antioxidant action of  $\alpha$ -tocopherol in liposomes, *Arch. Biochem. Biophys.* 280 (1990) 147-152